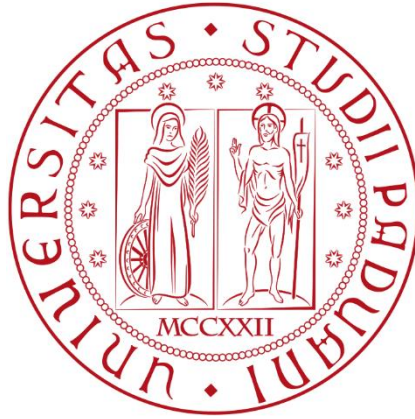# UNIVERSITÀ DEGLI STUDI DI PADOVA

DIPARTIMENTO DI GEOSCIENZE

Corso di laurea magistrale in

Geologia e Geologia Tecnica

Trasporto di microplastiche durante piene fluviali:

esempi dal fiume Arno (Toscana, Italia)

–

Microplastics transport during river floods:

examples from the Arno River (Tuscany, Italy)

Relatore: Prof. Massimiliano Ghinassi

Correlatore: Prof. Massimiliano Zattin

Laureando: Alessandro Michielotto

Matricola 1222696

Anno Accademico 2020 – 2021

Summary

Abstract

Microplastics are ubiquitous pollutants which pose a huge threat to ecosystems and human health. Plastic production has grown exponentially over time, and, consequently, also the plastic waste. Rivers are seen as the major vectors to deliver microplastics in marine environments, but they also are efficient temporary reservoirs. However, there is a lack of information on the dispersal pattern and transport of microplastics in river sediments, as previous researches mainly have focused on diversification and quantification of microplastics and their impacts on freshwater environments.

This study aims at providing new insights on this topic by analysing river sediments deposited after flood events and trying to identify any relationship between the depositional setting/process and the amount of microplastics accumulated in fluvial sediments. To achieve this goal, a total of 37 sediment samples form five alternate bars of the Arno River (Tuscany, Italy) were analysed to provide a complete spectrum for microplastic abundances and distributions in sediments accumulated in different conditions. Specifically study depositional conditions were: i) under dominant tractional processes during floods (samples T), ii) during brief episodes of standing water during the overall waning phase (samples S), iii) during the latest stages of the flood in standing to slowly moving water (samples M) and iv) during the highest flood water levels, associated with floating vegetation debris (samples F). The microplastics were extracted from the sediment by using the sodium polytungstate diluted to $1.6\ g/cm^3$ and the organic rich samples were previously oxidated with the Wet Peroxide Oxidation technique to eliminate the organic matter. The mechanical sieving was used to obtain the grain size distribution of the sampled sediments.

This approach led to the identification of some important features involving microplastic deposition in river sediments. As expected, the presence of microplastics was confirmed in all samples analysed, with variable concentrations ranging from 0.44 MPs/g up to 6.67 MPs/g, and a predominance of microfibres. Microplastic concentrations not only vary from a bar to another, but also within a single bar, suggesting there are different processes governing microplastics transport and depositions. Settling during the standing water, associated with the waning phase, seems to be the easier way for

Abstract

microplastics to deposit in river sediments, both within mud but also within interstitial space between gravelly clasts. Nevertheless, it was unexpected to see how many microplastics can be trapped in sandy deposits when they are moved under tractional conditions.

Riassunto

Le microplastiche sono inquinanti diffusi che rappresentano un'enorme minaccia per gli ecosistemi naturali e la salute umana. La produzione di plastica è cresciuta esponenzialmente nel tempo, e di conseguenza anche i rifiuti. I fiumi sono visti come i principali portatori di microplastiche negli ambienti marini, ma sono anche efficienti reservoir temporanei. Tuttavia, c'è una mancanza di informazioni sulle modalità di dispersione e trasporto delle microplastiche nei sedimenti fluviali, in quanto ad oggi le ricerche si sono principalmente concentrate sulla diversificazione e sulla quantificazione delle microplastiche e sul loro impatto negli ambienti continentali.

Questo studio vuole portare luce su questi temi, analizzando i sedimenti fluviali depositati dopo eventi alluvionali e cercando di identificare eventuali relazioni tra il processo deposizionale e la quantità di microplastiche accumulate nei sedimenti. Per fare questo, sono stati analizzati un totale di 37 campioni provenienti da cinque barre alternate del fiume Arno (Toscana, Italia) al fine di fornire uno spettro completo per le abbondanze e le distribuzioni di microplastiche nei sedimenti accumulati in diverse condizioni. Tali condizioni sono, nello specifico: i) di trasporto trattivo durante le piene (campioni T), ii) durante brevi episodi di stazionamento dell'acqua durante una generale fase calante (campioni S), iii) durante le ultime fasi della piena in acqua stagnante o in lento movimento (campioni M) e iv) durante i massimi livelli della piena, associati a detriti di vegetazione galleggianti (campioni F). Le microplasriche sono state estratte dal sedimento tramite separazione gravimetrica utilizzando il politungstato di sodio diluito a $1.6 \ g/cm^3$. I campioni ricchi in contenuto organico sono stati precedentemente ossidati con la tecnica della *Wet Peroxide Oxidation* per eliminare la materia organica. Per ottenere le curve granulometriche I campioni sono stati setacciati con il vibrovaglio.

Questo approccio ha portato all'identificazione di alcune importanti caratteristiche che riguardano il trasporto e la deposizione di microplastiche nei sedimenti fluviali. Come previsto, la presenza di microplastiche è stata confermata in tutti i campioni analizzati, con concentrazioni variabili che vanno da 0,44 MP/g fino a 6,67 MP/g, e una predominanza di microfibre. Le concentrazioni di microplastiche non solo variano da una

Riassunto

barra all'altra, ma anche all'interno di una singola barra, suggerendo che ci sono diversi processi che governano le deposizioni di microplastiche. La decantazione durante lo stazionamento d'acqua, associato alla fase calante, sembra essere il modo più facile per le microplastiche di depositarsi nei sedimenti fluviali. Tuttavia, è stato inaspettato osservare quante microplastiche possano accumularsi nei sedimenti sabbiosi quando messi in movimento in condizioni di trasporto trattivo.

1   Introduction

Plastic is a synthetic polymer which assumed a relevant role in our lives as it can be used in a multitude of application from domestic to industrial applications. Plastics are as much present in our daily lives as they are in the environment, and there is no country in the world that has not to deal with plastics.

Global plastic production shows a steady increase since the 1950s, reaching $368 \cdot 10^6 \ t$ in 2019 (PlascticsEurope, 2020) and as a result, more and more plastic litter is released into the environment every year. There is no place that is not contaminated: from rivers to oceans (Li et al., 2016), but also from the most remote polar regions (Mishra et al., 2021) to even the highest altitudes in the atmosphere (González-Pleiter et al., 2021) (*figure 1.1*).
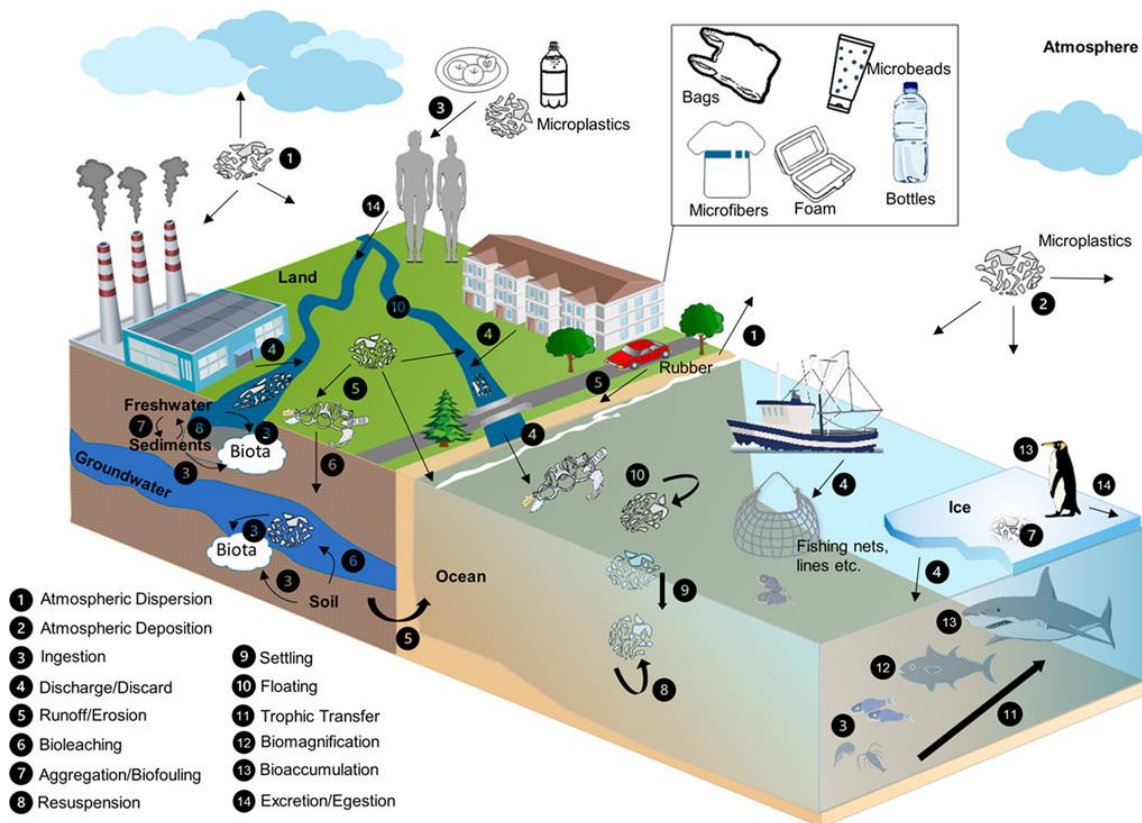

Figure 1.1. Plastic and microplastic production and dispersion, from Petersen et al., 2021

Plastics are persistent materials, so when discarded as a waste, they can accumulate in the environment for a long time and pose a threat, both direct and indirect, to ecosystems, biodiversity, and local economies (Frias et al., 2018).

1. Introduction

Plastic contamination has received an increasing attention from the scientific communities: first studies on marine environments began in the 1970s (Carpenter and Smith, 1972) and since that time, investigations have shown that plastic litter can be found in all aquatic environments such as beaches, deep-sea sediments, freshwater lakes, and rivers (Claessens et al., 2011; Eriksen et al., 2013; He et al., 2020; Kane & Clare, 2019).

When plastics are dispersed into the environment, they are exposed to weathering conditions which disaggregate the litter in smaller components producing microplastics. With the evolution of technology microplastics are appositely created for both industrial and domestic use.

In the last decade studies have focused in the microplastics, plastic particles which have dimensions from $1\ \mu m$ to $5\ mm$ (*figure 1.2*).
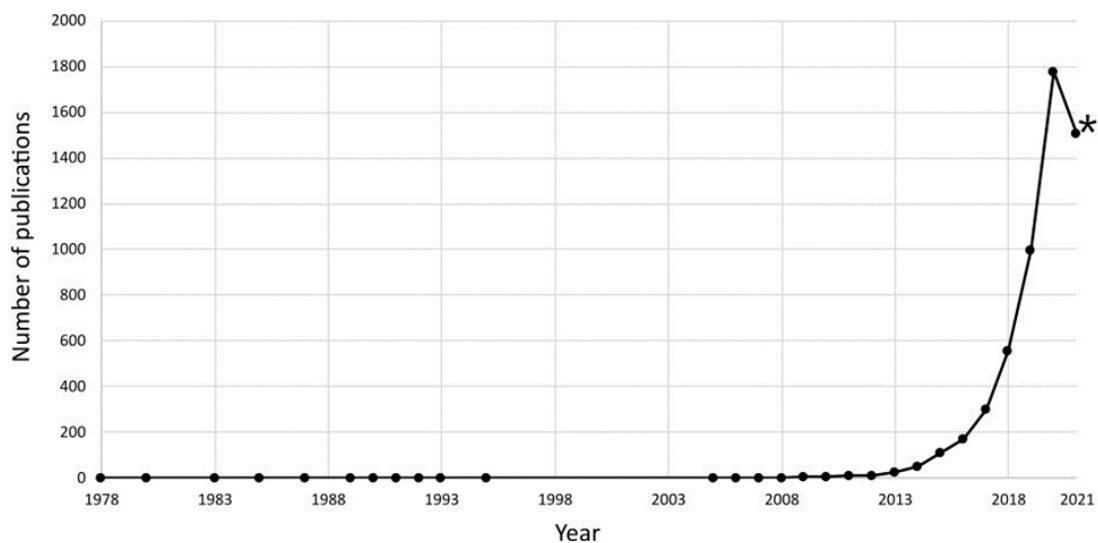

*Figure 1.2. Annual number of Scopus article containing the keyword "microplastics". *Last update in 06/20/2021.*

They can be divided into primary and secondary types. Primary microplastics are produced to have microscopic size and are commonly used for cosmetics and personal care products like microbeads for scrubbing or exfoliating (Napper et al., 2015), or glitter to shine (Yurtsever, 2019). Secondary microplastics derive from the breakdown of larger plastic debris (e. g. fragment and fibres from plastic bags) when exposed to weathering conditions (e. g. solar radiation, water temperature and abrasion processes) (Cole et al., 2013).

2

1. Introduction

Among plastic materials and related pollution, microplastics represent a huge concern due to their impacts resulting from their ability to adsorb persistent, bioaccumulative and toxic chemicals (PBTC) (e. g. polychlorinated biphenyls – PCBs, polycyclic aromatic hydrocarbons – PAHs) and trace elements (e. g. Cu, Zn, etc.) (Frias et al., 2019).

Plastic materials in marine environments can be found throughout the water column (Kane and Clare, 2019). When plastic litter is caught up in circular ocean currents, it can converge in the centre of these flows and create accumulations of mega- to micro-plastics creating actual plastic islands, that can cover areas from tens to even a million of km^2 as estimated by Lebreton et al. (2018) in the case of the Great Pacific Garbage Patch (*figure 1.3*).
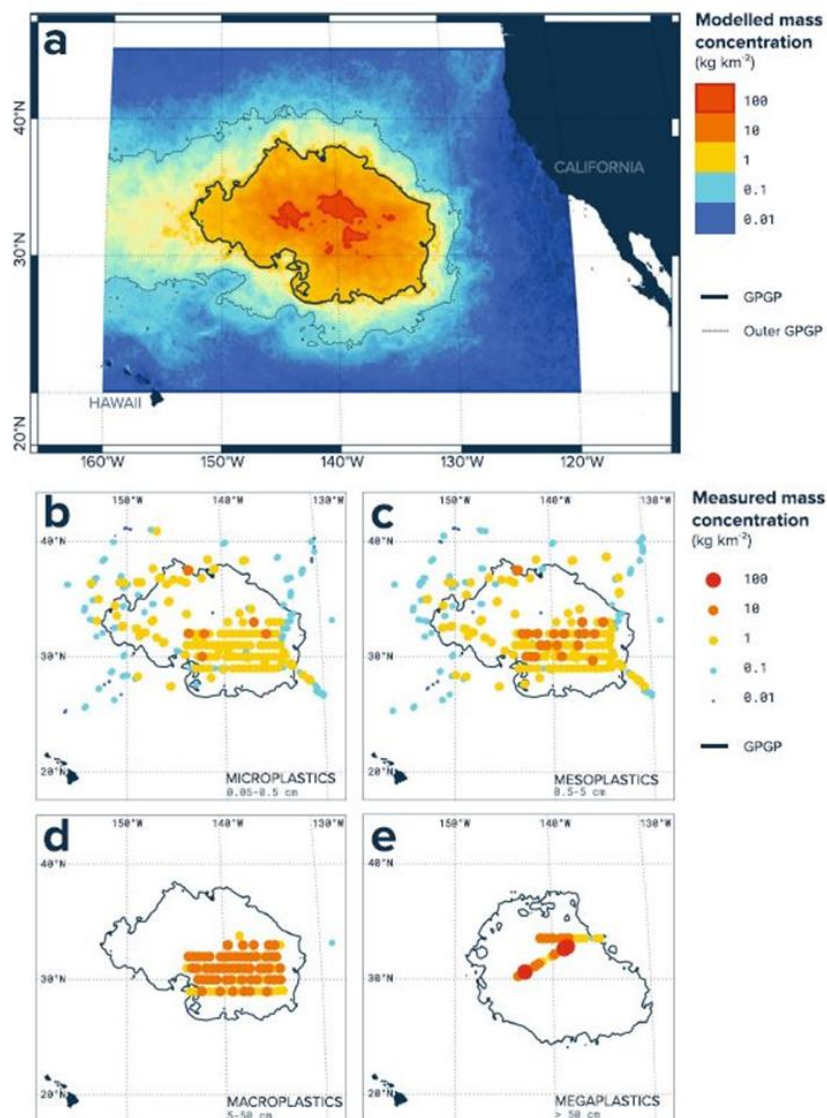

Figure 1.3. Modelled and measured mass concentration in the Great Pacific Garbage Patch (GPGP), from Lebreton et al., 2018.

1. Introduction

Plastic litter floating on the sea surface will undergo degradation processes that cause a continuous release of secondary microplastics. These are transported in suspension along the water column and may reach the seabed by underwater currents or by secondary processes linked first to ingestion and then to the death and decomposition of the organism that fed on them (Kane and Clare, 2019).

Rivers are seen as major pathways of microplastic transport from terrestrial areas to marine ecosystems, with estimated riverine fluxes up to $2.41 \cdot 10^6 \ t$ annually (Lebreton et al., 2017).

Rivers not only work as microplastic drivers to the seas, but also as temporary reservoirs, where they are efficiently retained in fluvial sediments (Besseling et al., 2017).

However, there is a lack of information on the dispersal pattern and transport of microplastics in river sediments as research up to now mainly has focused on diversification and quantification of microplastics and their impacts on freshwater environments, not considering microplastic distribution as function of variable sedimentary processes and different depositional environment (e. g. top of fluvial bars, abandoned channels) (*figure 1.4*).
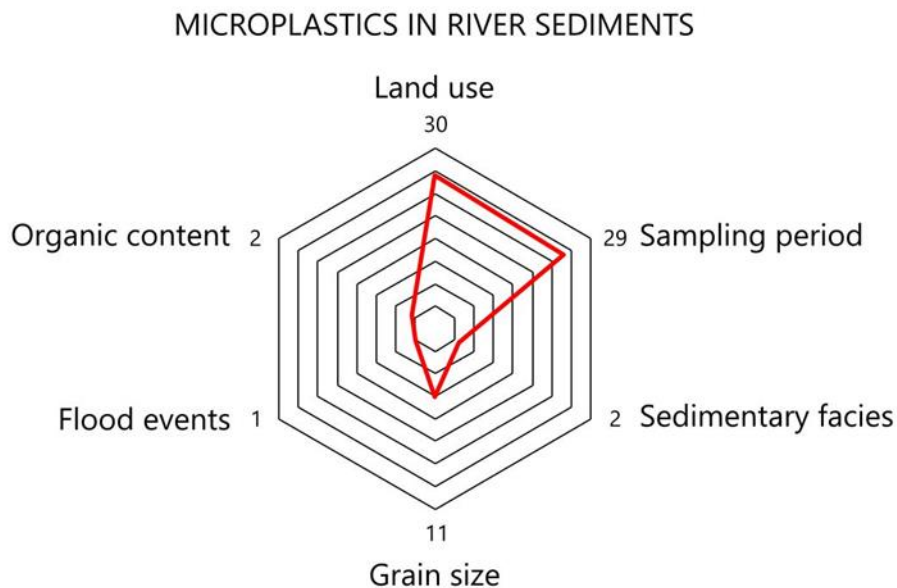

Figure 1.4. Factors considered in 35 articles dealing with microplastics in river sediments.

4

1. Introduction

The analysis of 35 different articles on microplastics in river sediments showed that most of them focus on land use near the study areas (e. g. industrial areas, agricultural areas) and indicate the days of sampling, but hardly ever take into account the hydrodynamic regime (e. g. flood events). The river sediments analysed are very often collected with grab samplers, so no distinction is made on the sedimentary facies they represent or even on the particle size and organic matter content. This study wants to bring a new insight on the topic by studying fluvial sediments collected in the Arno River, by considering on the depositional setting in which sampled sediments are accumulated. This approach aims at detecting possible relationships between the depositional setting/process and the amount of microplastics accumulated in sediments.

The aim of the study is to i) determine microplastics by their physical properties (e. g. shape, colour), ii) quantify the concentration of microplastics in different types of river sediments, and iii) identify any relationship between depositional environment and the quantity of microplastics in sediments.

2   Study area and sedimentary dynamics of alternate fluvial bars

This work focuses on sediments of the Arno River (*figure* 2.1), the 8th largest river in Italy (the 1th in Tuscany).
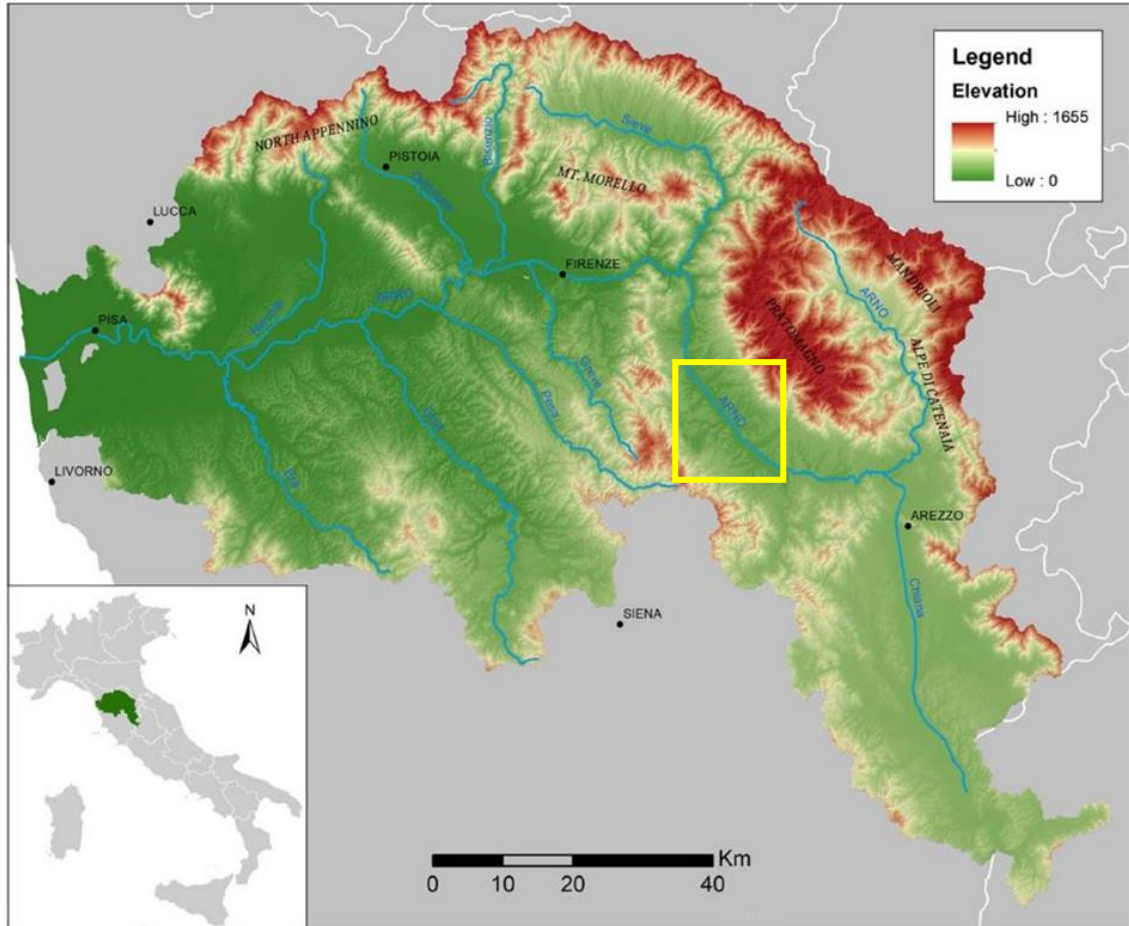

Figure 2.1. Location, elevation distribution, and main river network of the Arno River basin, from Stefanelli et al., 2020)
In yellow the study area.

The Arno River originates at $1385\ m$ a.m.s.l. (above mean sea level) form the Monte Falterona ($1658\ m$ a.m.s.l.) in the Casentino area (northern Apennines). It runs through the Provinces of Arezzo, Florence, and Pisa before it ends in the Tyrrhenian Sea.

The Arno catchment ($8228\ km^2$) is located within the mountain belt of the Northern Apennines, which was subject during the last phases of its evolution to an extensional tectonic phase caused by the aperture of the Tyrrhenian, starting from the upper Tortonian, producing a horst and graben system, aligned in a NW-SE direction, and a sequence of Neogene marine and fluvio-lacustrine sedimentary cycles. The physiography of the catchment is strongly influenced by the morphology of the region,

2. Study area and sedimentary dynamics of alternate fluvial bars

being characterized by a series of intermontane basins, alternated with bedrock-controlled gorge-like reaches (Caporali et al., 2005).

The Arno catchment drains the water of the following six drainage systems:

- Casentino 883 km^2
- Val di Chiana 1368 km^2
- Upper Val d'Arno 984 km^2
- Sieve 843 km^2
- Middle Val d'Arno 1383 km^2
- Lower Val d'Arno 2767 km^2

The Sieve River is the main tributary of the Arno, flowing into it on the hydrological right, as do other minor tributaries: the Mugnone and Terzolle (which flow through Florence like the Arno), the Bisenzio and Ombrone Pistoiese and the Usciana canal. On the hydrological left of the Arno there are the following tributaries: Greve, Pesa, Elsa, Egola and Era. The wide tectonic depression containing these tributaries resulted in the formation of an alluvial plain which, in the distal part of the Arno basin, joins a coastal plain (Nocita, 2007).

The rainfall regime of the Arno River catchment can be classified as sub-littoral in the higher portion of the basin and maritime closer to the Tyrrhenian Sea. Average annual runoff of the whole basin is about $3 \cdot 10^9 \ m^3$, with an average discharge of $90 \ m^3/s$ in its distal portion (San Giovanni alla Vena, Pisa) (Nocita, 2007). Flood periods occur between December and March, while the minimum discharges are reached in August. Annual peak discharges measured in the San Giovanni alla Vena (PI) gauging station range from 321 to 2290 m^3/s (recorded on November 4, 1966).

Between Arezzo and Firenze, the Arno Rivers flows northward along the Upper Valdarno Basin, where natural meandering channels were rectified during the XVIII century (Tartaro, 1989) and the Arno River was constrained to a straight course. This reach of the river trends SSE-NNW and is 6 km long.

2. Study area and sedimentary dynamics of alternate fluvial bars

The reach of the river chosen for this study is located between San Giovanni Valdarno and Montevarchi, in the Province of Arezzo, with a population density respectively of 800 and 430 $inhabitants/km^2$ (*figure2.2*).
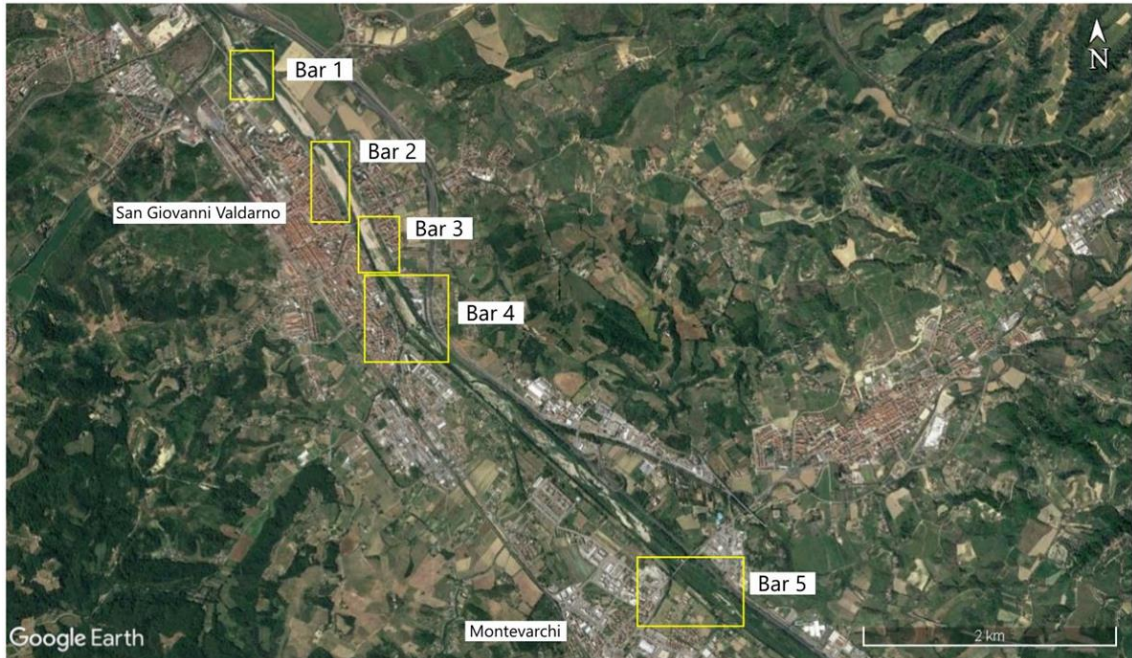

Figure 2.2.Section of the Arno River selected, in yellow the bars studied.

The selected reach has a width of 30 m when lean, while during floods can reach up to 130 m wide, and its natural course has been constrained to straight.

Straight watercourses are typical of rivers regulated by man which have lost their original conformations (*figure 2.3).*

Figure 2.3. Example of an urbanized river. Senne River (Bruxelles, Belgium).

2. Study area and sedimentary dynamics of alternate fluvial bars

Therefore, the study will deal with the deposition of anthropogenic material within the sediments of an "anthropogenic" river.

Sediments in rivers tend to accumulate in localized areas where conditions are unsuitable for sediment transport. In these areas, deposition occurs in different ways (tractional or suspension mechanisms) according to the local hydrodynamic regime. These accumulations, called bars, can be removed by a following flood or enter in the fossil record.

Bars can be considered complex sedimentary bodies, mainly growing during flood events (*figure2.4*), when the volume of sediment is "spread" onto the bar as an elongated and thin linguoid body accumulated where a decrease in flow velocity occurs.

Figure 2.4. Flood event almost covering the entire Bar 3, in San Giovanni Valdarno (AR), starting the erosion – deposition processes. Formation of a chute channel in the bank side.

2. Study area and sedimentary dynamics of alternate fluvial bars

Figure 2.5 shows a portion of the study area in a timeline from 2003 to 2020, highlighting the dynamic nature of some fluvial bars, migrating downstream with a northward flow.
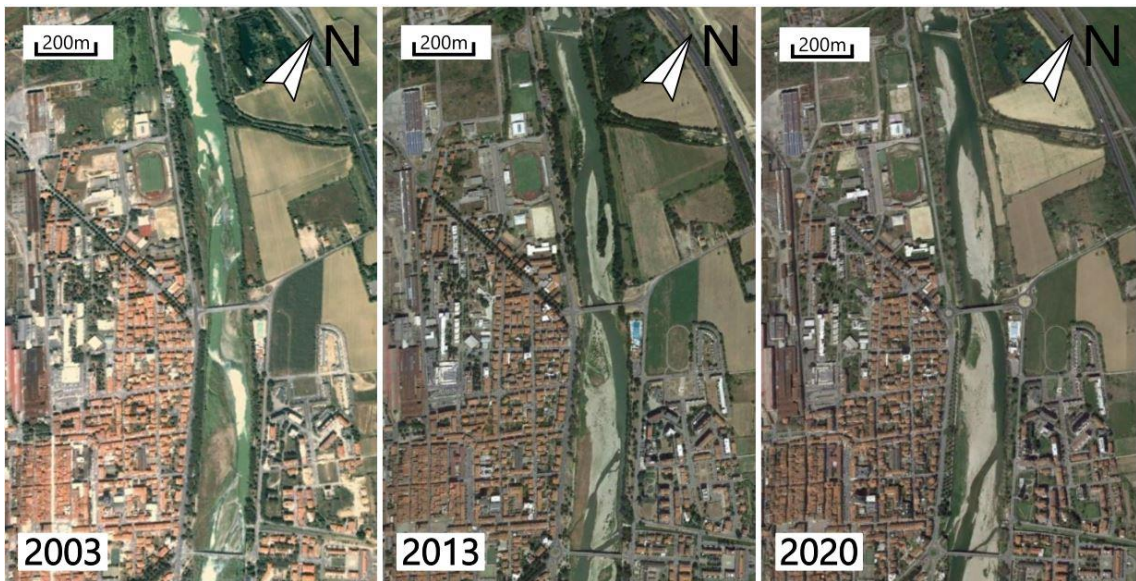

Figure 2.5. Pictures of the study area captured in 2003, 2013, and 2020. It can be appreciated the growth of the most downstream bar (northward) in just 7 years, from 2013 to 2020.

Based on their position in the watercourse, different types of bars can be distinguished (*figure 2.6*).
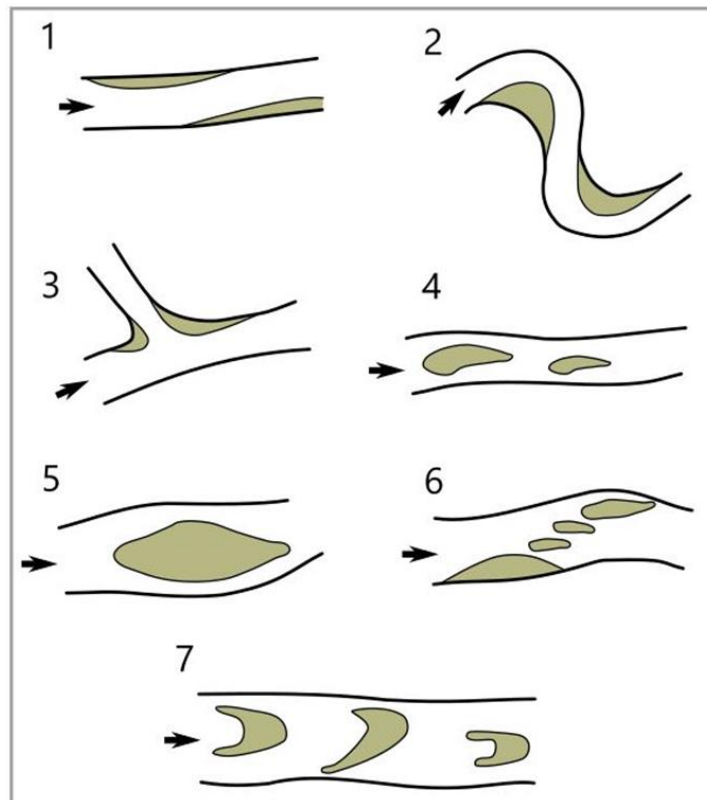
Figure 2.6. Classification of the principal type of bars: 1. Lateral bars; 2. Meandering bars; 3. Confluence bars; 4. Longitudinal bars; 5. Diamond bars; 6. Diagonal bars; 7. Lunate bars or dune. After Rinaldi et al. (2011).

2. Study area and sedimentary dynamics of alternate fluvial bars

 As the selected stretch is rectilinear, the sampled bars are classified as alternate. Alternate bars are sediment waves consisting of consecutive diagonal fronts with low slope riffles located upstream. The name "alternate" is due to the fact they tend to form alternately on the two sides of the channel (*figure* 2.7).


Tail (finer)   Head (coarser)
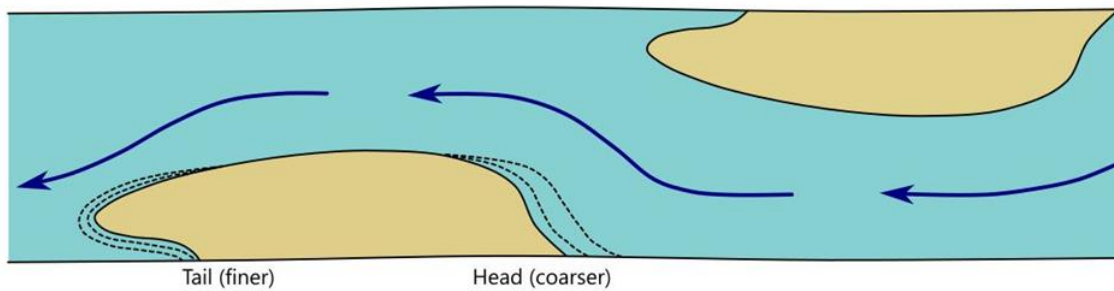
Figure 2.7. Alternate bars migrating downstream and moving from one side to the other of the channel.

They are generated by the instability of turbulent flows over an erodible bed during floods (Rodrigues et al., 2012). Their internal structure consists of large-scale sets of planar cross strata of coarse sands and gravels caused by the migration of ripples and dunes. Alternate bars tend to move mainly during flood events, where the head – made up of coarser grains – is exposed to erosion while the tail – made up of finer grains – receives sediments and deposition occurs. This leads the bar migrating downstream, grading from coarser to finer sediments in a process called armouring (*figure* 2.8).
While the central part of the bar tends to accrete univocally over time, the margins are subjected to sediment reworking. During the falling stage of the flood, when the flow intensity decreases, silty to muddy sediments tend to settle down and drape the bar.

2. Study area and sedimentary dynamics of alternate fluvial bars

Study bars consists of gravelly heads and sandy tails, and transition between these two grain sizes is commonly abrupt and marked by development of a gravelly avalanching front (picture 2 in *figure* 2.8). Study bars length ranges from 300 to 900 m, the width from 40 to 120 m and their maximum relief is generally $2.5 - 3.5 \, m$ above le lowest river level. The tail of these alternate bars is generally detached from the bank by a depression that hosts standing water and allows settling of suspended muddy deposits and plant debris (picture 1 in *figure* 2.8). The study bars are locally colonized by scattered permanent vegetation (*Populus nigra*) in their highest part, but host a dense seasonal vegetation in the tail zone.
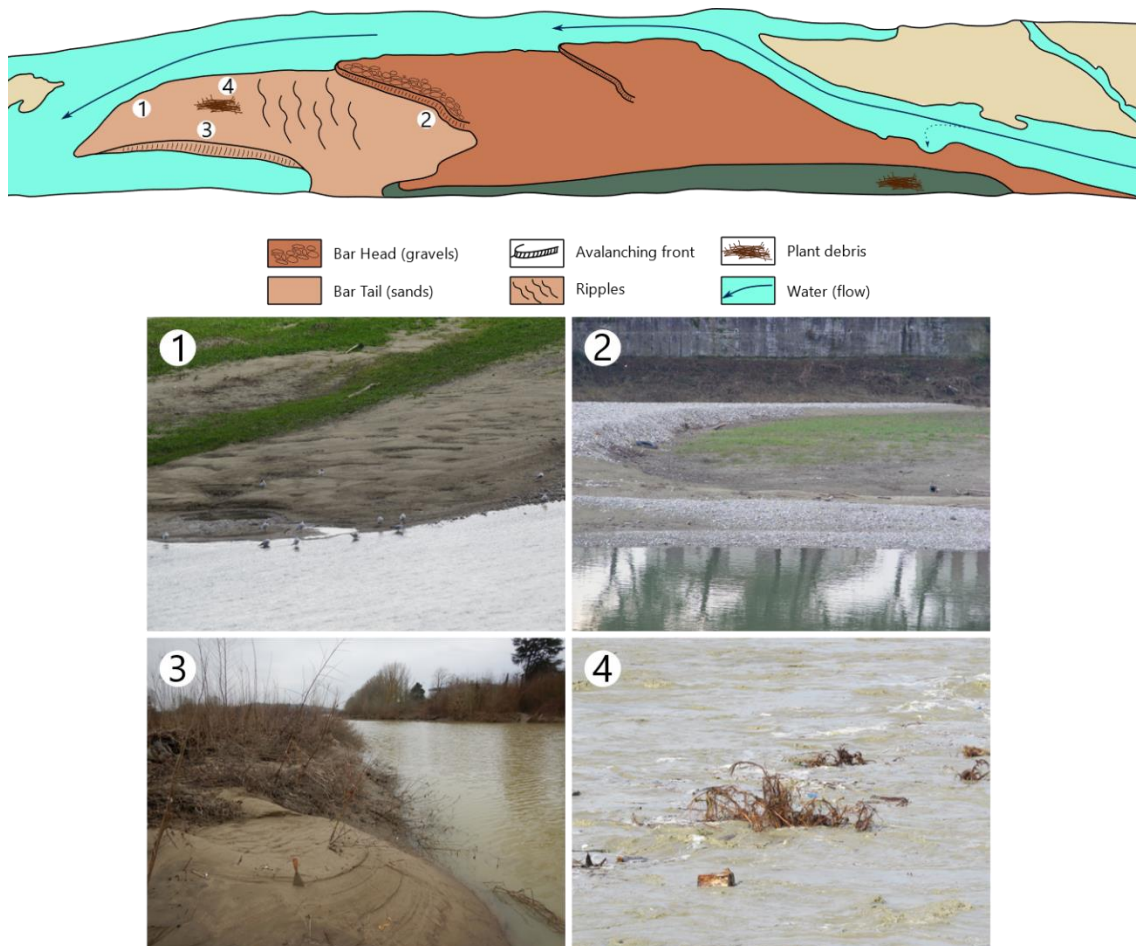
Figure 2.8. Representation of an actual alternate bar from the Arno River, highlighting the main characteristics. The downstream migration of the bar leads to an armouring process. 1. Sandy tail, with migrating ripples; 2. Gravelly avalanching front on bar tail; 3. Sandy avalanching front at the tip of the tail with evidence of slough water during the waning phase; 4. Floating vegetational and macroplastic elements deposited after flooding events.

3. Materials and methods

3 Materials and methods

3.1 Sample collection

Study samples were collected in 5 different alternate bars of the Arno River (*figure* 3.1) after two different flood events.
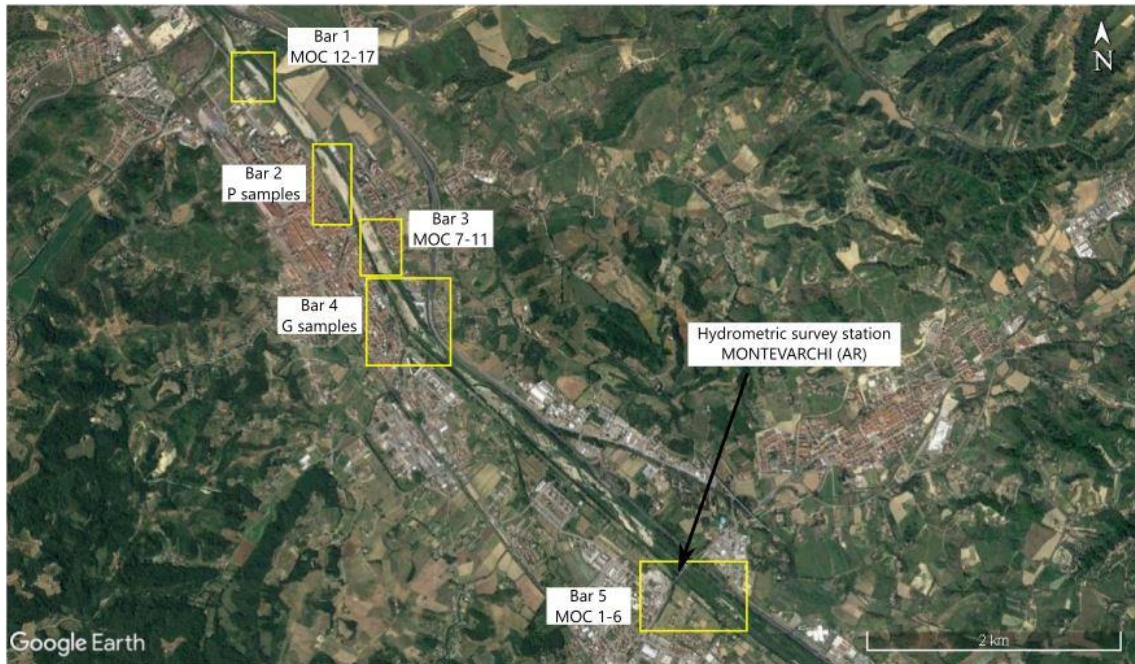

Figure 3.1. Sampling sites.

Collection of samples just after flood events allowed to pick up sediments which were not reworked by any process (e. g. bioturbation) that could have altered the content or distribution of microplastics.

Three series of samples were specifically collected: P, G and MOC. A total of 37 samples was collected.

P and G samples were collected on 12/23/2019 and come from two different alternate bars formed on the hydrographic left of the Arno River, in San Giovanni Valdarno (AR) area (Bar 2 and Bar 4). The intense flood reached his peak on 12/22/2019, whit a hydrometric elevation of more than $5\ m$ above hydrometric zero (m.s.z.i.), exceeding the first alert level (*figure 3.2 a*). At this stage, the top of both bars was covered 1-1.5 m of flowing water.

MOC samples were collected after a flood occurred on 02/10/2021 in three different bars, in San Giovanni Valdarno (AR) and Montevarchi (AR) areas (Bar 1, Bar 3 and Bar 5).

3. Materials and methods

Two bars are attached to the bank on the hydrological left, and one on the hydrological right. The flood reached a hydrometric peak of 3.7 m above hydrometric zero (m.s.z.i.) (*figure 3.2 b*).

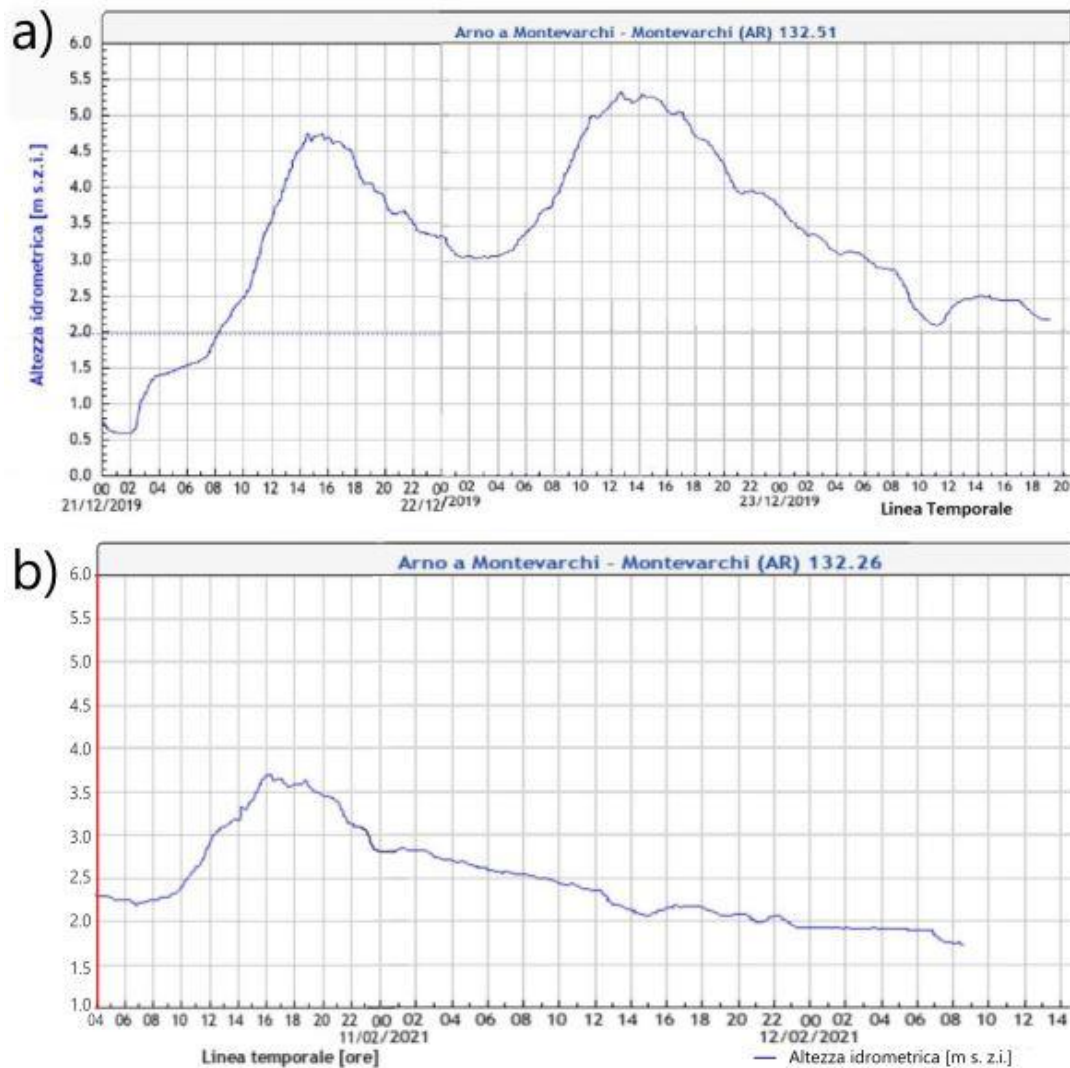Datas were provided from the Montevarchi hydrometric survey station, (*figure 3.1*).

Figure 3.2. a) Flood event occurred on 12/22-12/23/2019; b) Flood event occurred on 02/10-02/11/2021.

3. Materials and methods

Table 1 reports the GPS points per each sample and relative labels.

	Sample	TYPE	Latitude	Longitude
BAR 1	MOC12	S	43°34'38.97"N	11°31'30.38"E
	MOC13	T	43°34'38.97"N	11°31'30.38"E
	MOC14	S	43°34'39.25"N	11°31'30.08"E
	MOC15	T	43°34'39.25"N	11°31'30.08"E
	MOC16	F	43°34'38.59"N	11°31'32.60"E
	MOC17	F	43°34'38.13"N	11°31'31.91"E
BAR 2	P1	T	43°34'16.03"N	11°31'54.13"E
	P2	S	43°34'16.03"N	11°31'54.13"E
	P3	S	43°34'17.22"N	11°31'53.41"E
	P4	M	43°34'15.95"N	11°31'54.56"E
	P5	T	43°34'13.68"N	11°31'56.16"E
	P6	S	43°34'13.68"N	11°31'56.16"E
	P7	S	43°34'14.30"N	11°31'56.80"E
	P8	S	43°34'12.56"N	11°31'56.85"E
	P9	T	43°34'13.23"N	11°31'57.24"E
	P10	S	43°34'13.23"N	11°31'57.24"E
	P11	T	43°34'13.62"N	11°31'58.64"E
	P12	S	43°34'13.62"N	11°31'58.64"E
	P13	M	43°34'11.44"N	11°32'0.60"E
	P14	M	43°34'9.94"N	11°31'59.49"E
	P15	M	43°34'8.47"N	11°32'1.76"E
BAR 3	MOC7	S	43°33'53.01"N	11°32'14.00"E
	MOC8	T	43°33'53.01"N	11°32'14.00"E
	MOC9	S	43°33'56.30"N	11°32'12.12"E
	MOC10	T	43°33'56.30"N	11°32'12.12"E
	MOC11	F	43°33'53.30"N	11°32'14.66"E
BAR4	G2	T	43°33'41.93"N	11°32'18.34"E
	G3	S	43°33'41.93"N	11°32'18.34"E
	G4	T	43°33'40.86"N	11°32'18.80"E
	G5	S	43°33'40.86"N	11°32'18.80"E
	G12	S	43°33'38.91"N	11°32'20.29"E
BAR 5	MOC1	S	43°32'22.73"N	11°34'6.18"E
	MOC2	T	43°32'22.73"N	11°34'6.18"E
	MOC3	M	43°32'22.66"N	11°34'6.31"E
	MOC4	S	43°32'18.71"N	11°34'11.61"E
	MOC5	T	43°32'18.71"N	11°34'11.61"E
	MOC6	F	43°32'35.56"N	11°33'43.49"E

Table 1. GPS points and labels for the collected samples.

3. Materials and methods

In order to provide a complete spectrum for abundance and the distribution of microplastics accumulated in different conditions, sediments samples were picked up in different settings:

Samples T: deposits accumulated at the depositional interface under dominant tractional conditions during the flood. They mainly consist of sand with plane-parallel or ripple-cross laminations.

Samples S: sandy to muddy deposits accumulated during brief episodes of standing level during the overall waning phase of the flood. Temporary standing of water level was easily detected by continuous laterally – continuous accumulation of plant-debris.

Samples M: fine sand to mud accumulated at the latest stage of the flood in standing to slowly – moving water.

Samples F: mud to very-fine sand associated with floating vegetation debris that was plastered on the channel banks or bar-top zones during the highest flood water levels.

Samples were collected and stored using plastic-free instruments (e. g. aluminium foils) to avoid any kind of external contamination.

3. Materials and methods

3.2 Microplastics extraction

Microplastics extraction required a gravimetric separation process (*figure 3.3*).
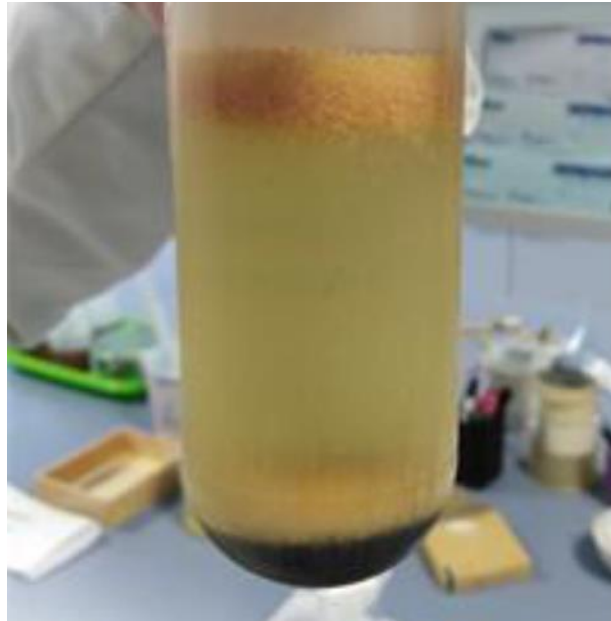
Figure 3.3. Example of a gravimetric separation on a synthetic sample. The particulate material (lighter than the heavy fluid) floats, while the heavier sediment sinks. From Bonotto, 2021.

For each sample, 25g of material (where possible) was placed into a centrifuge tube, where a heavy liquid, sodium polytungstate ($\rho = 3 \ g \cdot cm^{-3}$) diluted with distilled water to $\rho = 1.6 \ g \cdot cm^{-3}$ was added to separate the microplastics from heavier materials. The decision to use a liquid diluted to $\rho = 1.6 \ g \cdot cm^{-3}$ was due to the fact that previous analyses have shown an extraction yield of 97% (Bonotto, 2021).

3. Materials and methods

The samples were then centrifuged at $2000 \ RMP$ for $20 \ mins$ (*figure 3.4*). Once the samples have been centrifuged and left to rest, the suspended particulate matter, lighter than the liquid used in the process and containing microplastics, was collected with a pipette and gently transferred to two different filters with $0.1 \ \mu m$ pores: cellulose acetate for the P samples collected and glass microfibre for the G and MOC samples.

Figure 3.4. Centrifuge machine used to enhance the separation process.

Organic matter rich samples had a previous preparation with the Wet Peroxide Oxidation (WPO) technique, as suggested in (Masura et al., 2015). The WPO technique allow one to remove the organic matter present in the sample. The $0.3 \ mm$ fraction of sampled material was placed in a beaker with $20 \ mL$ of aqueous $0.05 M Fe(II)$ solution, as catalyst for the reaction, and $20 \ mL$ of 30% hydrogen peroxide, to oxidise the organic

matter present. The reaction started by stirring the solution inside the beaker, then, to prevent the reaction from reaching too high a temperature and degrading the microplastics, it was slowed down by placing the beaker in a cold bath. This procedure was repeated until all the natural organic material was not visible anymore.

Once the organic matter was eliminated and the samples were separated, the filters with microplastics rested for a night in an oven at a temperature of 55°C.

3.3   Grain size analysis

Grain size analysis required a mechanical sieving, using a stack of sieves with decrescent diameter of $2\ mm$, $1\ mm$, $500\ \mu m$, $250\ \mu m$, $125\ \mu m$ and $63\ \mu m$ (*figure 3.5*).

Figure 3.5. Vibrating plate used for the mechanical sieving.

3. Materials and methods

For each sample, 50 grams of sediment were put in the stack of sieves, one at the time, the stack was closed with a lid and then placed in a vibrating plate for ten minutes. After the sieving, the sediment retained in each sieve, including the one at the bottom, was weighed, in order to have all the information to build the granulometric distribution per each sample.

At the end of every measurement, the sieves were thoroughly cleaned to avoid any contamination between the samples.

For the fine sediment samples analysis (P11 to P15), an instrumental particle size analysis was carried out. These samples ($0.5\ cm^3$) were diluted in deionised water to obtain a suspension of the dispersed material and then analysed with a Mastersizer 2000 (Version 5.40, MALVERINE INSTRUMENTS) (Bonotto, 2021).

3.4   Microplastics analysis

The detection of microplastics required the use of a stereo microscope, equipped with a camera to obtain pictures of the microplastic items with the use of *Deltapix* software. The calibrations for the $3.2\ X$, $5\ X$, $8\ X$, and $11\ X$ magnifications were done with a $3000\ \mu m$ calibration slide.

The analyses have followed a standardized protocol for monitoring microplastics in sediments proposed by Frias et al. (2018), compiling a card per each sample (*figure 3.6*),

Figure 3.6. Filter observation datasheet provided by BASEMAN, from Frias et al., 2018.

3. Materials and methods

by briefly describing each item according to shape (e. g. fibres, fragments, films, microbeads, pellets), colour (e. g. transparent, white, red) and position. This allows one the quantification and determination of the microplastics present.

In few samples, the major limitation was represented by abundance of plant debris, which made microplastic difficult to be detected. In these cases, the use of a hot needle has proved to be very helpful as the plastic material reacts to heat, while the organic matter does not. Ultraviolet light has turned out to be a useful tool in detecting microplastics, as some of them react to the UV and assume a blue-violet colour (*figure 3.7*).
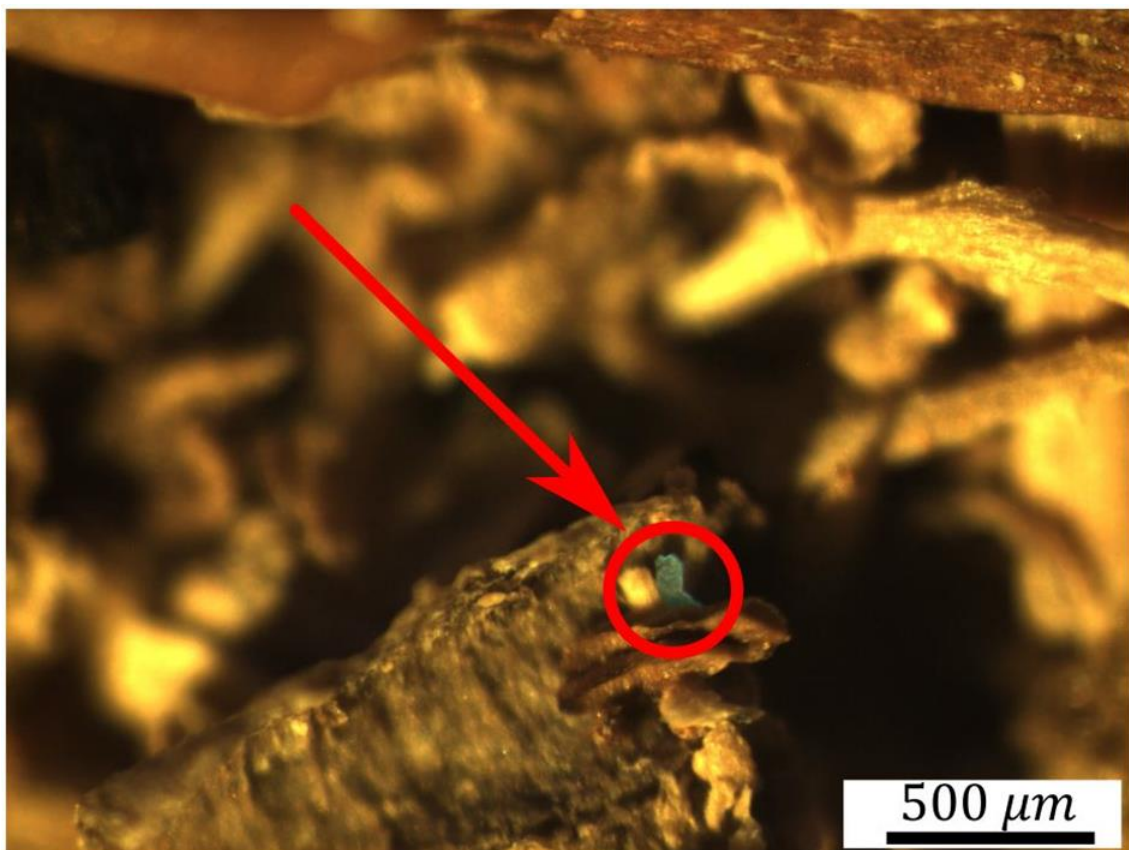
Figure 3.7. Microplastic film hidden in vegetational debris. Thanks to the reaction with UV light, identification was possible.

4   Results

Results concerning amount of microplastics and grainsize for each sample are presented in this section by keeping group of samples as related to bars where they were picked up.

4.1   Bar 1

In this bar, located on the hydrographic left of the channel (see *figure 3.1*), 6 samples were collected (*figure 4.1*).

Figure 4.1. Bar 1, containing MOC12 - MOC17 samples

Two couples of samples (MOC12-13 and MOC14-15) were collected in a sandy avalanching front at different depth to better evaluate the deposition of microplastics under tractional conditions and settling.

The last two samples (MOC16 and MOC17) come from the floating vegetational debris deposited on both sides of the bar.

4. Results

The results are summarized in table 2.

Henceforth, for sake of simplicity, microplastics could be indicated with the acronym MPs. The T, S, F, and M abbreviations, refer to the type of deposit that samples represent as indicated in paragraph 3.1. Respectively: sediments deposited under tractive conditions, sediments deposited by settling, floating vegetational debris, and standing water markers. The F samples do not have the D_{50} as they represent vegetational debris and not sediment.

Sample	TYPE	$D_{50}(mm)$	Wentworth class	Material analysed	Items	Concentration (MPs/g)
MOC12	S	0,323	Medium sand	25 g	29	1,16
MOC13	T	0,319	Medium sand	25 g	11	0,44
MOC14	S	0,181	Fine sand	25 g	24	0,96
MOC15	T	0,363	Medium sand	25 g	22	0,88
MOC16	F	null	null	3,6 g	24	6,67
MOC17	F	null	null	8 g	22	2,75

Table 2. Results of Bar 1 samples

4. Results

4.1.1 MOC12 – MOC13

This couple of samples comes from a sandy avalanching front sites in the bar tail (*figure 4.2*), collected at different depths.

Figure 4.2. Sandy avalanching front where MOC12-MOC13 samples were collected.

MOC 13

MOC13 represents the sediment deposited under tractional conditions. The sample is composed by clean sand in which 11 microplastic items were counted during the microscopic analysis. Figures 4.3 and 4.4 show forms and abundance of microplastics within the sample.
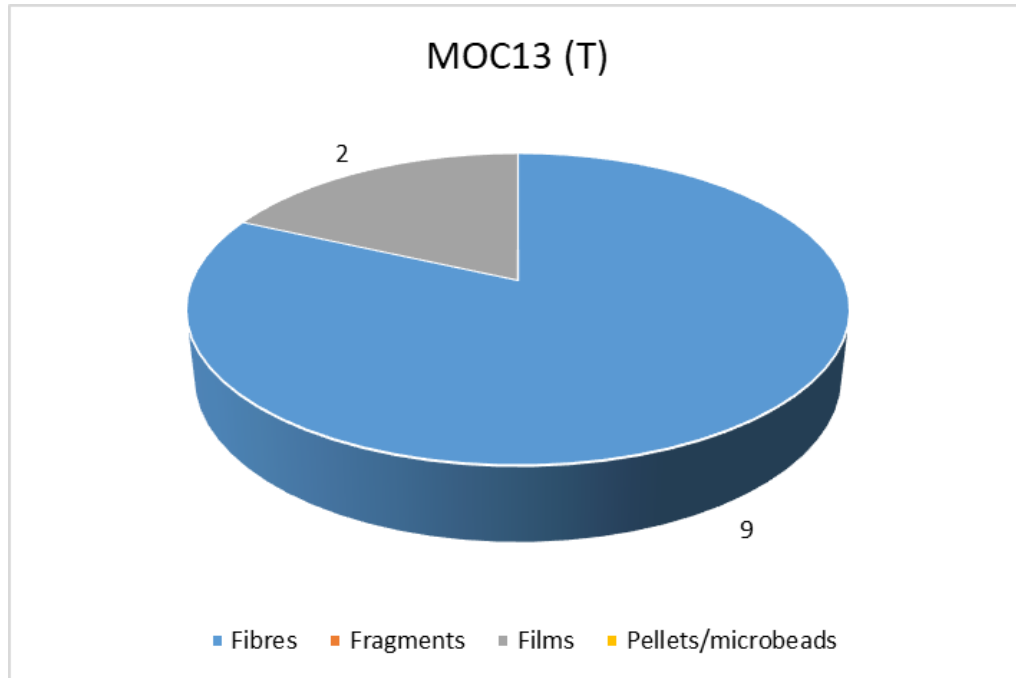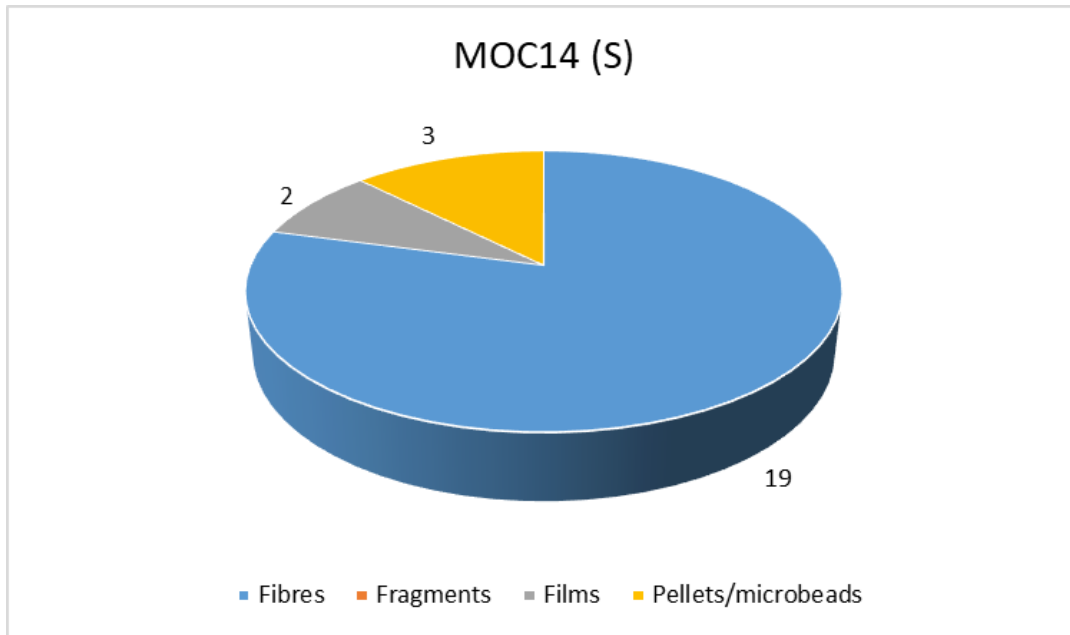
4. Results

*Figure 4.3. Forms and abundance of microplastics in MOC13.*

Figure 4.4. Pictures of microplastics found in MOC13. 1. Blue fibre; 2. Transparent fibre; 3. Transparent film.

4. Results

MOC12

The sediment covering the MOC13 sample, deposited for settling during the latest waning phase, is represented by the MOC12 sample. The microscopic analysis permitted to identify 29 microplastic items. Figures 4.5 and 4.6 show forms and abundance of microplastics within the sample
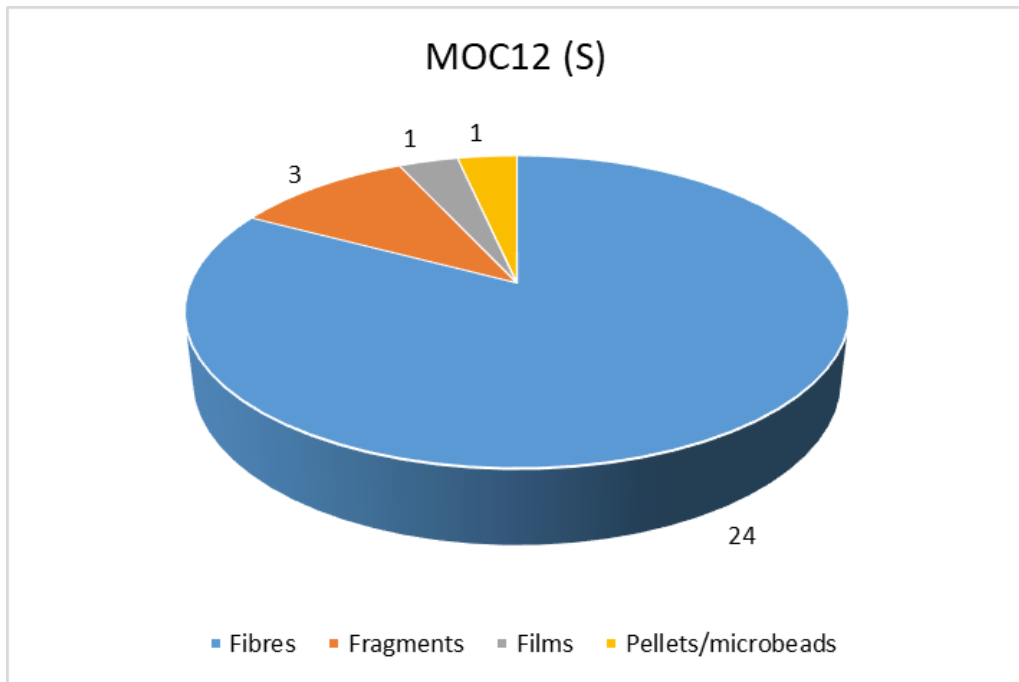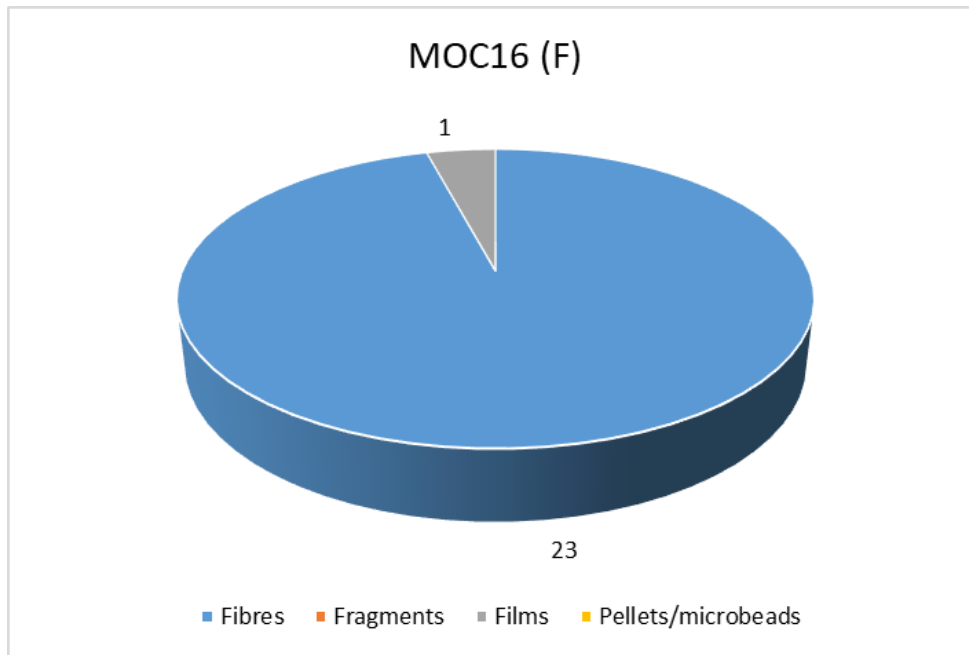

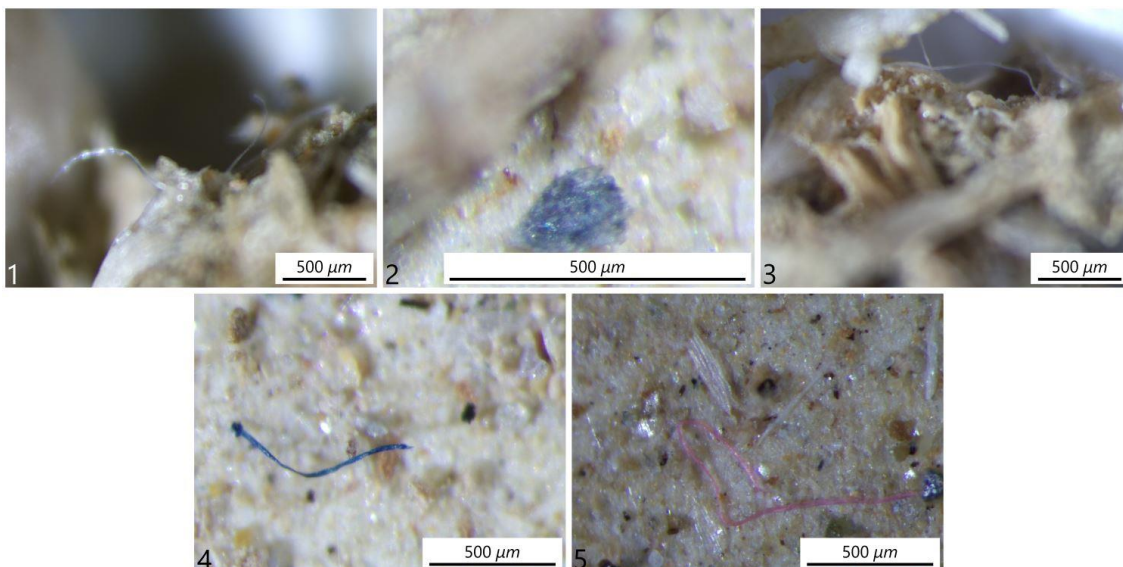
Figure 4.5. Forms and abundance of microplastics in MOC12.
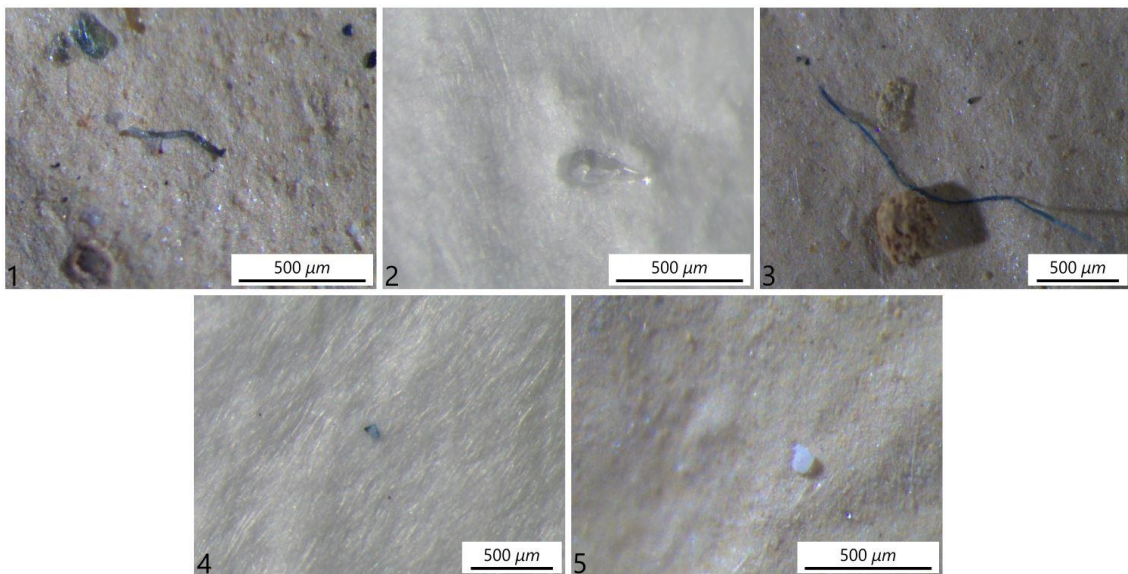
Figure 4.6. Pictures of microplastics found in MOC12. 1. Blue fibre; 2. Transparent microbead; 3. Blue fibre; 4. Blue fragment; 5. Transparent fragment.

4. Results

4.1.2 MOC14 – MOC15

This couple of samples comes from the same avalanching front, but from a site placed more toward the tail of the bar in respect to MOC12 and MOC13 (*figure* 4.7).

Figure 4.7. Sandy avalanching front with evidence of standing water periods during the waning phase.

4. Results

MOC15

MOC15 represents the sediments deposited under tractive conditions. The sample is composed by clean sand, and contains 22 microplastic items, all belonging to the microfibre class (*figures 4.8* and *4.9*).
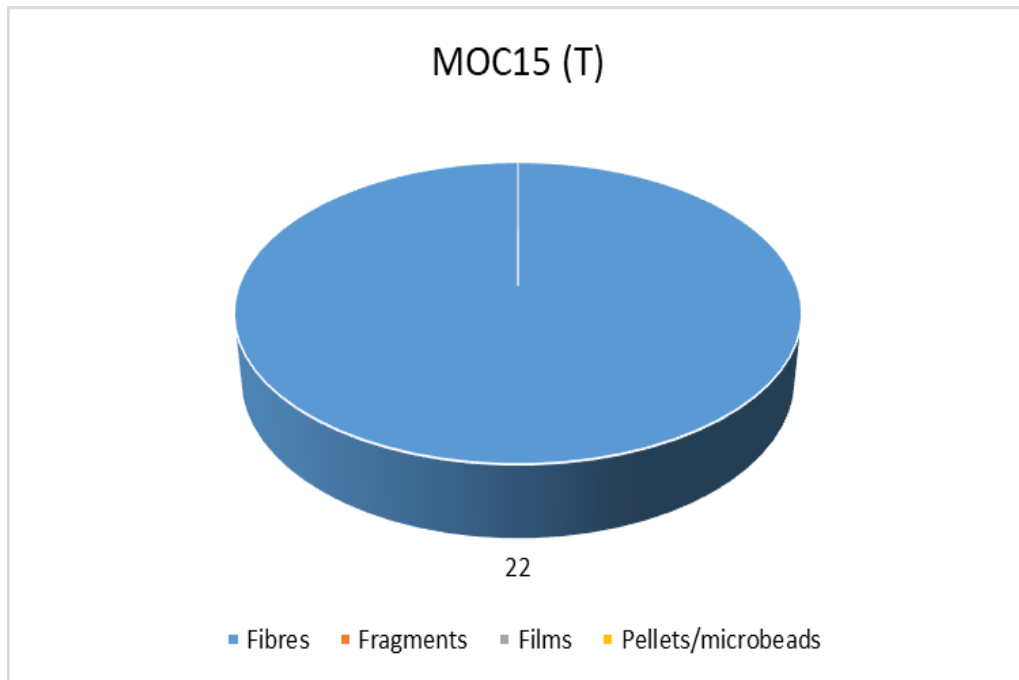
Figure 4.8. Microplastics found in MOC15.
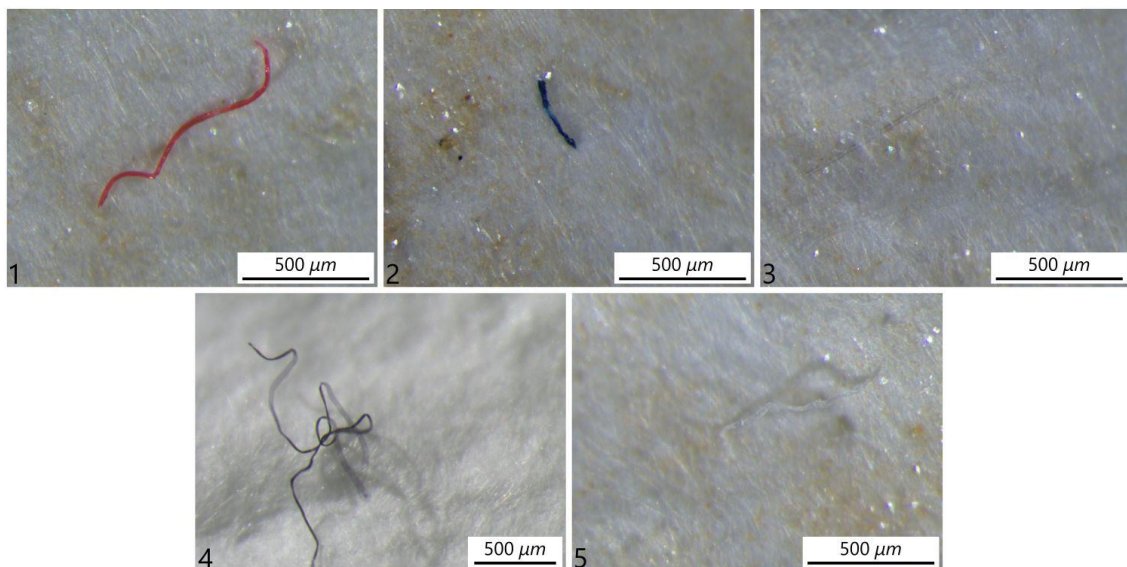
Figure 4.9. Picture of microfibres found in MOC15. 1. Red fibre; 2. Blue fibre; 3. Transparent fibre; 4. Black fibre; 5; White fibre.

4. Results

MOC 14

The sediment deposited for settling at the top of the avalanching front during the waning phase, and covering the MOC15 sample, is represented by the MOC14 sample. The microscopic analysis led to the identification of 24 microplastic items. Figures 4.10 and 4.11 show forms and abundance of microplastics within the sample.

Figure 4.10. Forms and abundance of microplastics in MOC14.
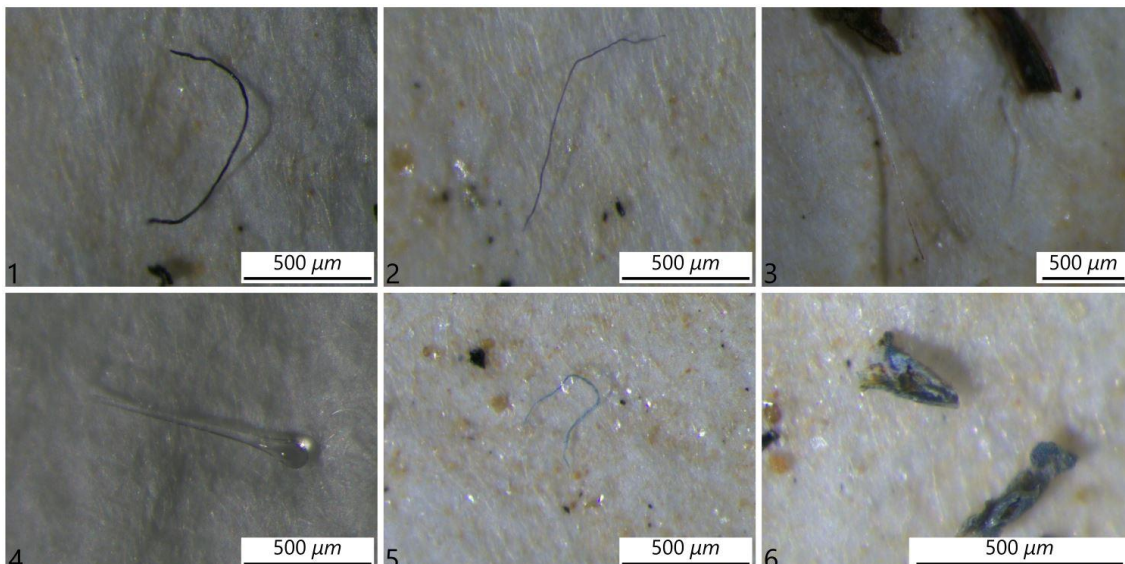
Figure 4.11. Pictures of microplastics found in MOC14. 1. Black fibre; 2. Blue fibre; 3. Transparent fibre; 4. Transparent fibre; 5. Blue fibre; 6. Blue films.

4.1.3 MOC16 – MOC17

These two samples come from the floating vegetational debris transported during the flood event (*figures 4.12*). Here, microscopic analysis proved more difficult, because the organic matter was so abundant that a large amount of it did not react with WPO (see methods).

Figure 4.12. Example of vegetational debris transported during floods (MOC16).

4. Results

MOC16

This sample was collected in the right side of the bar. The large amount of organic matter made the investigation harder as microplastic fibres were knotted to the roots and broken twigs. 24 microplastic items were identified in the sample. Figures 4.13 and 4.14 show forms and abundance of microplastics within the sample.

Figure 4.13. Forms and abundance of microplastics found in MOC16.

Figure 4.14. Picture of microplastics found in MOC17. 1. Transparent fibre; 2. Blue fragment; 3. Transparent fibre; 4. Blue fibre.

4. Results

MOC17

This sample was collected in the left side of the bar. In here as well, investigation was harder due to the large amount of organic matter present. 23 microfibres were identified in the microscopic analysis. Figures 4.15 and 4.16 show forms and abundance of microplastics within the sample.
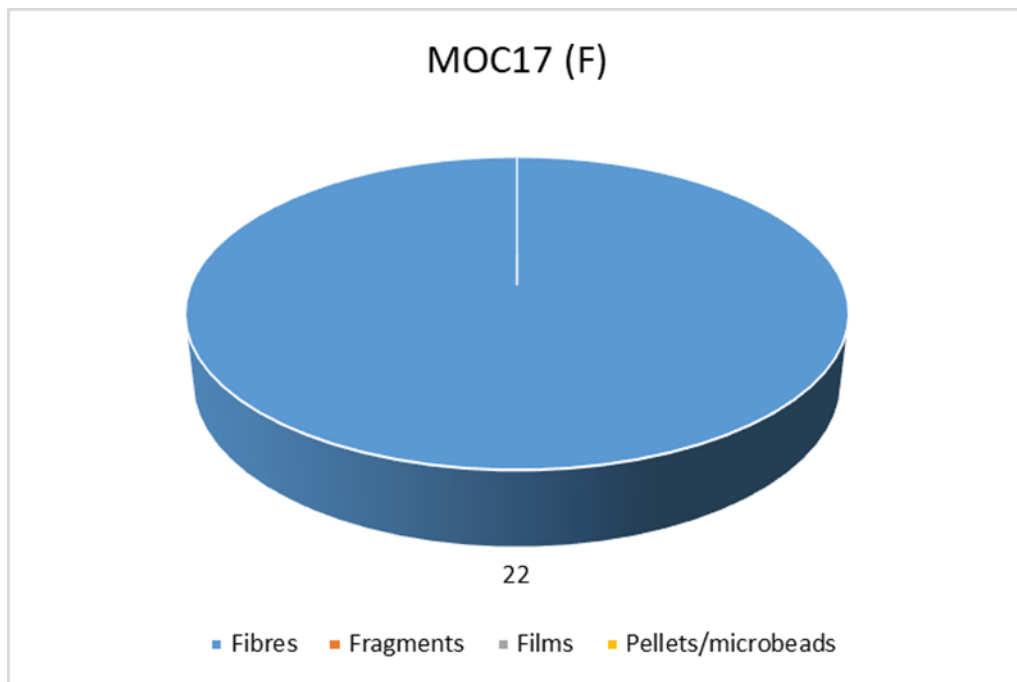
Figure 4.15. Microplastics in MOC17.
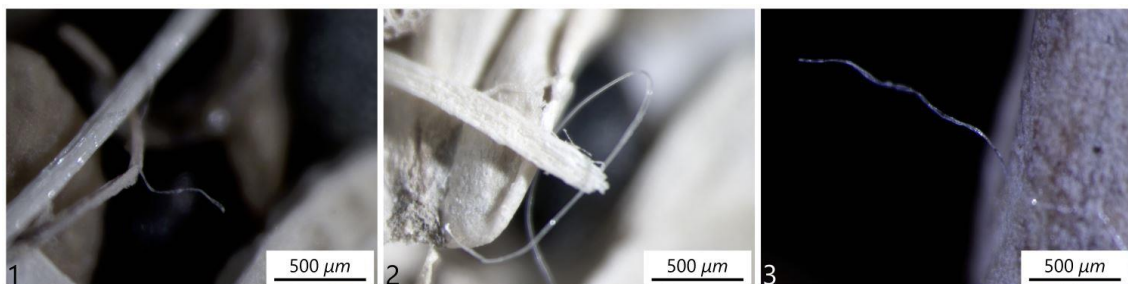
Figure 4.16. Pictures of transparent microfibres found in MOC 17.

4. Results

4.2   Bar 2

Bar2 is located $500\ m$ upstream of Bar1 (see *figure* 3.1), on the hydrographic left of the channel (*figure 4.17*).

Figure 4.17. Bar 2, containing P samples.

This is the most sampled bar in this work and provided a total number of 15 samples. Samples were collected all along the bar, starting from the gravelly avalanching front in the head region, to the sandy tongue in the tail region.

4. Results

The results are summarized in table 3.

Sample	TYPE	$D_{50}(mm)$	Wentworth class	Material analysed	Items	Concentration (MPs/g)
P1	T	0,41	Medium sand	25 g	80	3,2
P2	S	0,22	Fine sand	25 g	142	5,68
P3	S	0,2	Fine sand	25 g	60	2,4
P4	M	0,3	Medium sand	25 g	45	1,8
P5	T	0,31	Medium sand	25 g	61	2,44
P6	S	0,23	Fine sand	25 g	61	2,44
P7	S	0,15	Fine sand	25 g	26	1,04
P8	S	0,4	Medium sand	25 g	69	2,76
P9	T	2,7	Very fine gravel	25 g	40	1,6
P10	S	2	Very fine gravel	25 g	130	5,2
P11	T	0,18	Fine sand	25 g	24	0,96
P12	S	0,11	Very fine sand	25 g	88	3,52
P13	M	0,09	Very fine sand	25 g	56	2,24
P14	M	0,09	Very fine sand	25 g	61	2,44
P15	M	0,11	Very fine sand	25 g	21	0,84

*Table 3. Results of Bar 2 samples. **P** indicates fine matrix within gravels.*

4. Results

4.2.1   P1 – P2

This couple of samples come from a sandy tongue, where the picking occurred at different depth to better evaluate the deposition of microplastics under tractive condition and settling. The sharp change in grain size shown in *figure 4.18* marks the passage from deposition under tractional conditions (characterized by sands in plane parallel stratification) to deposition by settling during waning phase. At the bottom, the evidence of a previous flood event.
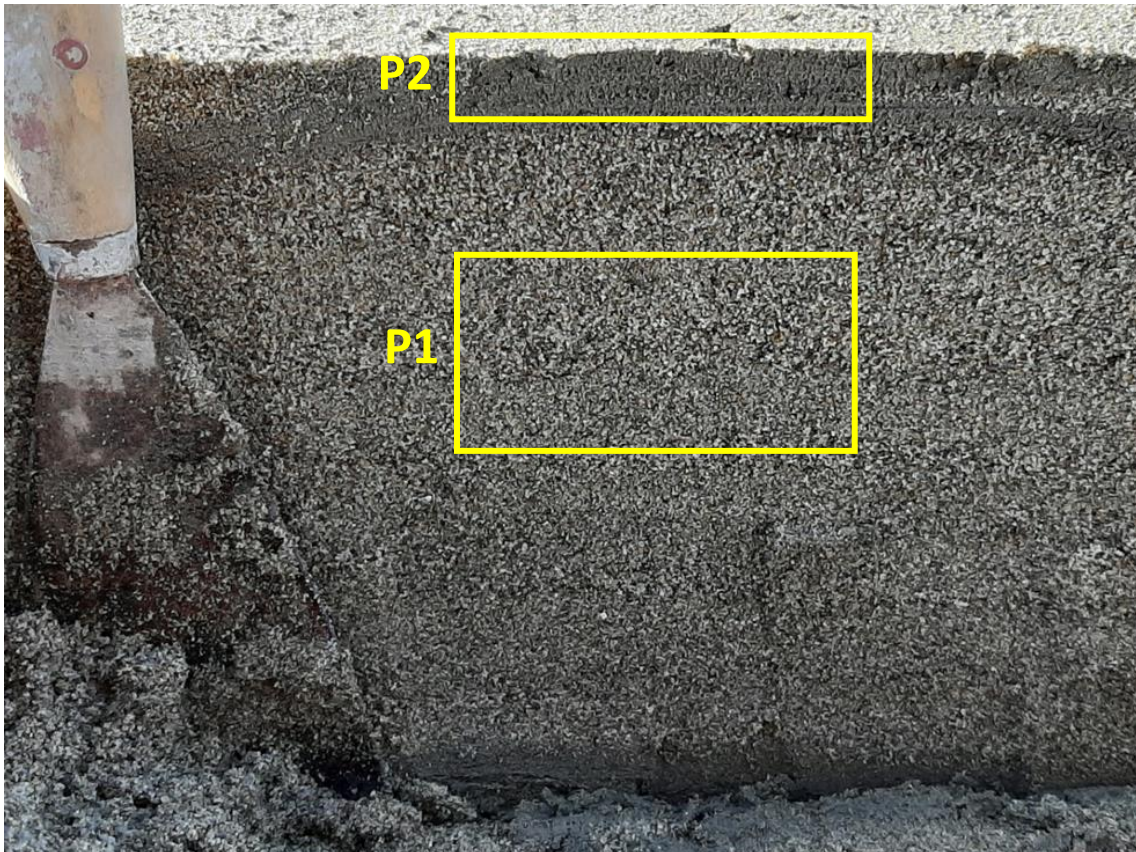
Figure 4.18. P1 – P2. P1 represents the sands in plane parallel stratification and P2 the finer sediment settled above.

4. Results

P1

P1 has deposited in plane parallel stratification under tractional conditions. It is composed by medium clean sand and contains 80 microplastic items. Figures 4.19 and 4.20 show forms and abundance of microplastics within the sample.
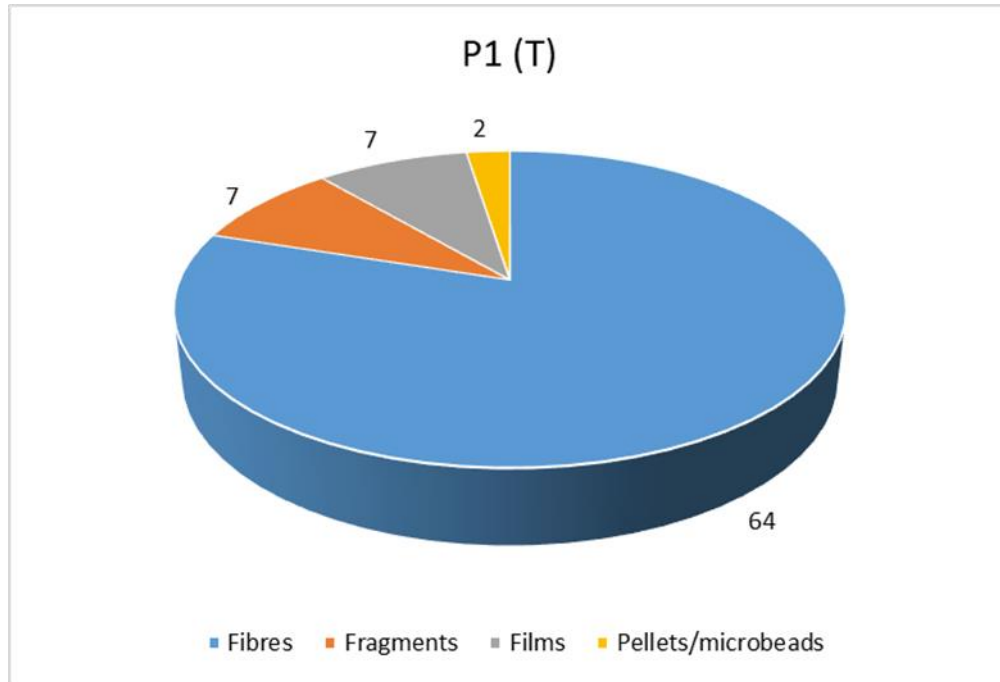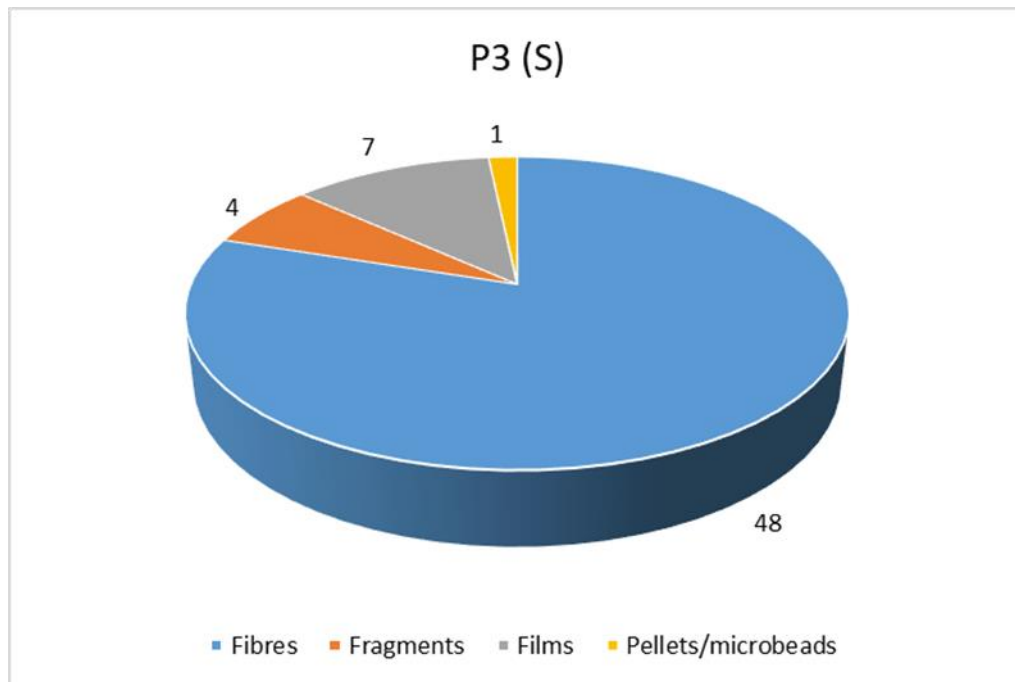

Figure 4.19. Forms and abundance of microplastics in P1.
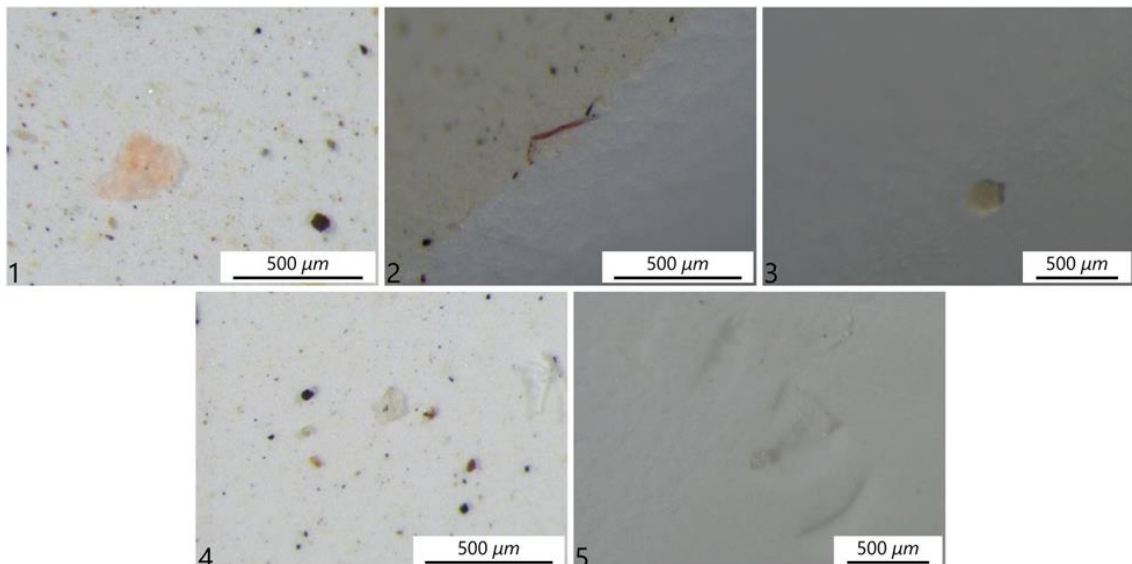
Figure 4.20. Pictures of microplastics found in P1. 1. Pink film; 2. Red fibre; 3. White fragment; 4. Transparent film; 5. Transparent microbead.

4. Results

P2

P2 represents the sediment which deposited for settling and covered P1. It is composed by fine – silty sand and 142 microplastic items were counted. Figures 4.21 and 4.22 show forms and abundance of microplastics within the sample.
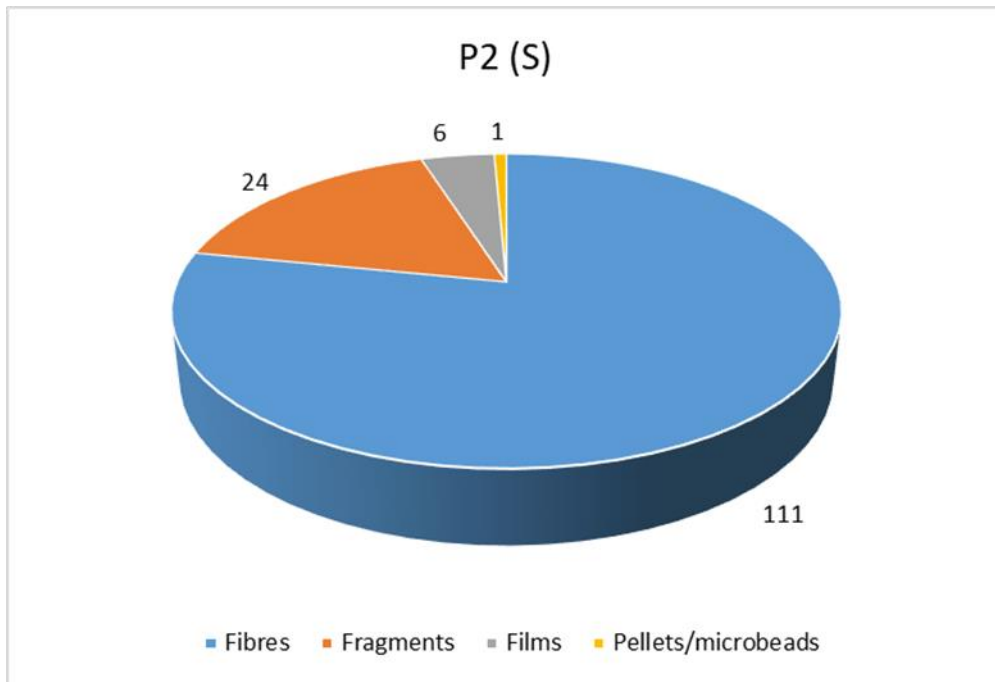
Figure 4.20. Forms and abundance of microplastics in P2.
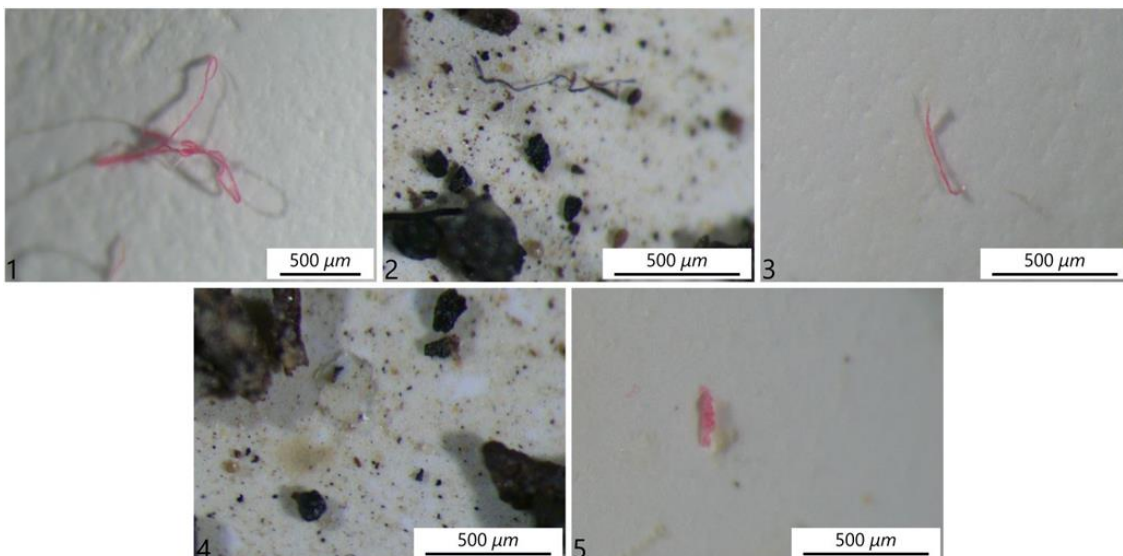
Figure 4.21. Pictures of microplastics found in P2. 1. Red fibre; 2. Blue fibre; 3. Red fibre; 4. Transparent film; 5. Red fragment.

4.2.2 P3

P3 represents a fine sand sediment deposited during the waning phase, near the tip of the tail (*figure* 4.23). Here the microplastic items recognized are 60. Figures 4.24 and 4.25 show forms and abundance of microplastics within the sample.

Figure 4.22. P3. Silty sediments slightly depressed

4. Results

Figure 4.23. Forms and abundances of microplastics in P3.
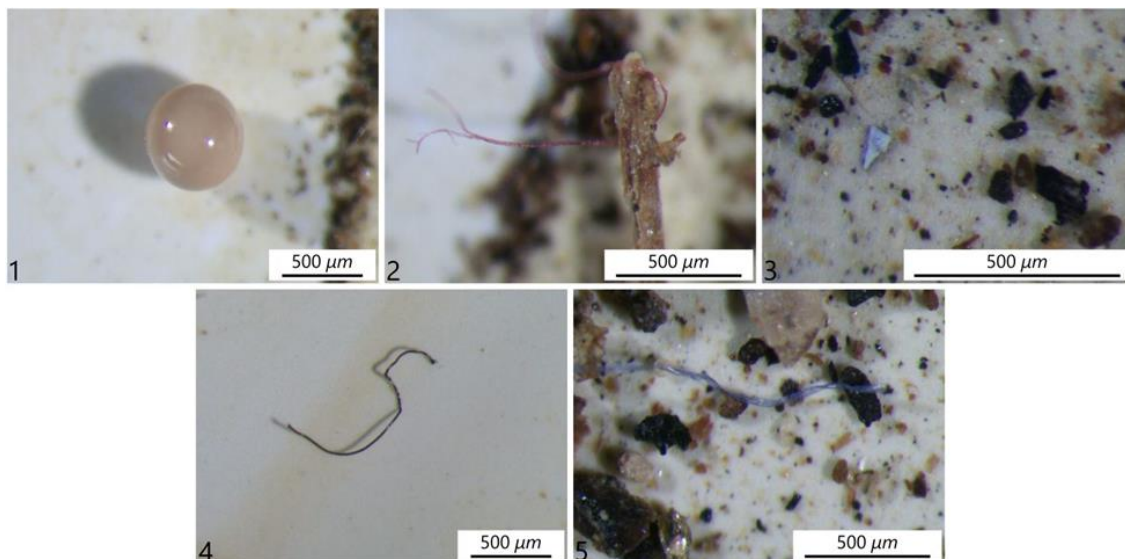
Figure 4.24. Pictures of microplastics found in P3. 1. White pellet; 2. Red fibre; 3. White fragment; 4. Black fibre; 5. Blue fibre.

4.2.3   P4

P4 represents slough water level markers in a sandy tongue (*figure 4.26*). The high abundance of frustules made the WPO unable to completely remove the organic matter, and the residues hampered the analysis, nevertheless, 45 microplastic items were identified. Figures 4.27 and 4.28 show forms and abundance of microplastics within the sample.

Figure 4.25. P4. Slough water levels markers in a sandy tongue.

4. Results
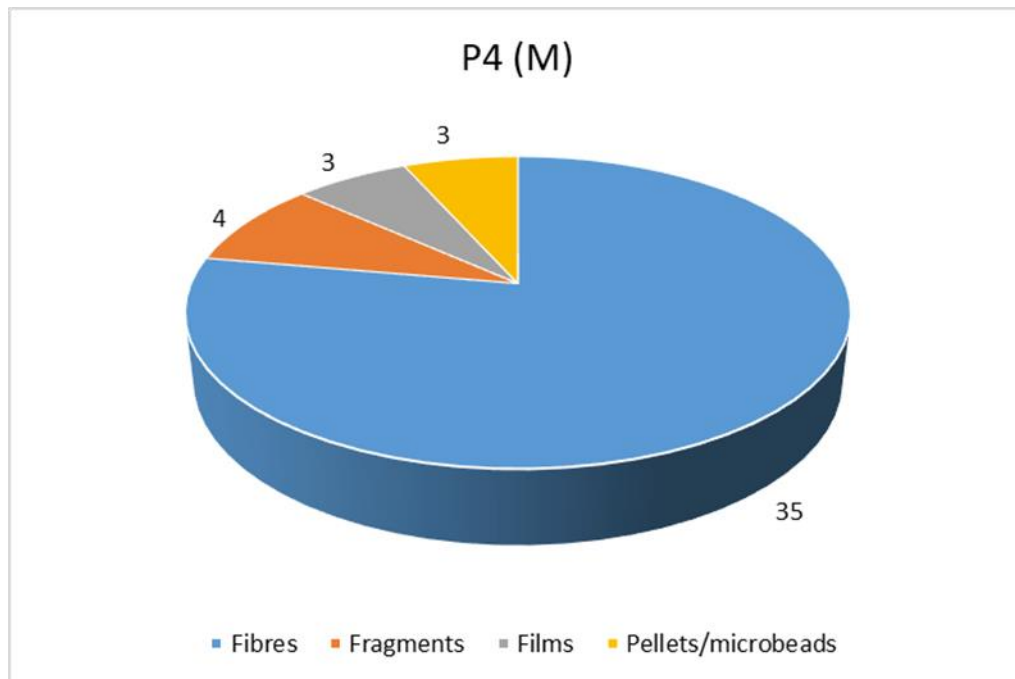
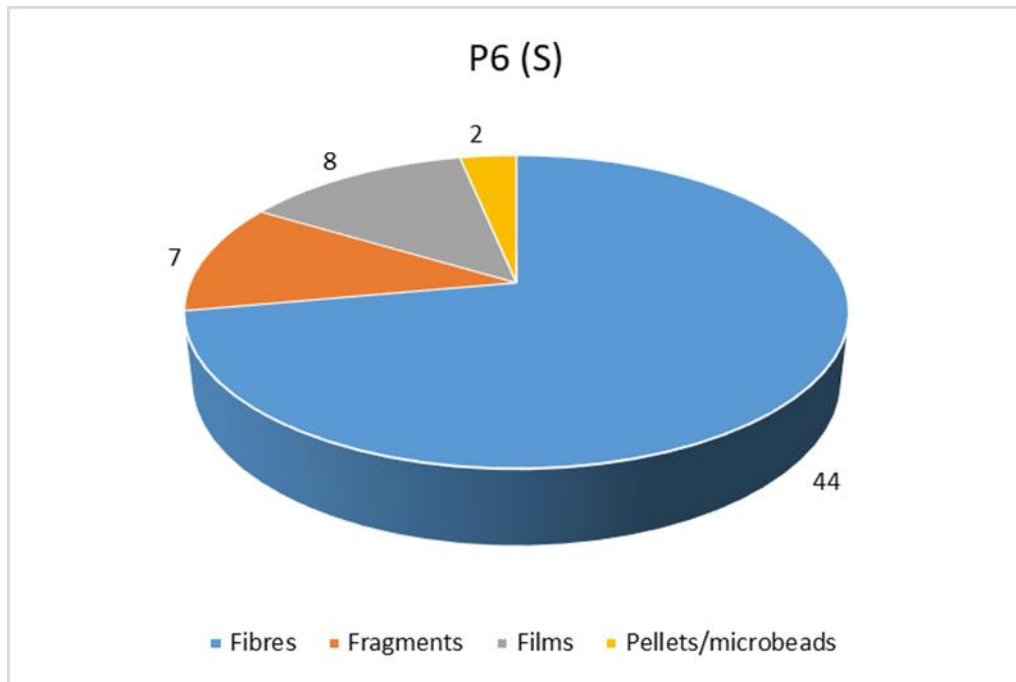*Figure 4.26. Forms and abundance of microplastics in P4.*
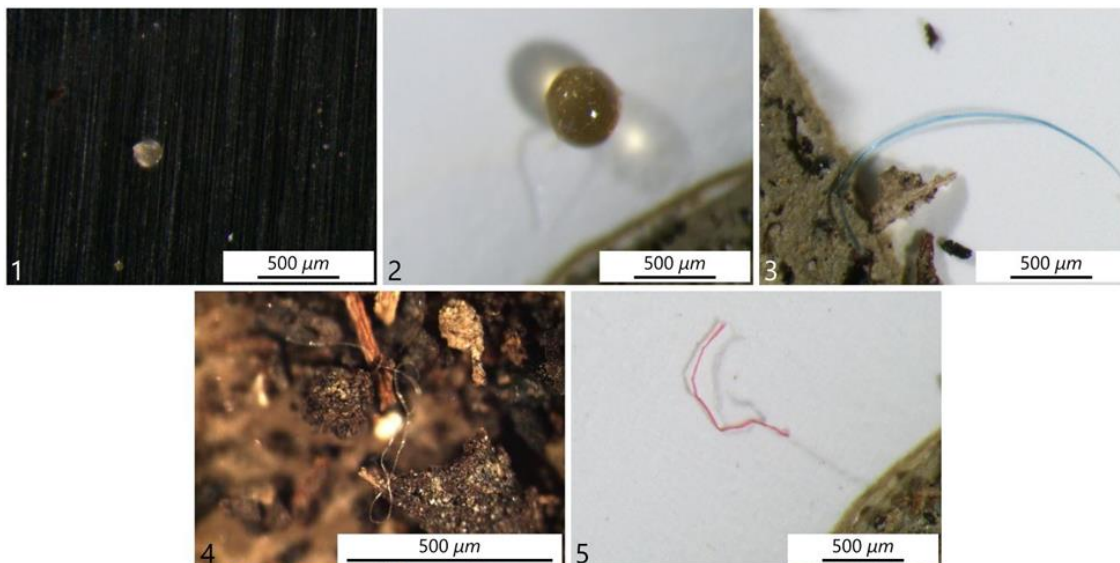
Figure 4.27. Pictures of microplastics found in P4. 1. Transparent microbead; 2. Yellow pellet; 3. Blue fibre; 4. Transparent fibre; 5. Red fibre

4.2.4   P5 – P6

This couple of samples was collected few meters downstream of the gravelly avalanching front of the bar and consists of sandy deposits. The two samples were collected at different depths in order to discern the sediment deposited under tractive condition in plane parallel stratification from the sediment settled above it (*figure 4.29*).

Figure 4.28. P5 – P6. Sands next to the avalanching front in a vegetated area.

4. Results

P5

P5 was collected at $5\,cm$ depth and it is composed by the sand deposited under tractional conditions. 61 microplastics items were counted. Figures 4.30 and 4.31 show forms and abundance of microplastics within the sample.
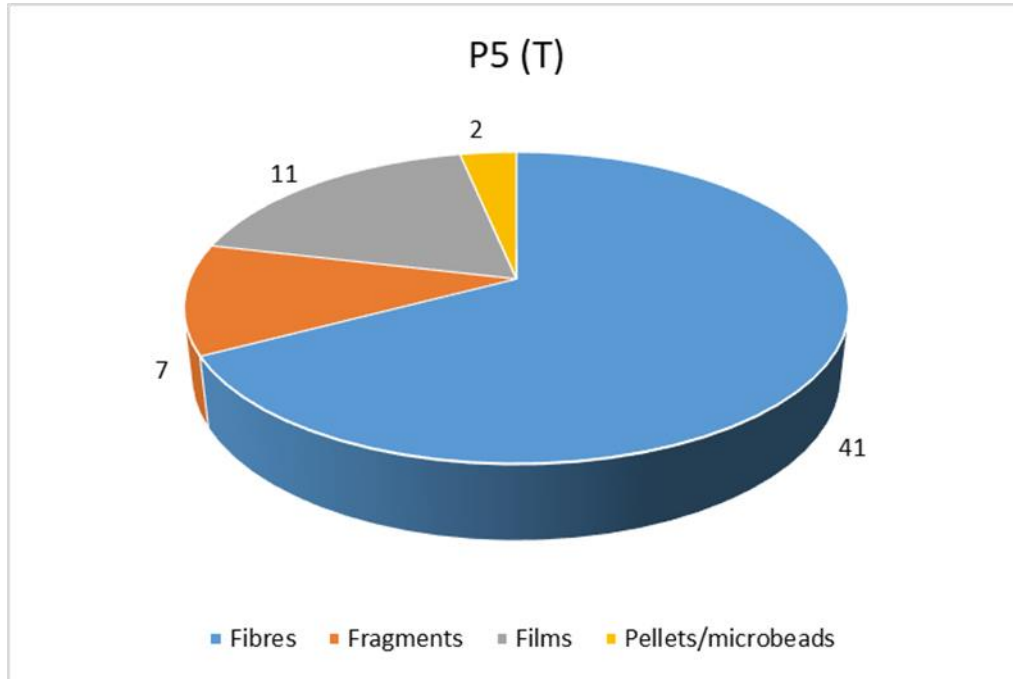


Figure 4.29. Forms and abundance of microplastics in P5.
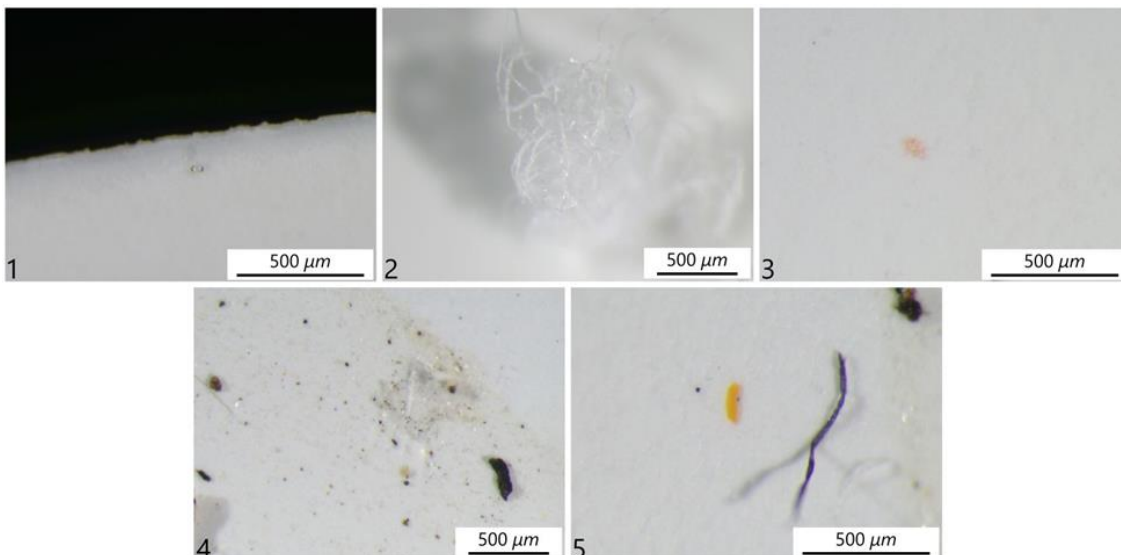
Figure 4.30. Pictures of microplastics found in P5. 1. Transparent microbead; 2. White fibres; 3. Pink fragment; 4. Transparent film; 5. Blue fibre.

4. Results

P6

P6 represents the sediment deposited during the waning phase, composed by fine sand settled above P5. The microscopic analysis led to the identification of 61 microplastic items, with proportions in forms similar to P5. Figures 4.32 and 4.33 show forms and abundance of microplastics within the sample.
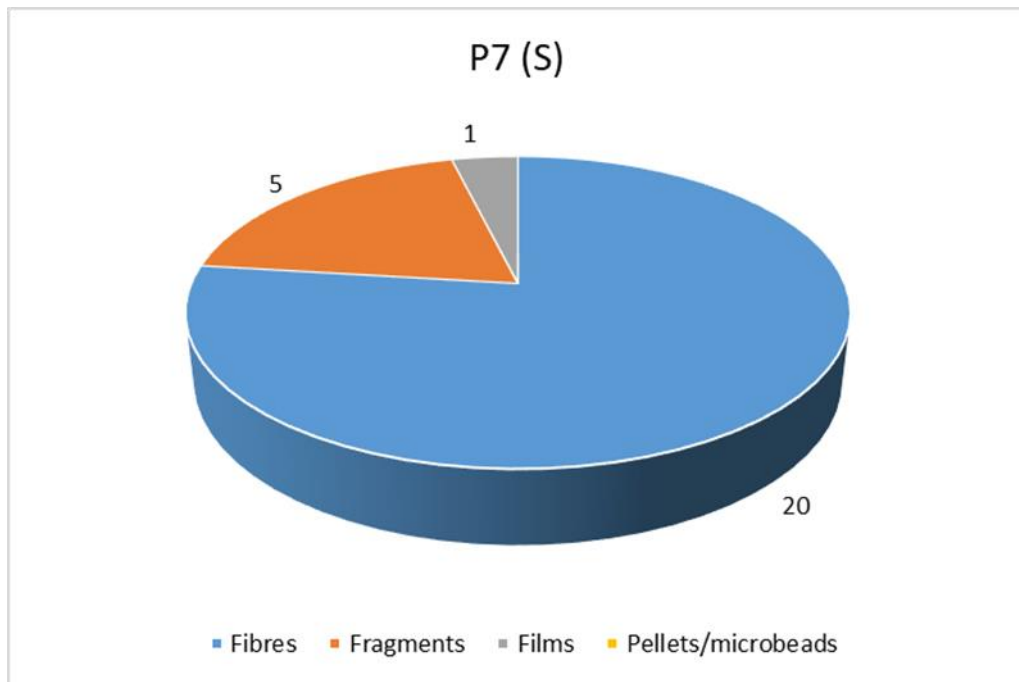

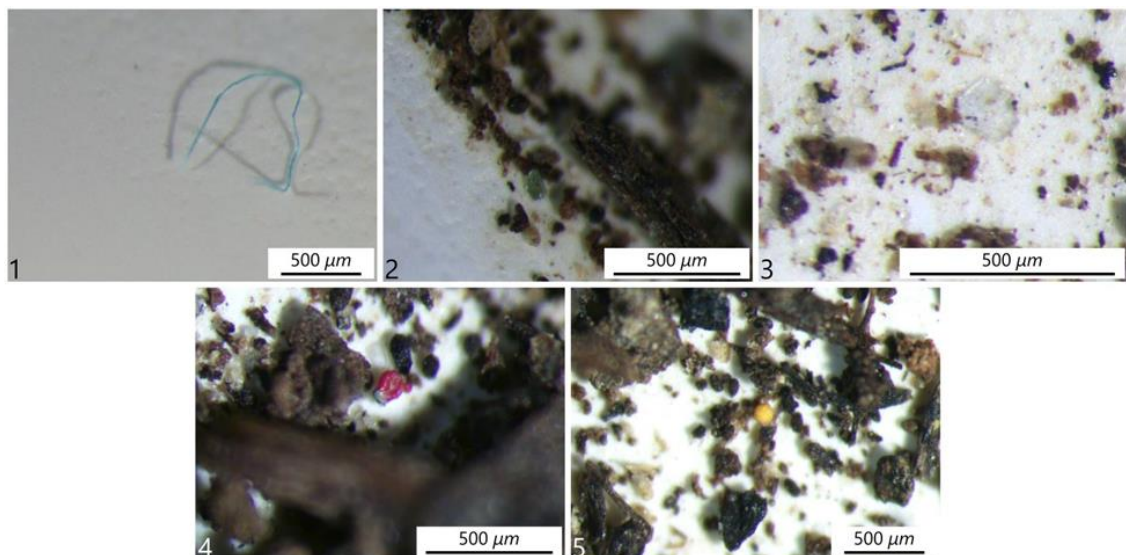
Figure 4.31. Forms and abundances of microplastics in P6.
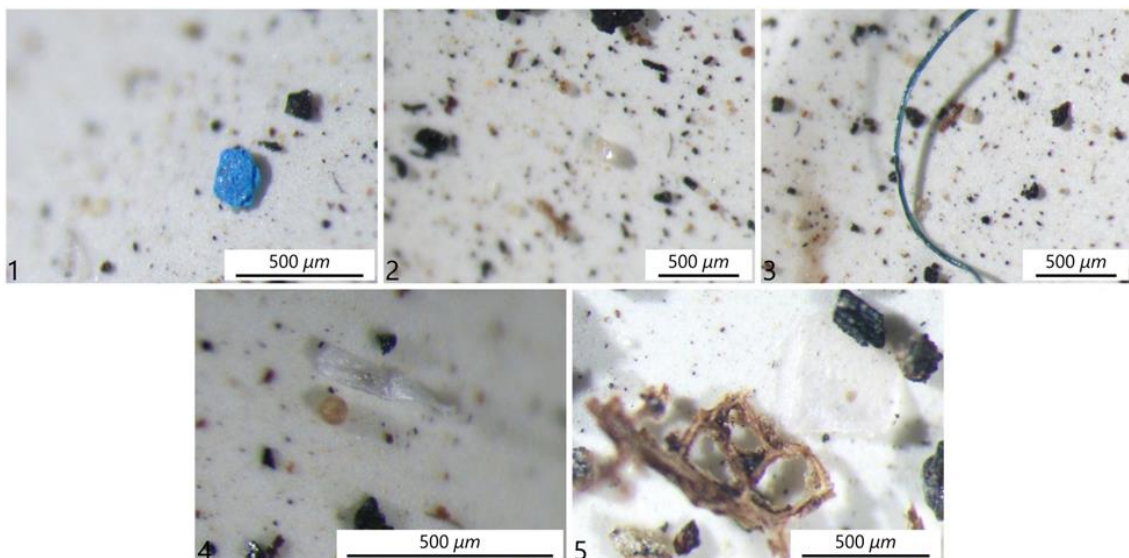
Figure 4.32. Pictures of microplastics found in P6. 1Blue fragment; 2. Transparent microbead; 3. Blue fibre; 4. Transparent fragment; 5. Transparent film

4. Results

4.2.5 P7 – P8

P7 and P8 were collected at the toe of the gravelly avalanching front (*figure 4.17*). They both represent the sediment deposited during the waning phase, rich in frustules (*figure 4.33*).

Figure 4.33. Frustules deposited at the toe of the gravelly avalanching front during the waning phase (P8).

4. Results

P7

In P7, the frustules present did not completely react with the *WPO,* and this made the microscopic analysis harder as they prevented to fully investigate the sample. 26 microplastic items were counted. Figures 4.34 and 4.35 show forms and abundance of microplastics within the sample.
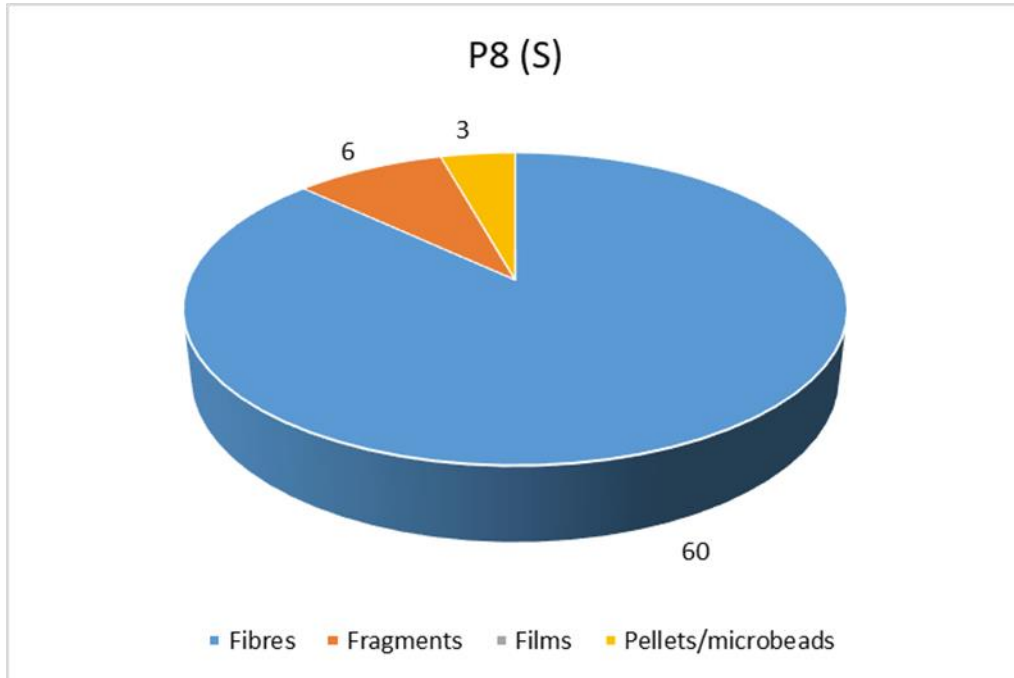

Figure 4.34. Forms and abundance of microplastics in P7.

Figure 4.35. Pictures of microplastics found in P7. 1. Blue fibre; 2. Green fragment; 3. Transparent film; 4. Red fragment; 5. Yellow fragment.

4. Results

P8

The microscopic analysis in P8 led to the identification of 69 microplastic items. Figures 4.36 and 4.37 show forms and abundance of microplastics within the sample.

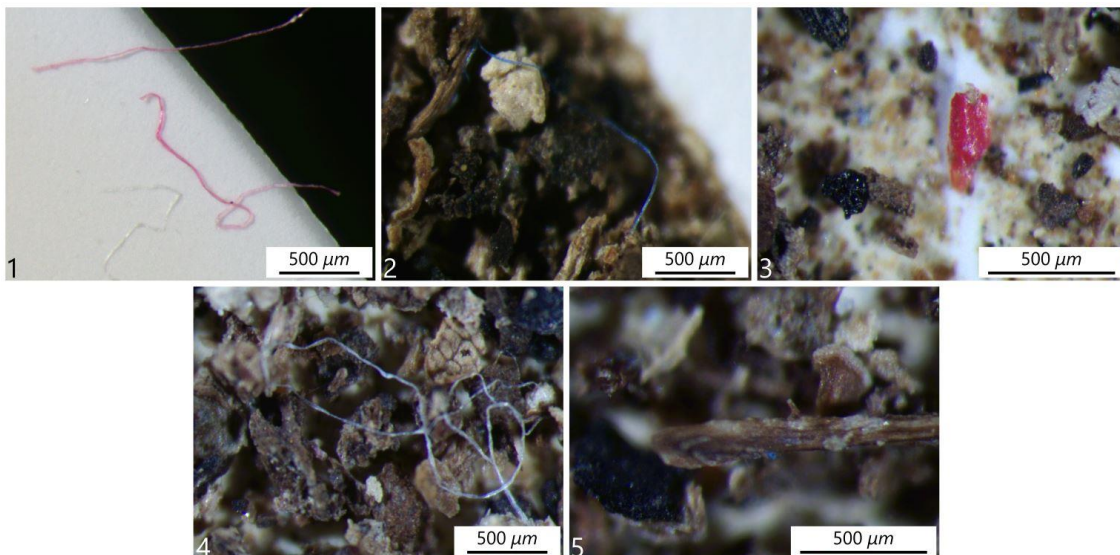*Figure 4.36. Forms and abundances of microplastics in P8*

Figure 4.37. Pictures of microplastics found in P8. 1; Red fibres; 2. Blue fibre; 3. Red fragment; 4. Transparent fibre; 5. Blue fragment.

4. Results

4.2.6 P9 – P10

This couple of samples was collected in the gravelly avalanching front of the bar (see *figure 4.33* to observe part of the sampled avalanching front).

The sediment deposited under tractional conditions, with high water flows, is represented by the sandy-gravelly matrix found between the pebbles while the sediment deposited during the waning phase consists in matrix infiltrated in shadow zones under gravels (*figure 4.38*).
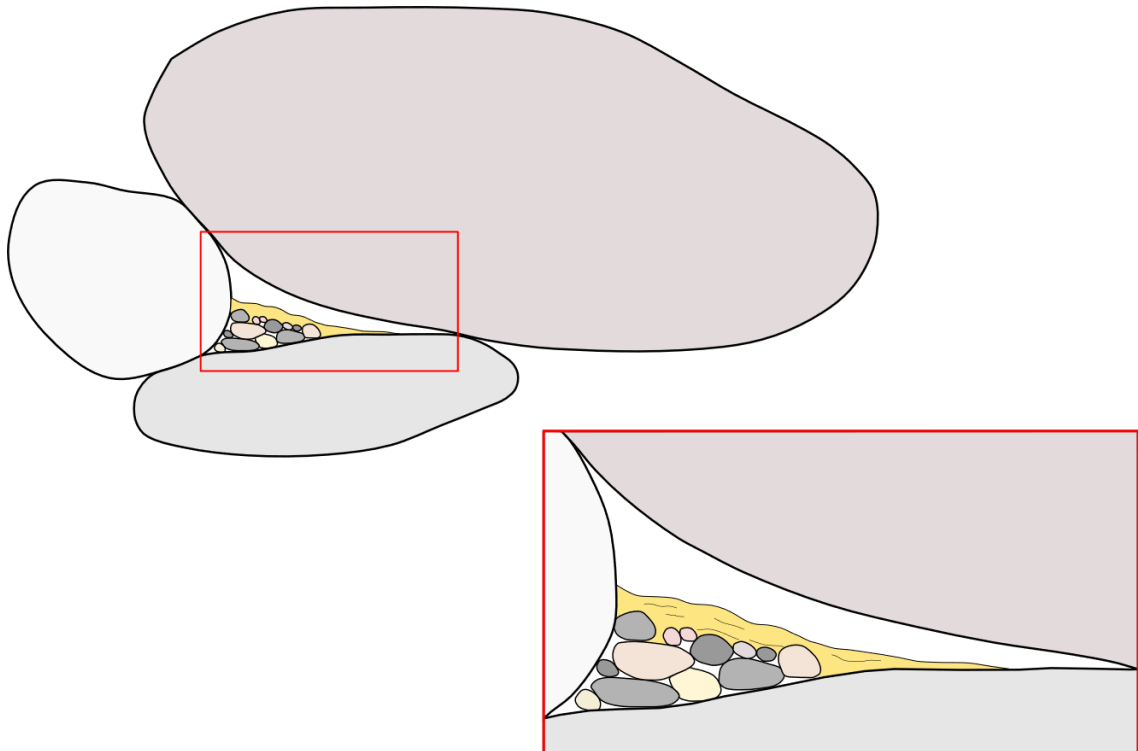
Figure 4.38. Very fine sand infiltrated within gravels and pebbles. The sampled portion (yellow) is minimum compared to the volume of the available space between the large clasts (mainly occupied by air).

4. Results

P9

P9 represents the sediment deposited under sustained water flows between the coarser grains, collected at $15\ cm$ below the surface. It contains 40 microplastic items. Figures 4.39 and 4.40 show forms and abundance of microplastics within the sample.
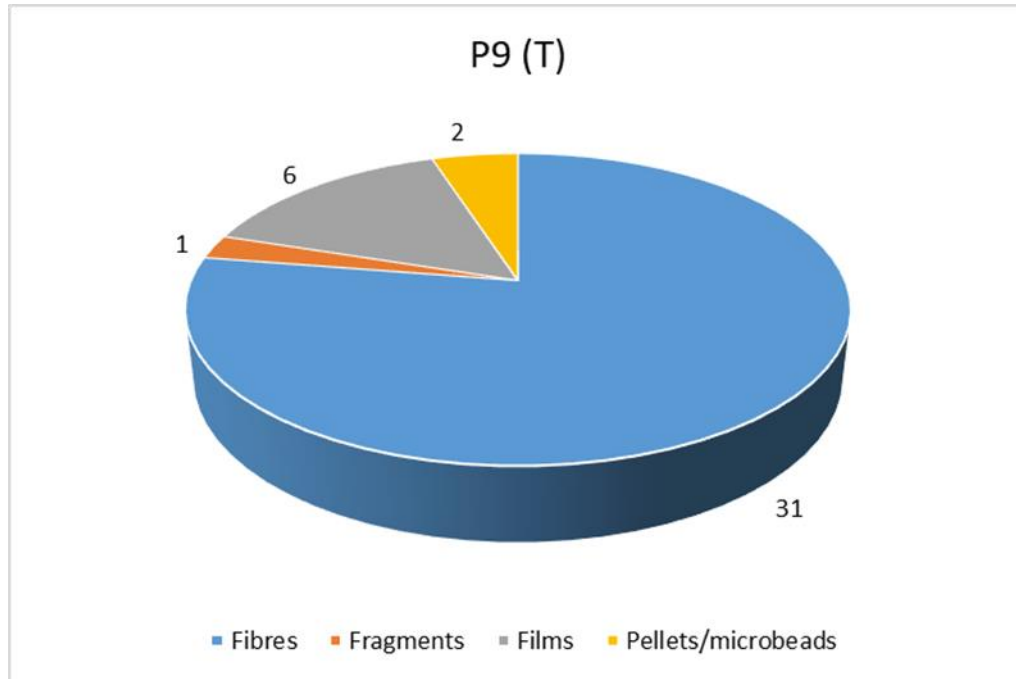

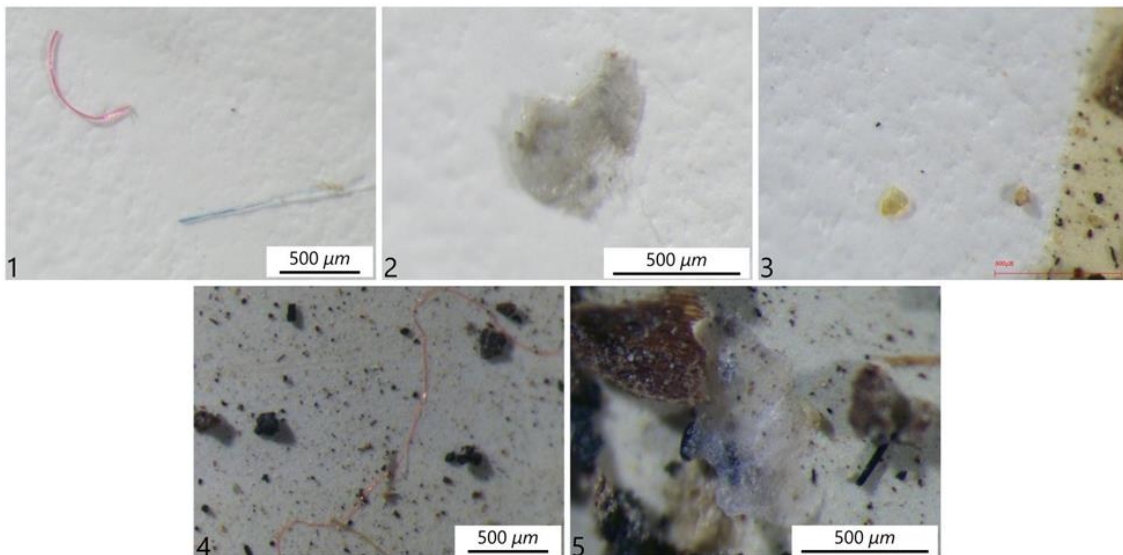*Figure 4.39. Forms and abundance of microplastics in P9*

Figure 4.40. Pictures of microplastics found in P9. 1. Blue and red fibres; 2 Transparent film; 3. Yellow fragment; 4. Red fibre; 5. Transparent film.

4. Results

P10

P10 represents the sediment deposited in the topset of the avalanching front during the waning phase, in the shadow zones under gravels. The microscopic analysis led to the identification of 130 microplastic items. Figures 4.41 and 4.42 show forms and abundance of microplastics within the sample.
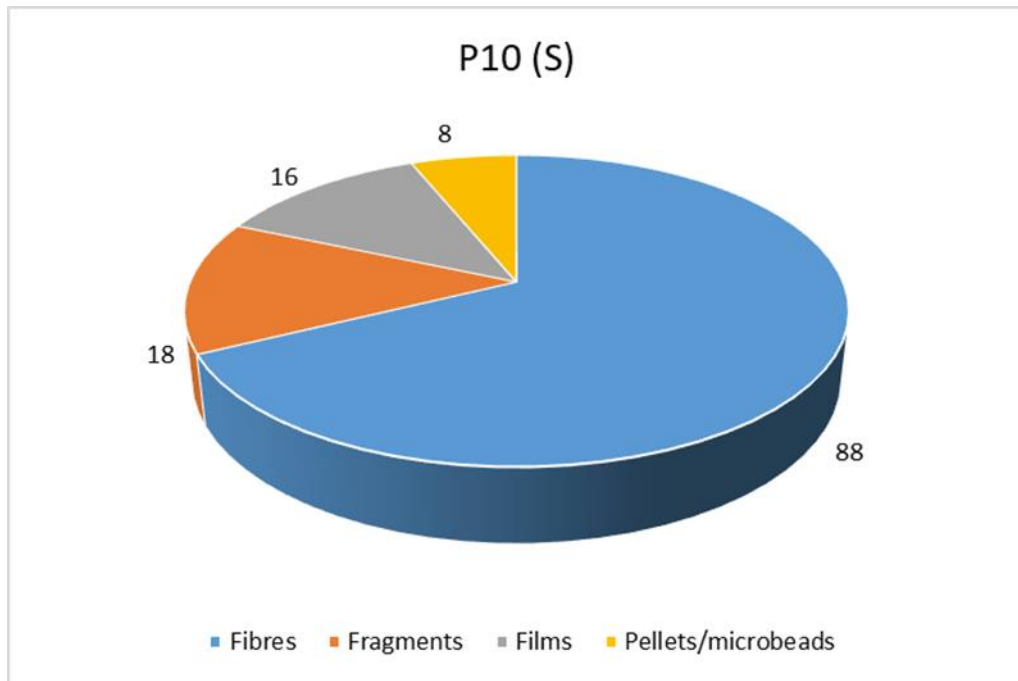

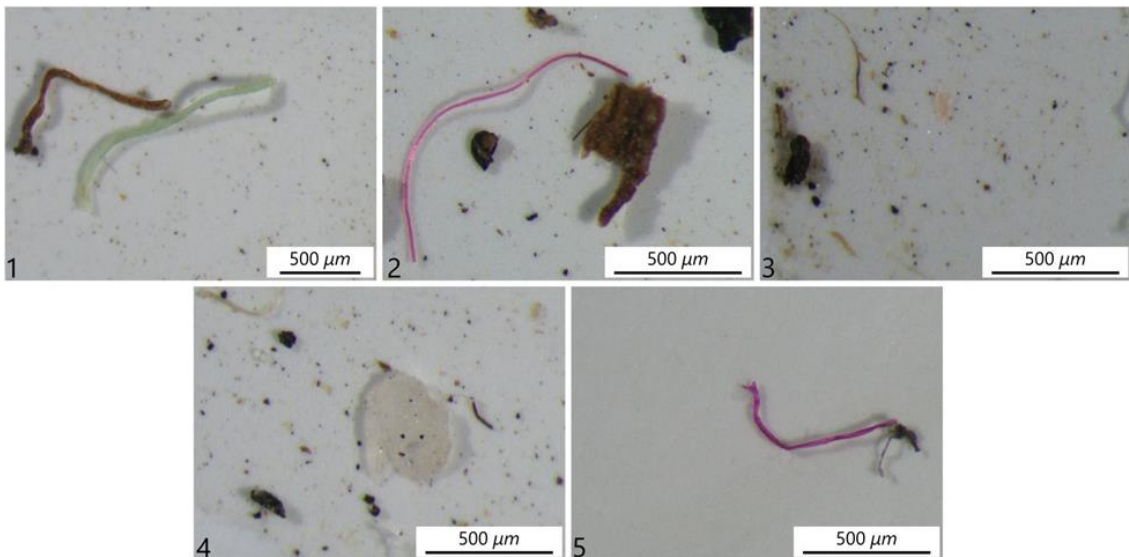*Figure 4.41. Forms and abundance of microplastics in P10.*

Figure 4.42. Picture of microplastics found in P10. 1. Green fibre; 2. Red fibre; 3. Pink fragment; 4 Transparent fragment; 5. Violet fibre.

4.2.7   P11 – P12

This couple of samples represent a similar situation to P9 – P10. They come from the gravelly avalanching front and represent the matrix between the gravels deposited during different flood stages (*figure 4.43*).

Figure 4.43. Muddy to sandy matrix infiltrated between gravels and pebbles.

4. Results

P11

P11 represents the matrix deposited between coarser clasts under sustained water flows, collected at $10\ cm$ depth. It contains 24 microplastics items. Figures 4.44 and 4.45 show forms and abundance of microplastics within the sample.
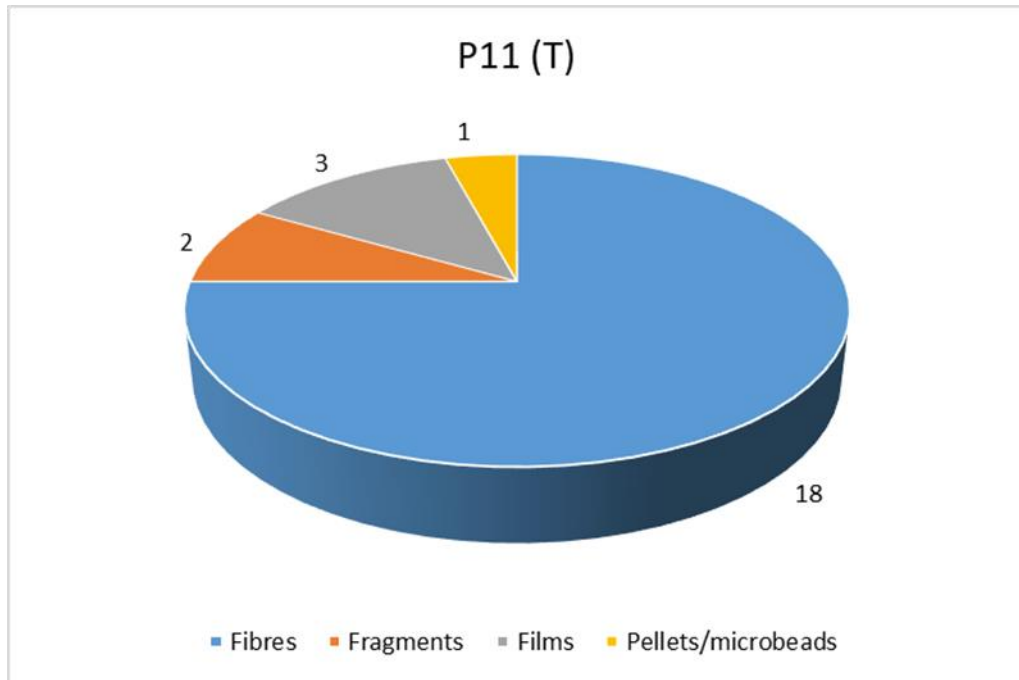

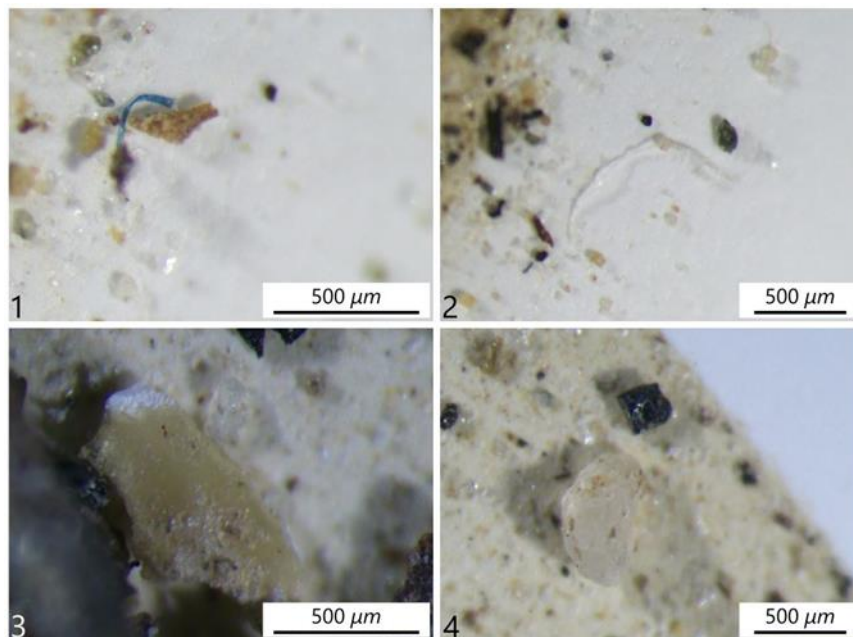
Figure 4.44. Forms and abundance of microplastics in P11.

Figure 4.45. Pictures of microplastics found in P11. 1. Blue fibre; 2. Transparent fibre; 3. Yellow fragment; 4. Transparent fragment

4. Results

P12

P12 represents the matrix infiltrated in the shadow zones created by coarser gravels during the waning phase. The microscopic analysis let to the identification of 88 microplastic items. Figures 4.46 and 4.47 show forms and abundance of microplastics within the sample
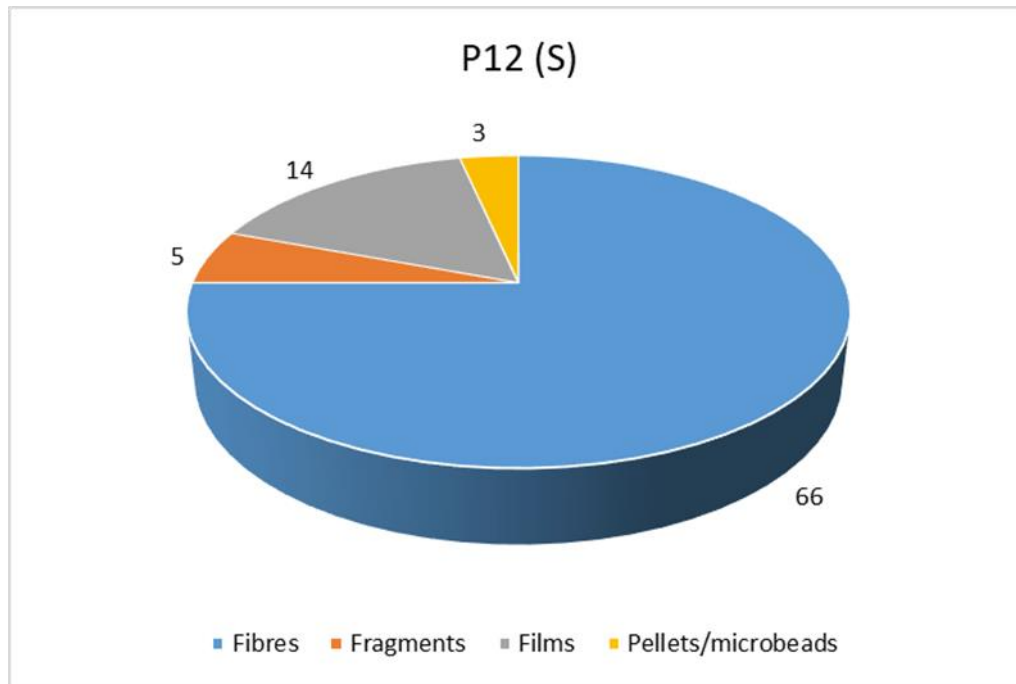

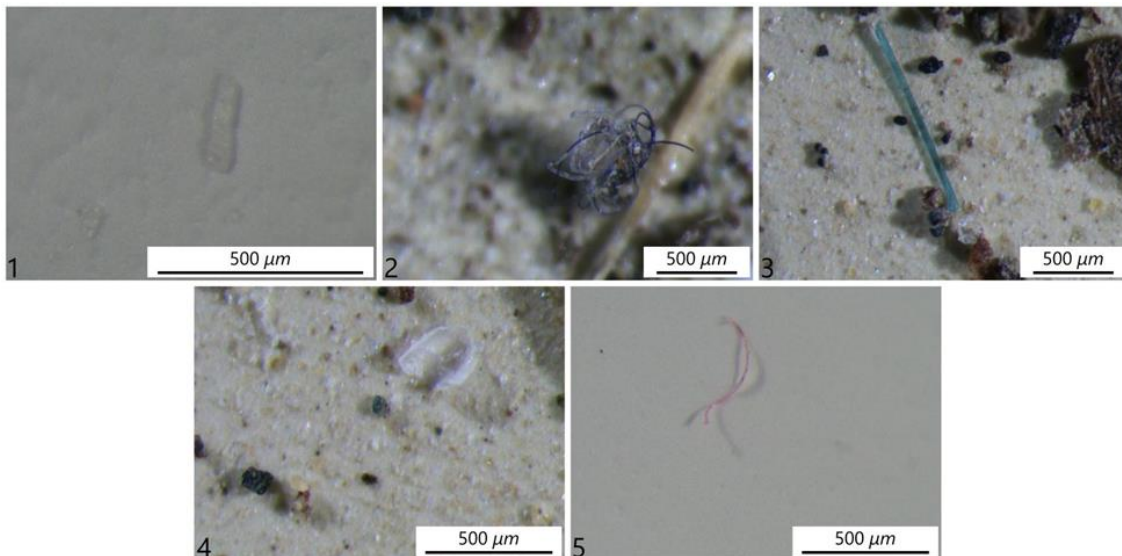*Figure 4.46. Forms and abundance of microplastics in P12.*

Figure 4.47. Pictures of microplastics found in P12. 1. Transparent fragment; 2. Blue and white fibres; 3. Blue fibre; 4. Transparent film; 5. Red fibre.

4.2.8 P13 – P14 – P15

These three sediments come from the gravelly part of the bar, but they were not collected in the same sites. They all represent a stand condition of the water level during the waning phase. In this case, differently from P4, the muddy sediment infiltrates within gravels and pebbles (*figure 4.48*).

Figure 4.48. Example of depositional setting represented by the P13-P15 samples: gravels and pebbles with spots of plant debris. The sampled sediment (mud to sand) infiltrated within coarser grains. Here it is represented the maximum erosion zone of the bar head (P15).

4. Results

P13

P13 represents the sediment infiltrated in gravels, under plant debris which marks a water standing during the waning stage. The microscopic analysis led to the identification of 56 microplastics items. Figures 4.49 and 4.50 show forms and abundance of microplastics within the sample.
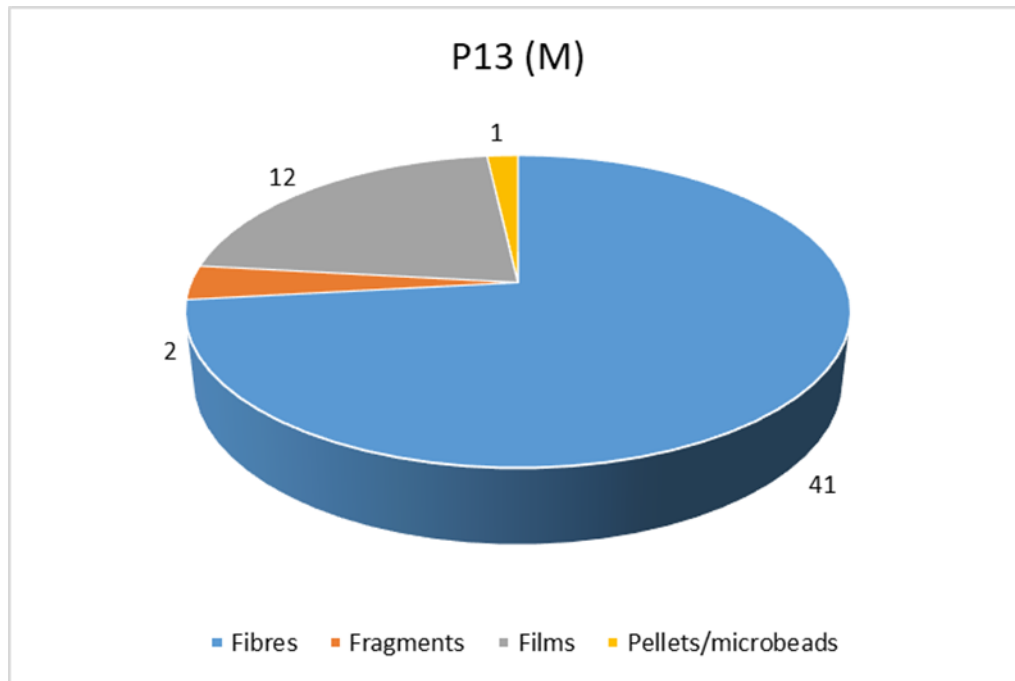

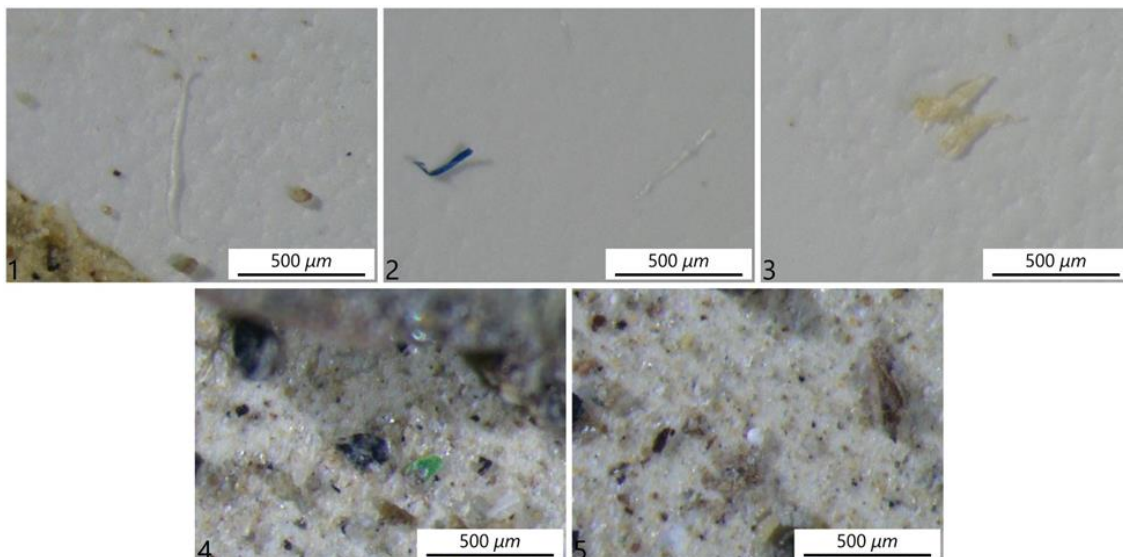*Figure 4.49. Forms and abundances of microplastics in P13.*

Figure 4.50. Pictures of microplastics found in P13. 1. Transparent fibre; 2. Blue fibre; 3 Yellow films; 4. Green fragment; 5. White pellet.

4. Results

P14

P14 comes from the highest zone of the bar. The sampled sediment has infiltrated the gravels in a slightly depressed area. In here, 51 microplastics items were identified. Figures 4.51 and 4.52 show forms and concentration of microplastics within the sample.
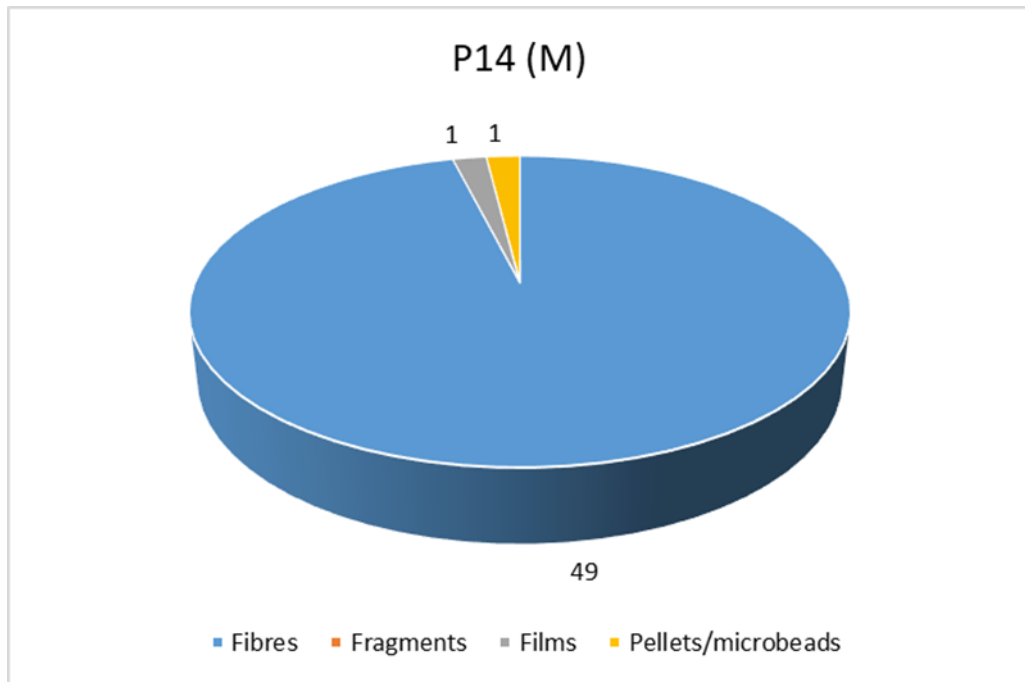

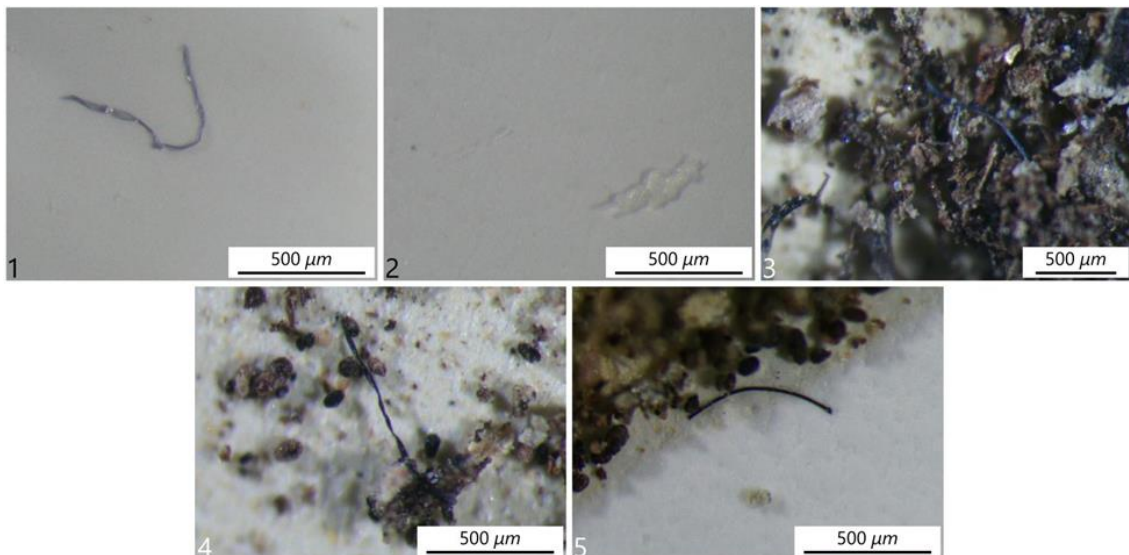*Figure 4.51. Forms and abundance of microplastics found in P14.*

Figure 4.52. Pictures of microplastics found in P14. 1. Blue fibre; 2. Transparent film; 3. Green fibre; 4. Blue fibre; 5. Black fibre.

4. Results

P15

P15 comes from the maximum erosion zone, in the upstream side of the bar. This zone was poor in fine sediment infiltrated into the gravels due to the strong erosion caused by high water fluxes. The analysis led to the identification of 21 microplastic items. Figures 4.53 and 4.54 show forms and concentration of microplastics within the sample.
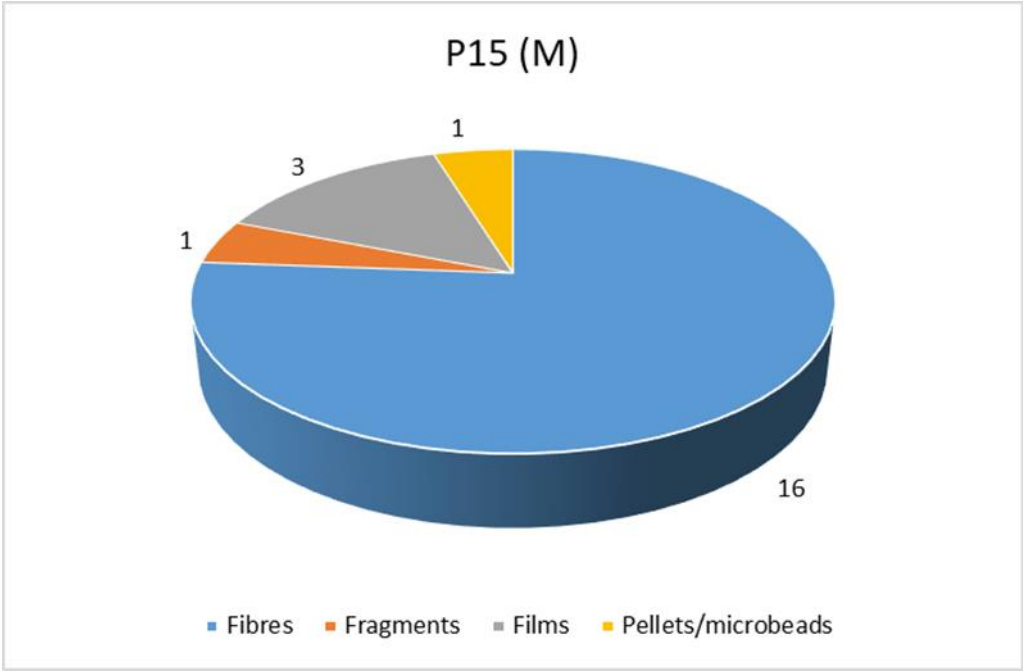

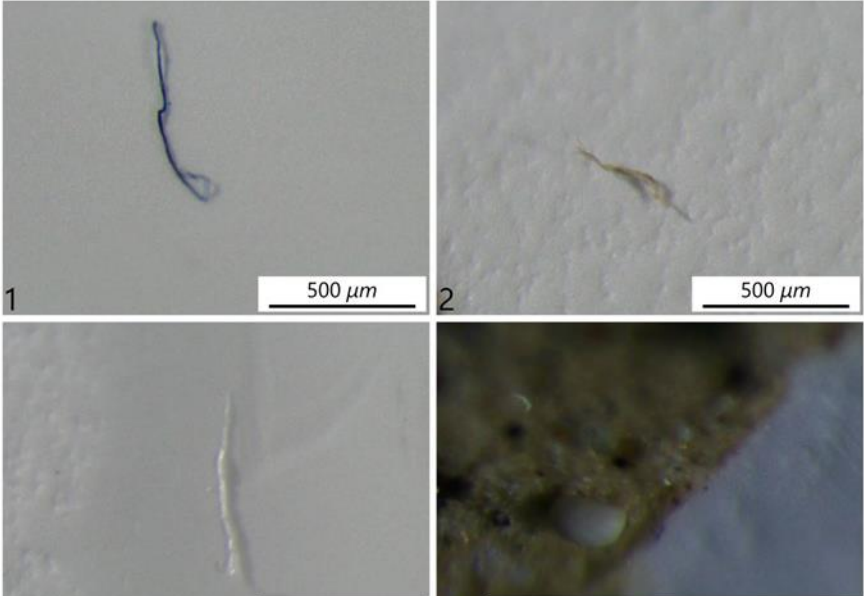*Figure 4.53. Forms and abundance of microplastics in P15.*

Figure 4.54. Pictures of microplastics found in P15. 1. Blue fibre; 2. Yellow fibre; 3. Transparent fibre; 4. White pellet.

4. Results

4.3 Bar 3

Bar3 is just next upstream of Bar 2 (see *figure* 3.1), on the opposite side (hydrographic right). 5 samples were collected in here (*figure 4.55*).

Figure 4.55. Bar 3. Containing MOC7 – MOC11 samples

Two couples of samples (MOC7-8 and MOC9-10) come from the sandy zone of the bar, where ripples migrate downstream, at different depth to distinguish sediments deposited during different flood stages. The last sample (MOC11) represent the vegetational debris floating during the flood.

4. Results

Results are summarized in table 4:

Sample	TYPE	$D_{50}(mm)$	Wentworth class	Material analysed	Items	Concentration (MPs/g)
MOC7	S	0,316	Medium sand	25 g	19	0,76
MOC8	T	0,337	Medium sand	25 g	33	1,32
MOC9	S	0,242	Fine sand	25 g	42	1,68
MOC10	T	0,314	Medium sand	25 g	22	0,88
MOC11	F	*null*	*null*	5 g	14	2,8

Table 4. Results of Bar 3 samples

4.3.1   MOC7 – MOC8

Samples were collected in the sandy region of the bar. The MOC8 sample represents the sediment deposited under tractive condition, where ripple formed. The MOC7 sample represents the terminal phase of the flood, when the finer sediments settled and draped the ripples (*figure* 4.56).

Figure 4.56. P7 – P8. Sandy ripples in cross lamination migrating downstream.

4. Results

MOC8

MOC8 has deposited during under tractive conditions, where high water flows led the formation of ripples in the tail region of the bar. 33 microplastic items were identified during the microscopic analysis. Figures 4.57 and 4.58 show forms and abundance of microplastics within the sample.
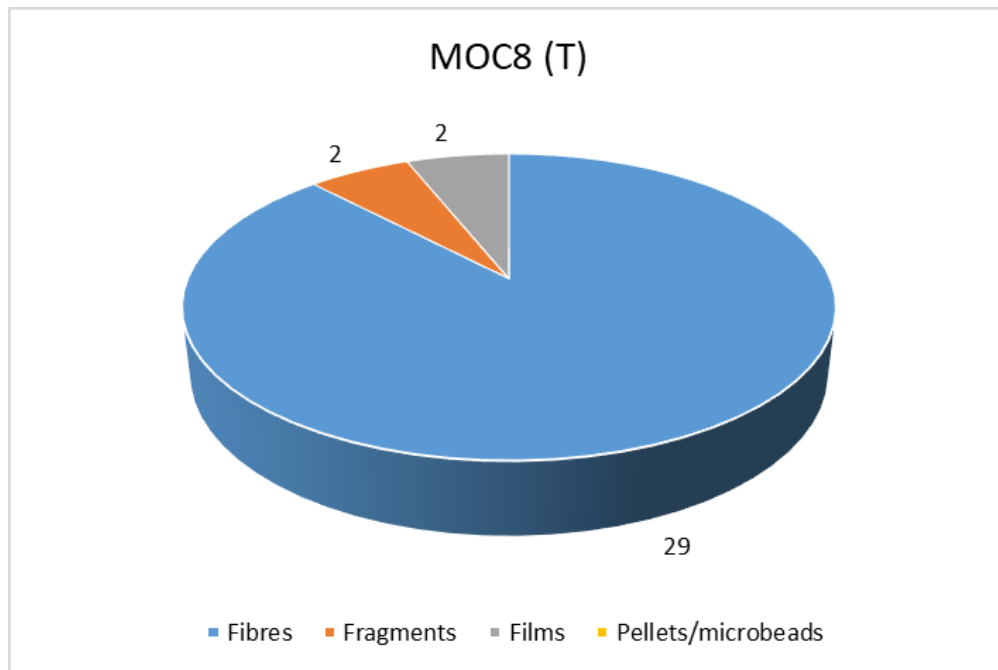

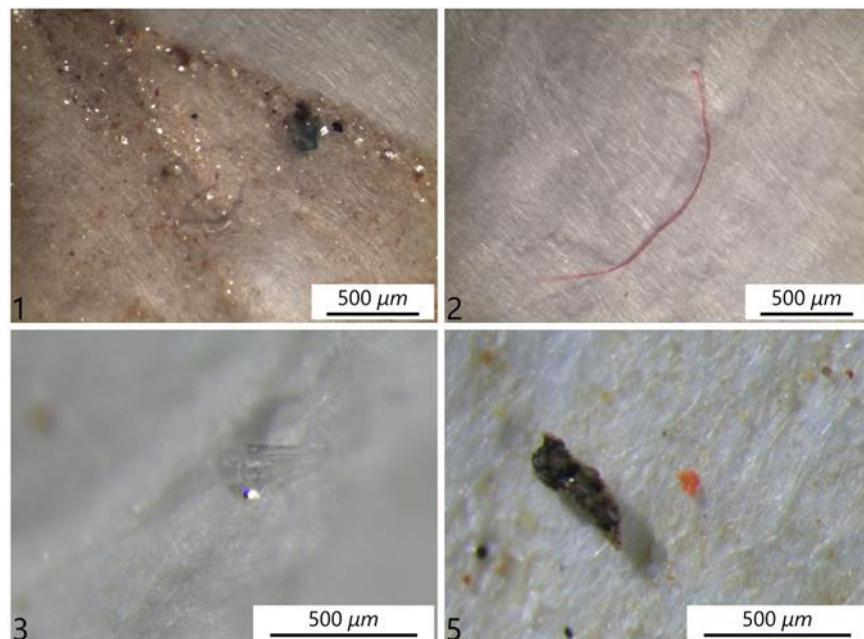*Figure 4.57. Forms and abundance of microplastics in MOC8.*

Figure 4.58. Pictures of microplastics found in MOC8. 1. Green fragment; 2. Red fibre; 3. Transparent microbead; 4. Orange fragment.

4. Results

MOC7

MOC7 should represent the finer sediments settled during the waning phase which draped the ripples. The microscopic analysis led to the identification of 19 microplastic items. Figures 4.59 and 4.60 show forms and abundance of microplastics within the sample.
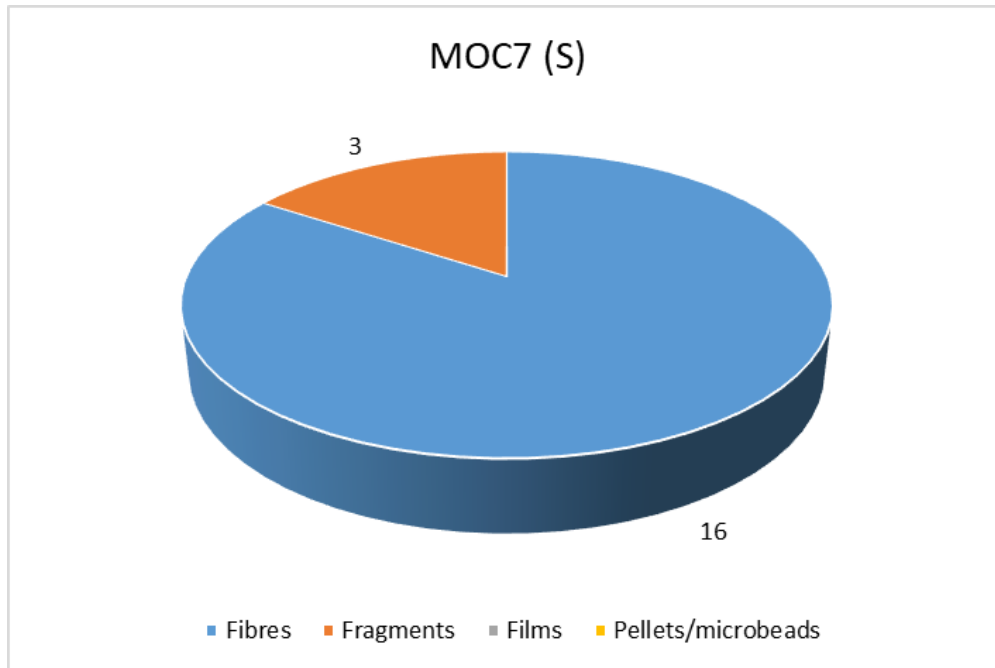

Figure 4.59. Forms and abundance of microplastics in MOC7.
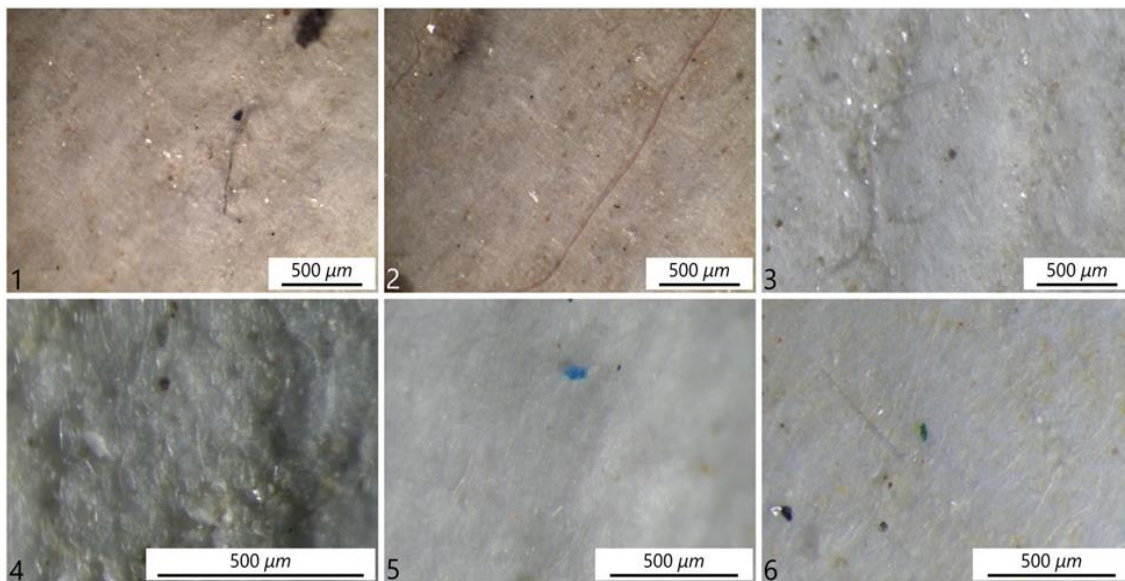
Figure 4.60. Pictures of microplastics in MOC7. 1. Transparent fibre; 2. Red fibre; 3. Transparent fibre; 4. White fragment; 5. Blue fragment; 6. Green fragment.

4. Results

4.3.2 MOC9 – MOC10

This couple of sediment represents the same conditions found with MOC7 − MOC8. Sands in ripple cross stratification were sampled, with finer sediments settled above it (*figure 4.61*).

Figure 4.61. P9 – P10. Migrating ripples with frustules.

4. Results

MOC10

MOC10 comes from the ripples in cross stratification which moved under tractional conditions during the flood phase whit higher water flows. 22 microplastic items were identified during the microscopic analysis. Figures 4.62 and 4.63 show forms and abundance of microplastics within the sample.

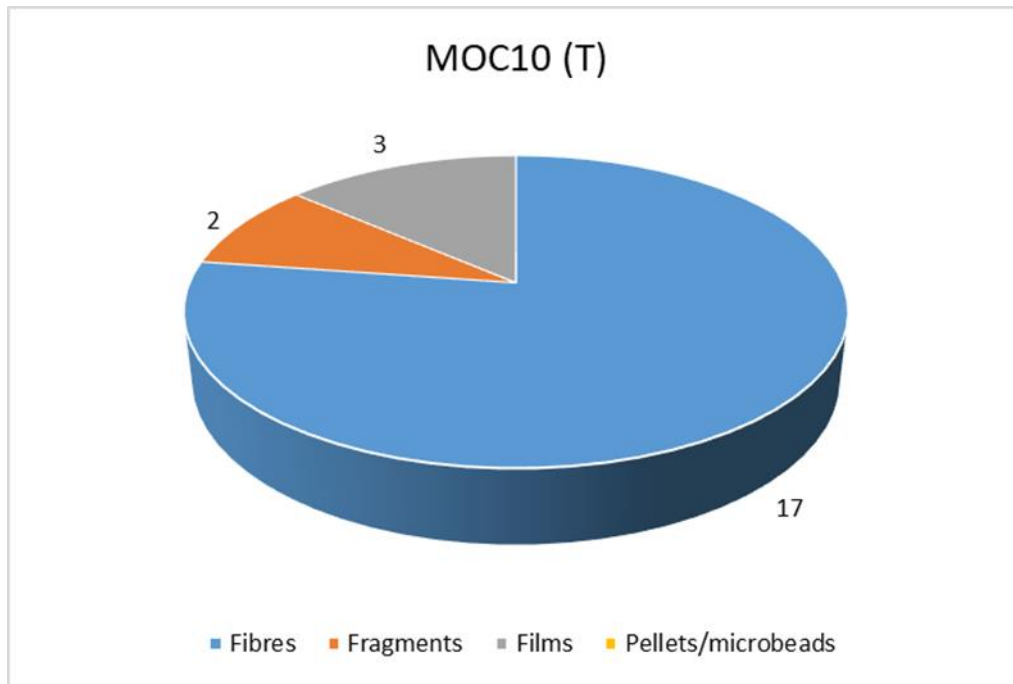

Figure 4.62. Forms and abundance of microplastics in MOC10.

Figure 4.63. Pictures of microplastics in MOC10. 1. Red fragment; 2. White fibre; 3. Transparent fibre; 4. Transparent films.

4. Results

MOC9

MOC 9 represents the finer sediment settled due to the low flow conditions in the terminal phase of the flood. 42 microplastic items were identified. Figures 4.64 and 4.65 show forms and abundance of microplastics within the sample.

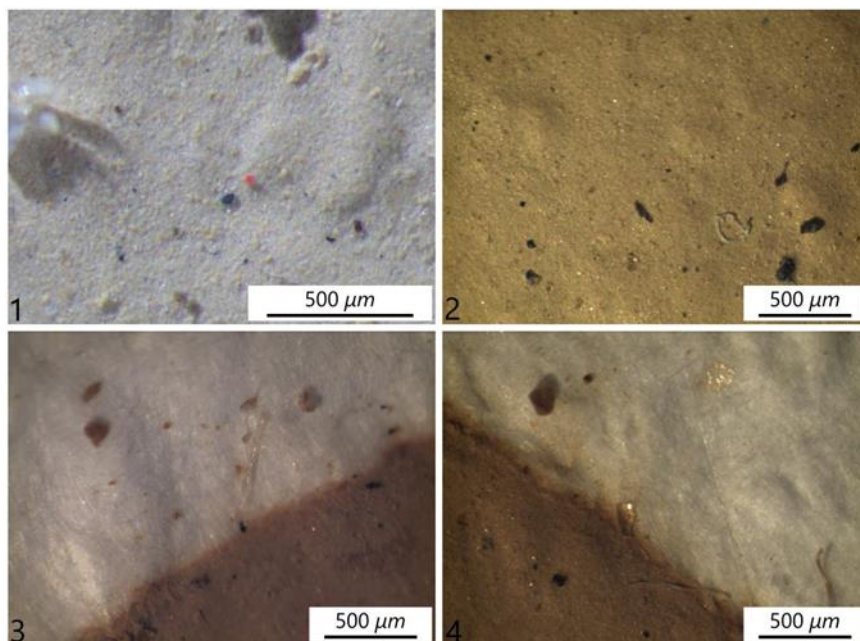*Figure 4.64. Forms and abundance of microplastics in MOC9.*

Figure 4.65. Pictures of microplastics found in MOC9. 1. Blue and red fibres; 2. Red fibre; 3. Transparent fibre; 4. Blue fibre; 5. Transparent fragment.

4. Results

4.3.3 MOC11

This sample was collected from the floating vegetational debris transported by high water fluxes during floods (*figure 4.66*). The high concentration in organic matter made the microscopic analysis hard.

Figure 4.66. MOC11. Vegetational debris accumulated on the riverbank.

The microscopic analysis led the identification of 14 microplastic items. Figures 4.67 and 4.68 show forms and abundance of microplastics within the sample.

4. Results

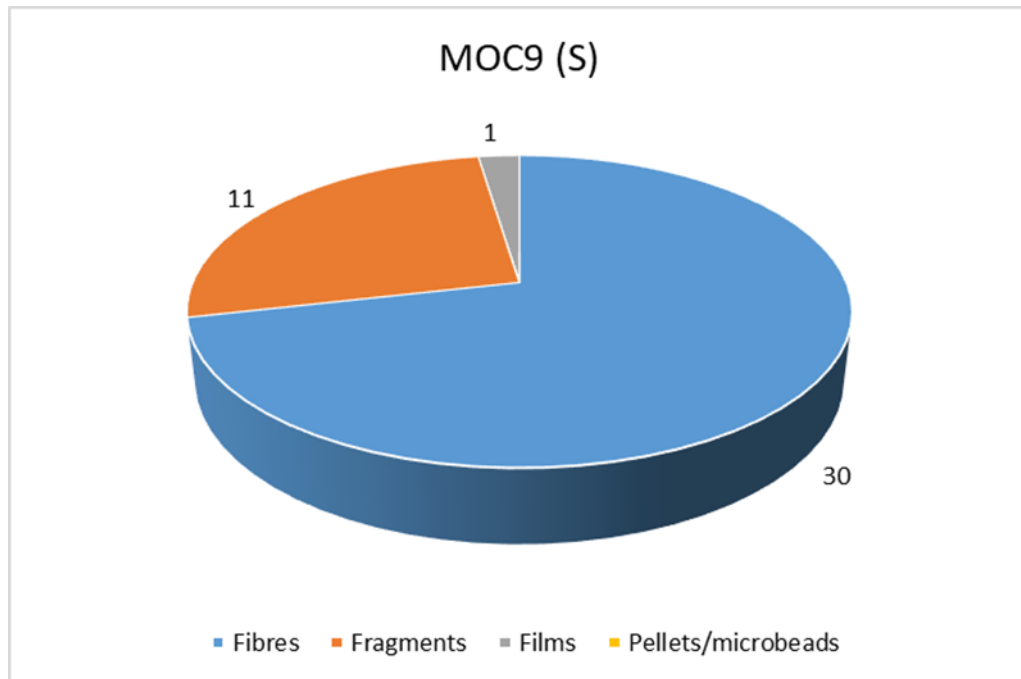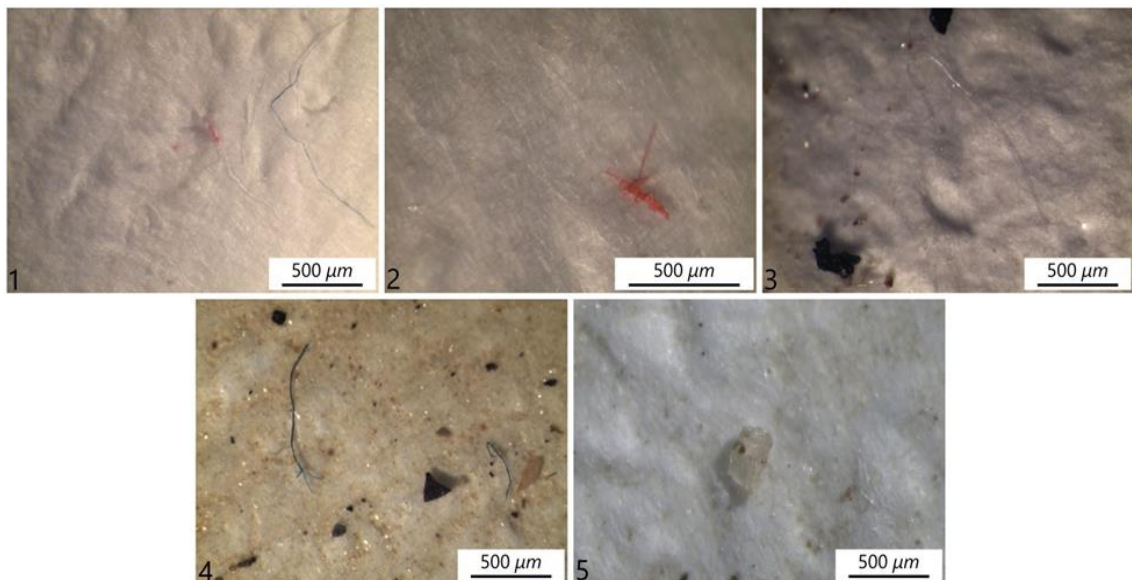*Figure 4.67. Forms and abundance of microplastics in MOC11.*

Figure 4.68. Pictures of microplastics found in MOC11. 1. Blue fibre; 2. Transparent beads and fibres; 3. Transparent fragment; 4. Transparent fibre; 5. Blue fibre; 6. Pink fibre.

4. Results

4.4 Bar 4

Bar 4 (*figure 4.75*) is on the hydrological left of the channel, and it is just next upstream of Bar3 (see *figure 3.1)*. 5 samples were collected.

Figure 4.69. Bar 4, containing G samples.

Two couples of samples (G2-3 and G4-5) come from a sandy tongue in a vegetated shadow zone, which was sampled at different depth in order to represent sediments deposited under different conditions during the flood event.

The last sample (G12) come from the finer sediment settled at the top of the gravelly front during the waning phase.

4. Results

The results are summarized in table 5.

Sample	TYPE	$D_{50}(mm)$	Wentworth class	Material analysed	Items	Concentration (MPs/g)
G2	T	0,231	Fine sand	*25 g*	24	0,96
G3	S	0,142	Fine sand	*25 g*	22	0,88
G4	T	0,193	Fine sand	*25 g*	24	0,96
G5	S	*null*	*null*	*25 g*	36	1,44
G12	S	0,088	Very fine sand	*25 g*	28	1,12

Table 5. Results of Bar 4 samples.

4.4.1 G2 – G3

This couple of sediment comes from the sandy tongue of the bar, deposited in shadow created by seasonal vegetation.

The sediment deposited under tractive condition is characterized by ripple in cross lamination moving upstream, while the sediment settled above it represents the one deposited during the waning phase (*figure* 4.70).

Figure 4.70. G2 – G3. Ripples in cross lamination draped by finer sediment.

4. Results

G2

The G2 sample consists in fine sand ripples in cross lamination, thus representing the sediment deposited under tractive conditions.

The microscopic analysis led the identification of 24 microplastic items. Figures 4.71 and 4.72 show forms and abundance of microplastics within the sample.
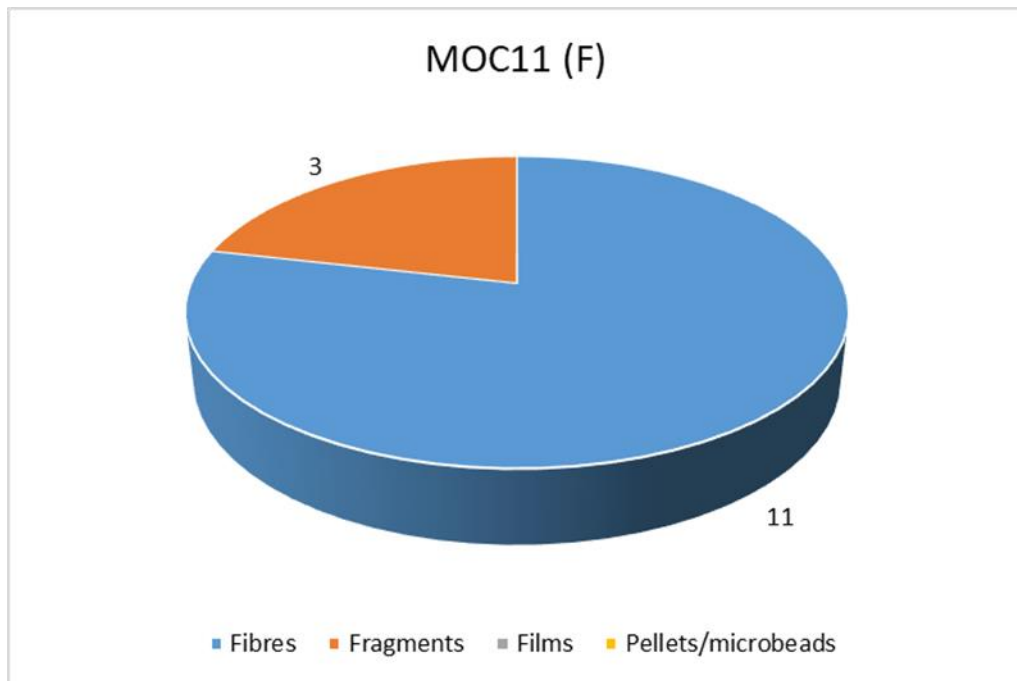

Figure 4.71. Forms and abundance of microplastics in G2.

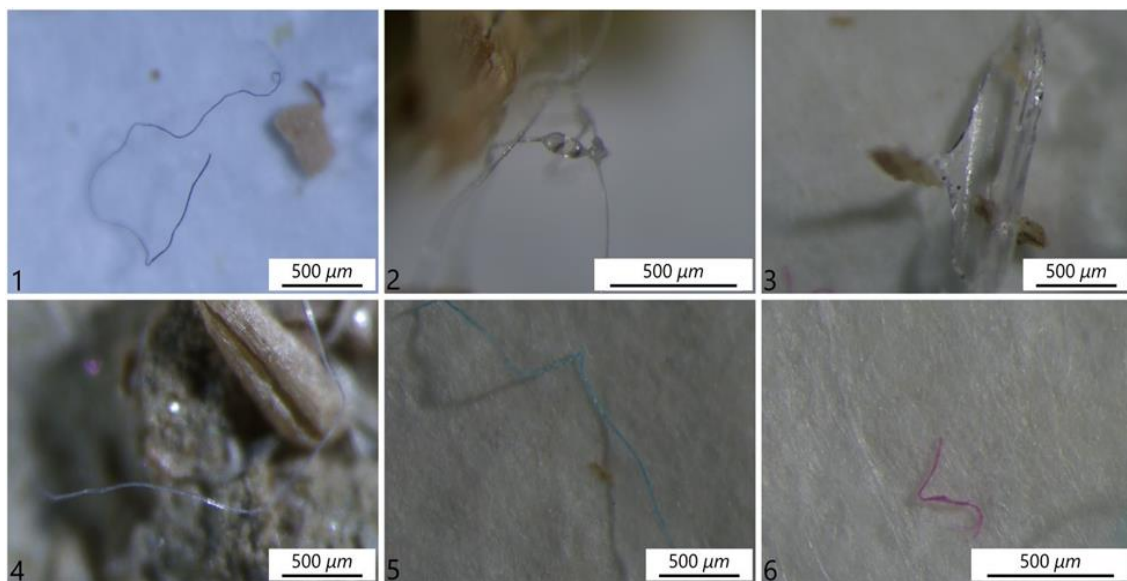*Figure 4.72. Pictures of microplastics found in G2. 1. Transparent fibre; 2. Blue fibre; 3. Transparent fibre; 4. Green fragment.*

4. Results

G3

G3 represents the finer sediment draping ripples settled down during the waning phase.

22 microplastic items were identified during the microscopic analysis. Figures 4.73 and 4.74show forms and abundance of microplastics within the sample.
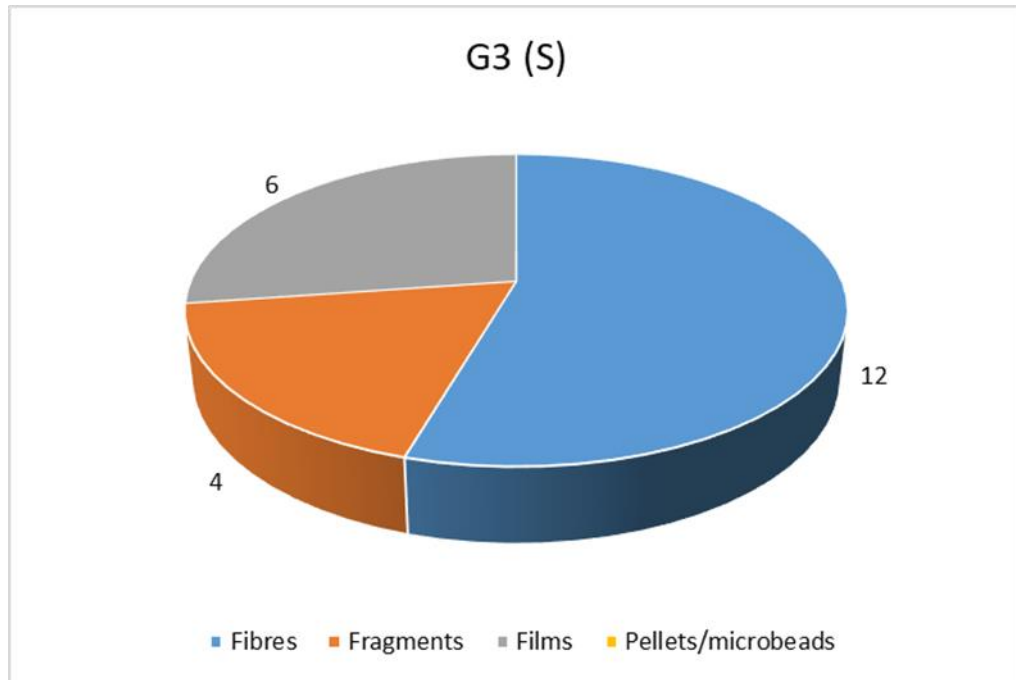
Figure 4.73. Forms and abundance of microplastics in G3.

Figure 4.74. Pictures of microplastics found in G3. 1. Transparent fibre; 2. Transparent fragment; 3. Transparent fibre under UV light; 4. Yellow fragment; 5. Red fragment; 6. Transparent film.

4.4.2   G4 – G5

G4 and G5 samples were collected in the same sandy tongue of, G2 and G3, and represent a similar condition. However, the main difference is represented by the material deposited during the waning phase, that in this case consists of a large amount of plant debris (*figure 4.75*).

Figure 4.75. G4 – G5. Ripple in cross lamination covered with plant debris.

4. Results

G4

The G4 sample is composed by fine sand ripples deposited under tractional conditions.

The microscopic analysis led the identification of 24 microplastic items. Figures 4.76 and 4.77 show forms and abundance of microplastics within the sample.
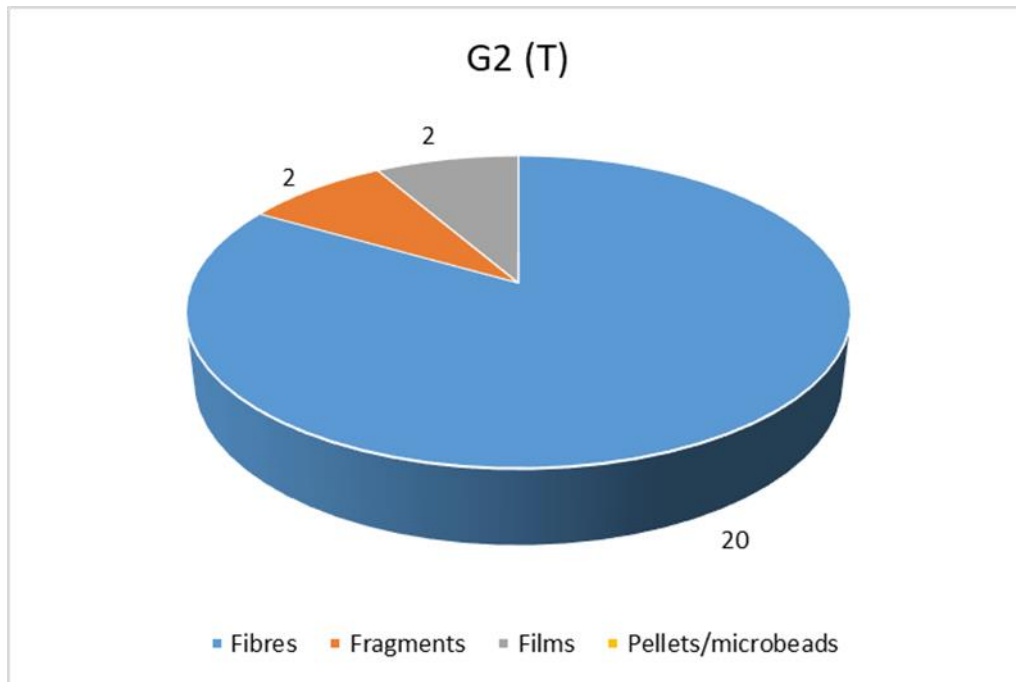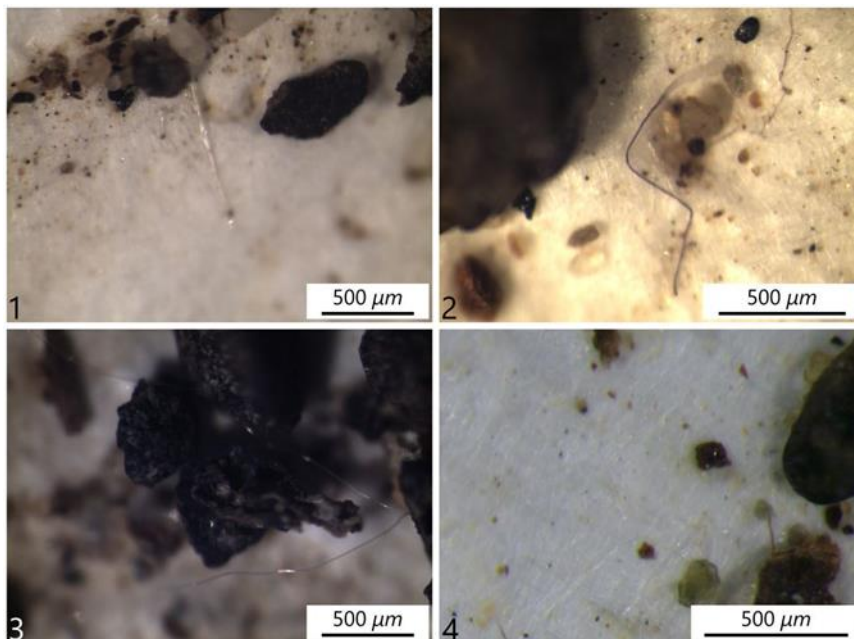

Figure 4.76. Forms and abundance of microplastics in G4.

Figure 4.77. Pictures of microplastics found in G4. 1. Very small blue fragment; 2. Blue fibre; 3. Transparent fibre; 4. Blue fibre; 5. Blue fibre; 6. Blue fragment.

4. Results

G5

G5 represents the plant debris deposited on G4 during the waning phase. Due to the large amount of organic matter, WPO process did not completely work, and microscopic analysis proved more difficult. 36 microplastic items were identified. Figures 4.78 and 4.79 show forms and abundance of microplastics within the sample.

Figure 4.78. Forms and abundance of microplastics in G5.
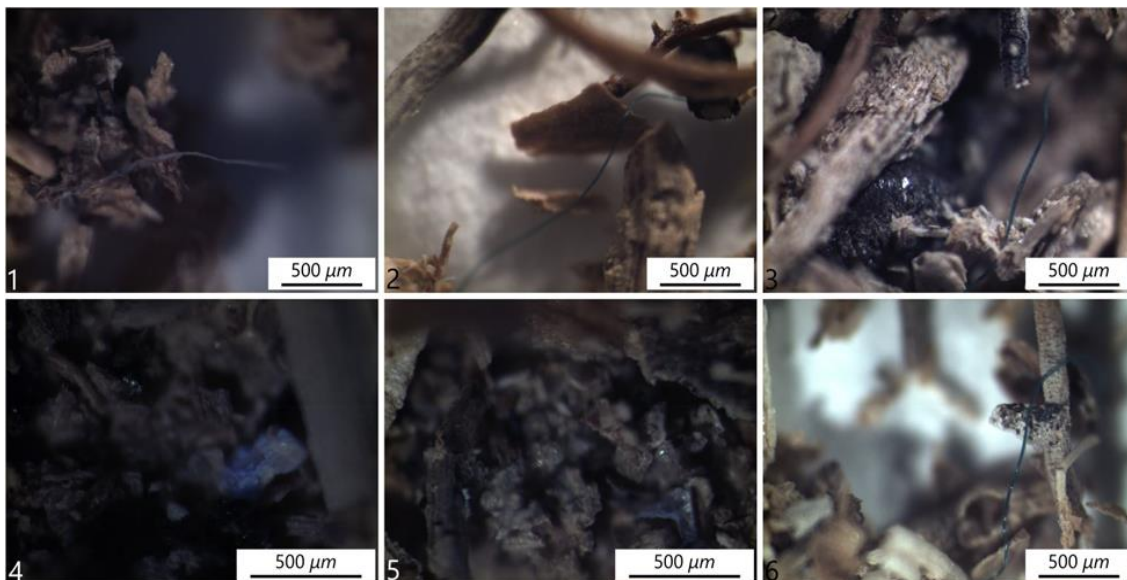
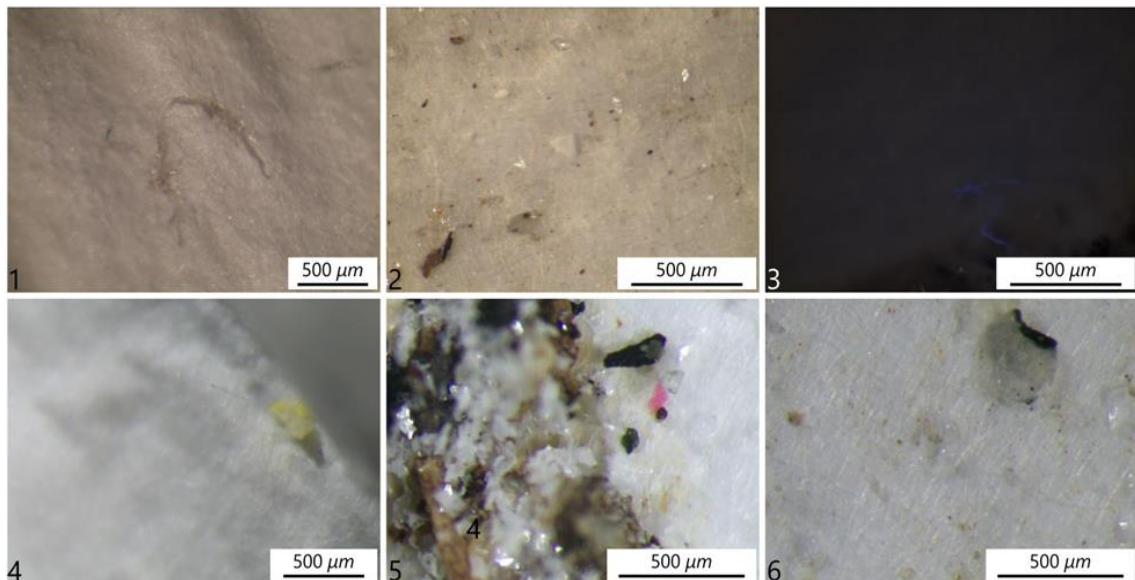*Figure 4.79. Pictures of microplastics found in G5. 1. Transparent fibre; 2. Green fibre; 3. Green fibre; 4. Transparent fragment under UV light; 5. Transparent film slightly lit by UV light. 6. Green fibre.*

4.4.3   G12

G12 comes from the head region, where sediments mainly consist of gravels and pebbles. Nevertheless, during the waning phase, when the erosive force calms down, finer sediments can settle and deposit. The G12 sample represents such a condition (*figure 4.80*).

Figure 4.80. Silty to sandy sediments at the top of a gravelly front.

The microscopic analysis let the identification of 28 microplastic items. Figures 4.81 and 4.82 show forms and abundance of microplastics within the sample.
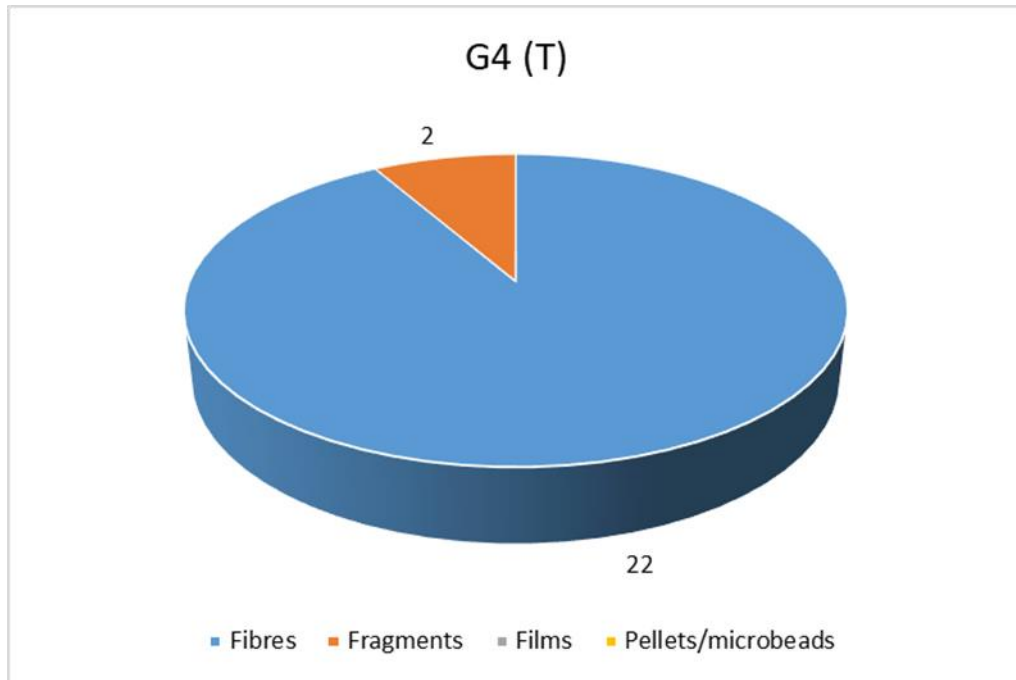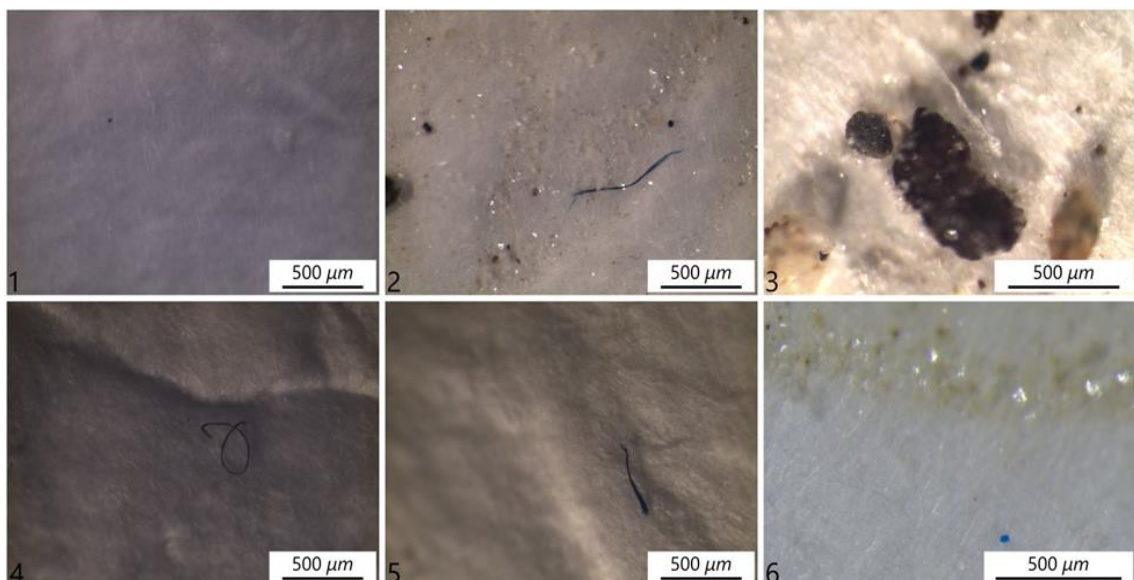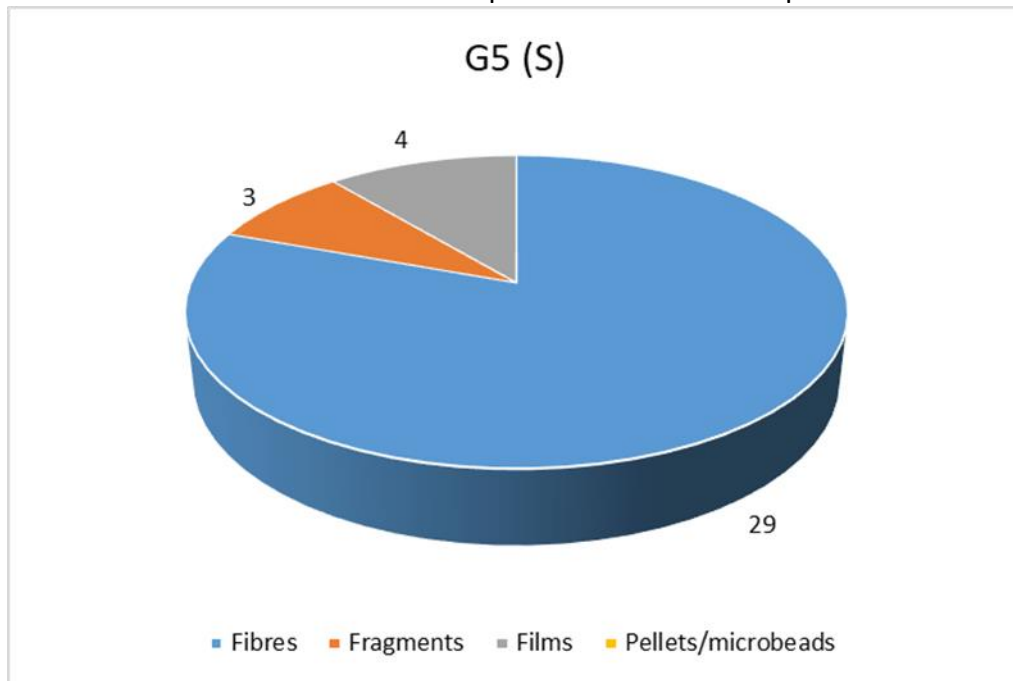
Figure 4.81. Forms and abundance of microplastics in G12.
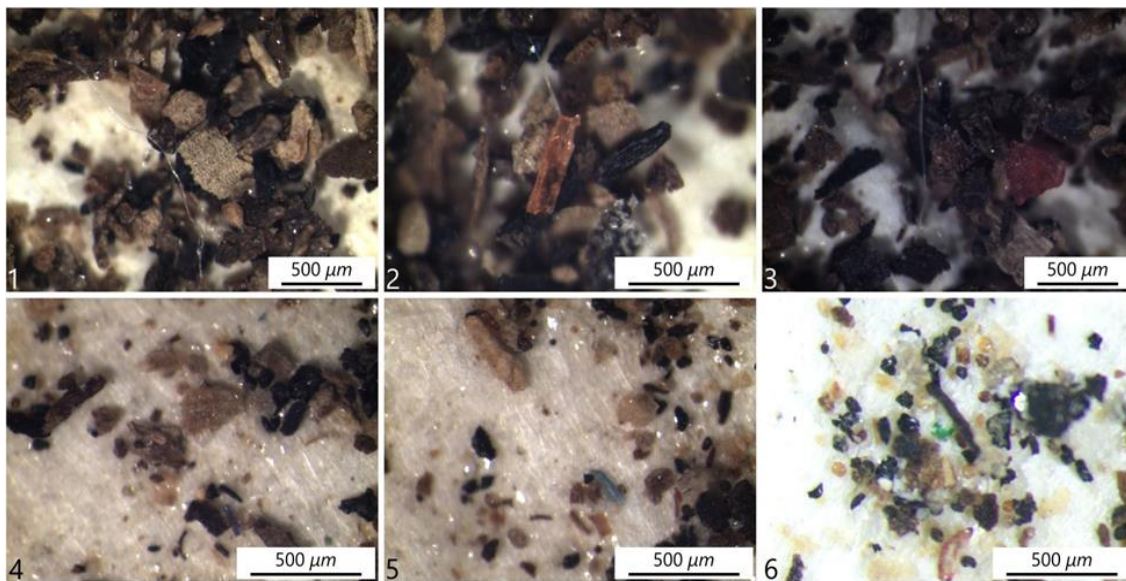
Figure 4.82. Pictures of microplastics found in G12. 1. Transparent fibre; 2. Red fragment; 3. Red fragment and a transparent fibre; 4. Blue fibre; 5. Blue fibre; 6. Green fragment.

4.5 Bar 5

Bar 5 is the most upstream sampling site, 3.5 km far from Bar 4 (see *figure 3.1*). It is on the hydrographic left of the channel, in proximity of the Montevarchi hydrometric survey station (*figure 4.83*).
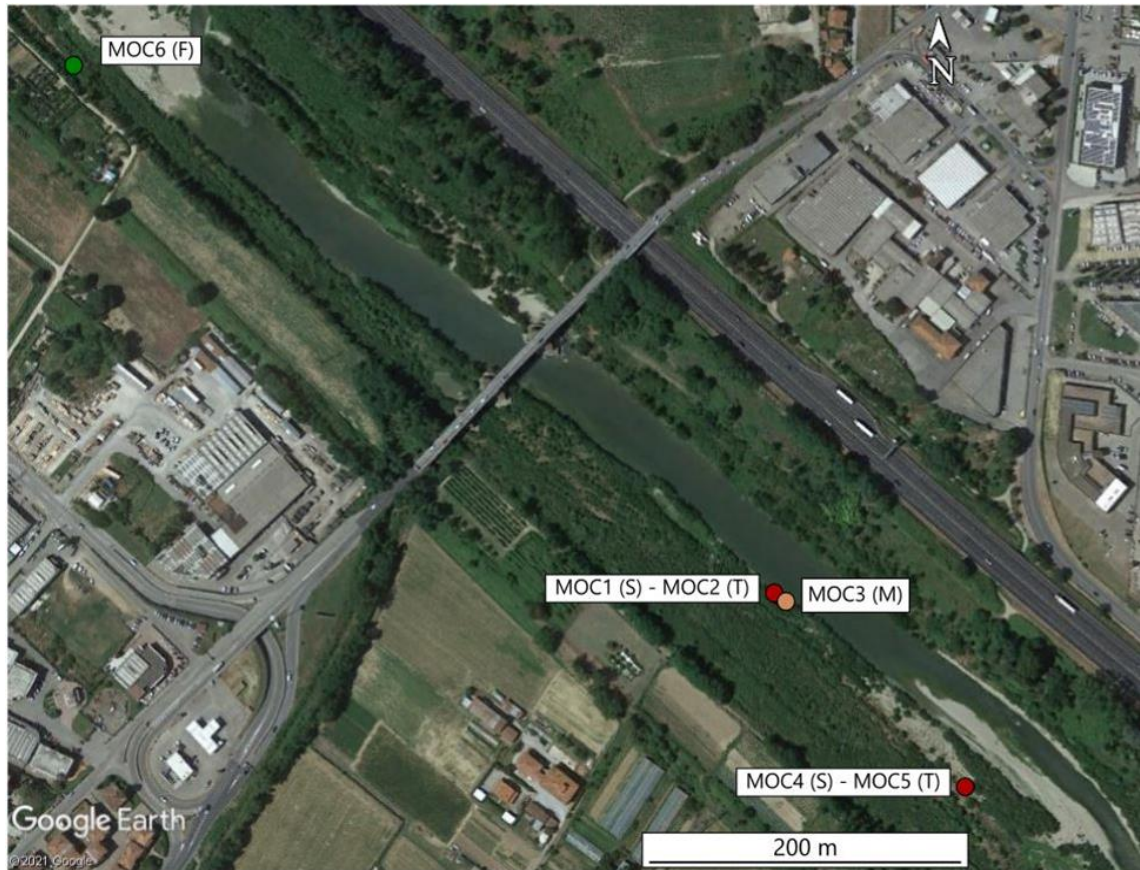
Figure 4.83. Bar 5, containing MOC1 – MOC6 samples.

Here 6 samples were collected. Two couples of samples (MOC1-2 and MOC4-5) come from the tail and represent both sediments deposited at different flood stages, a single sample (MOC3), collected in proximity of the two couples, represents the material marking a standing water condition during the waning phase. One sample (MOC6) is actually sited in the downstream riffle zone of the bar and represents the floating vegetational debris.

4. Results

The results are summed up in the table 6.

Sample	TYPE	$D_{50}(mm)$	Wentworth class	Material analysed	Items	Concentration (MPs/g)
MOC1	S	0,228	Fine sand	25 g	33	1,32
MOC2	T	0,317	Medium sand	25 g	28	1,12
MOC3	M	null	null	25 g	28	1,12
MOC4	S	0,202	Fine sand	25 g	22	0,88
MOC5	T	0,357	Medium sand	25 g	22	0,88
MOC6	F	null	null	25 g	26	1,04

Table 6. Results of Bar 5 samples.

4.5.1   MOC1 -MOC2

This couple of sediments comes from the tail region of the bar, where deposition processes are mainly associated with migration of ripples, or dunes, under tractive conditions. When the river regime slows down the sedimentation occurs for settling of finer sediments over bedforms previously deposited (*figure 4.84*).

Figure 4.84. Migrating ripples in cross lamination.

4. Results

MOC2

The MOC2 sample represents the medium sand ripples deposited under tractional conditions.

The microscopic analysis let the identification of 28 microplastic items. Figures 4.85 and 4.86 show forms and abundance of microplastics within the sample.
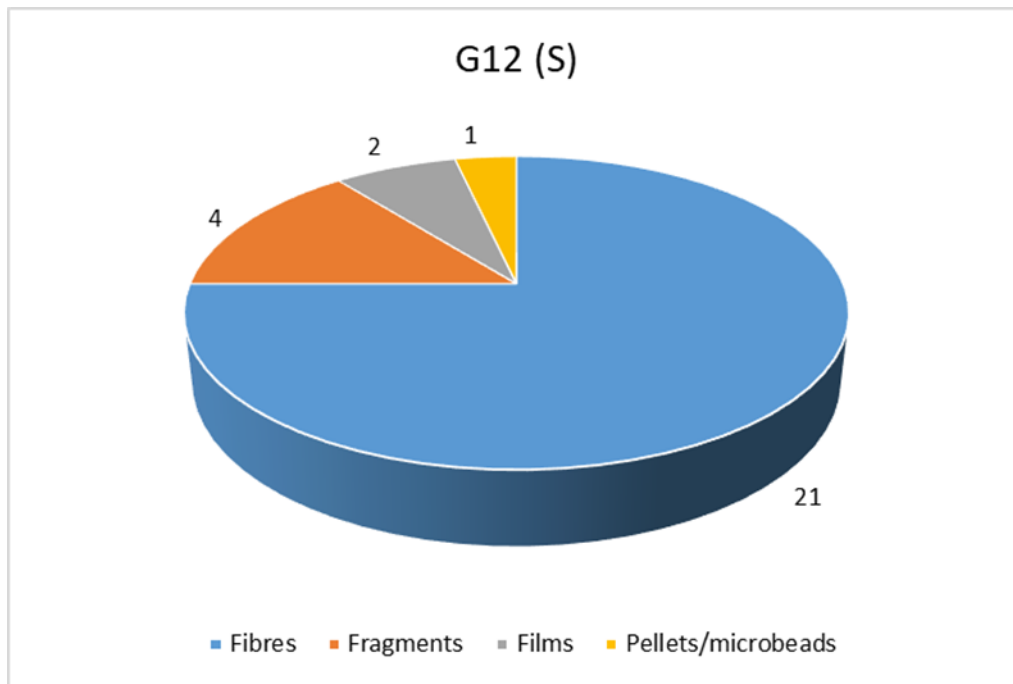

*Figure 4.85. Forms and abundance of microplastics in MOC2.*

Figure 4.86. Pictures of microplastics found in MOC2. 1.Red fibre; 2. Blue fibre; 3. Black fibre.

4. Results

MOC1

The MOC1 sample has deposited during the waning phase and consists of finer sand draping ripples.

33 microplastic items were identified thanks to the microscopic analysis. Figures 4.87 and 4.88 show forms and abundance of microplastics within the sample.

Figure 4.87. Forms and abundance of microplastics in MOC1.
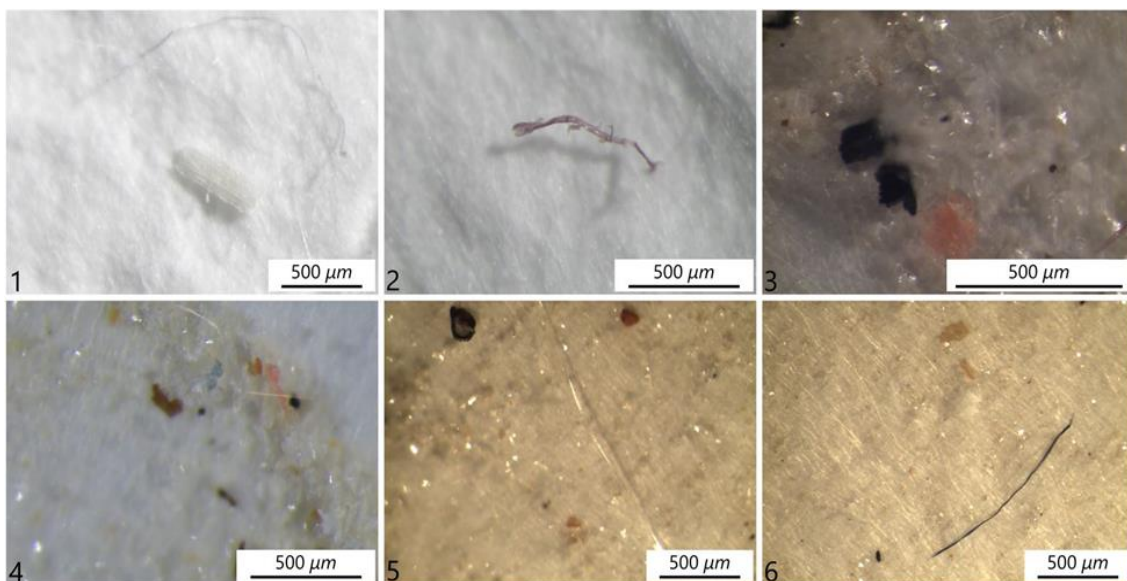
Figure 4.88. Pictures of microplastics found in MOC1. 1. Transparent fibre with organic debris; 2. Violet fibre; 3. Pink fragment; 4. Blue and pink fragments; 5. Transparent fibre; 6. Blue fibre.

4.5.2 MOC3

The MOC3 sample is close to MOC1-MOC2 couple, and it is composed of frustules marking a previous standing water condition (*figure 4.89*).

Figure 4.89. Plant debris marking a slough water level.

The high concentration of organic matter made the WPO process not entirely efficient, leaving a significant concentration of material that was not fully digested.

28 microplastic items were identified thanks the microscopic analysis. Figures 4.90 and 4.91 show forms and abundance of microplastics within the sample.

4. Results

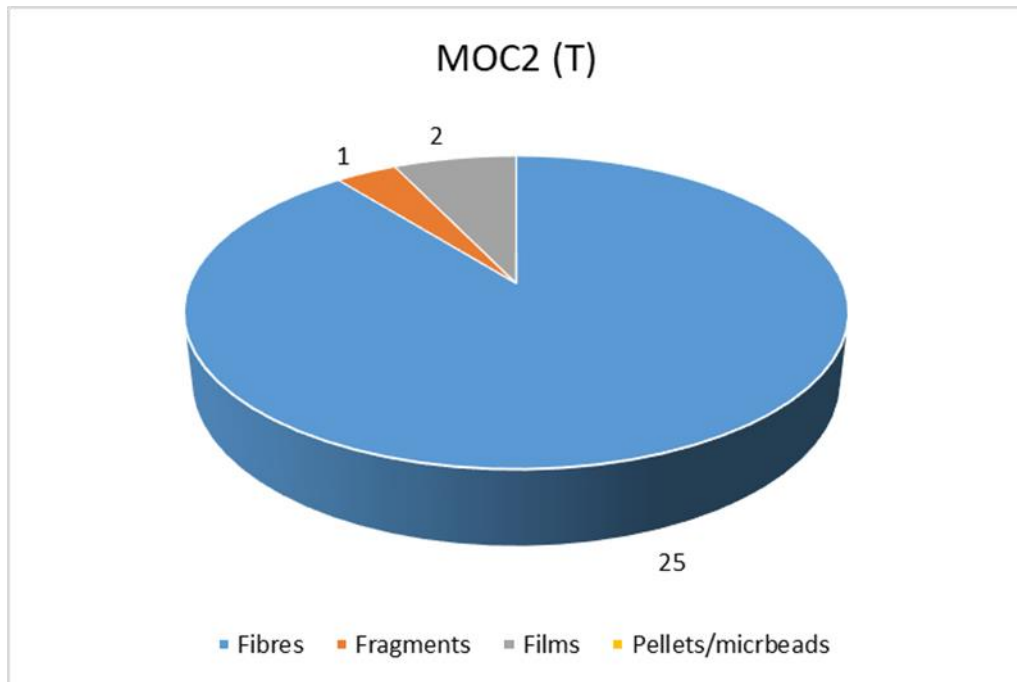*Figure 4.90. Forms and abundance of microplastics in MOC3.*
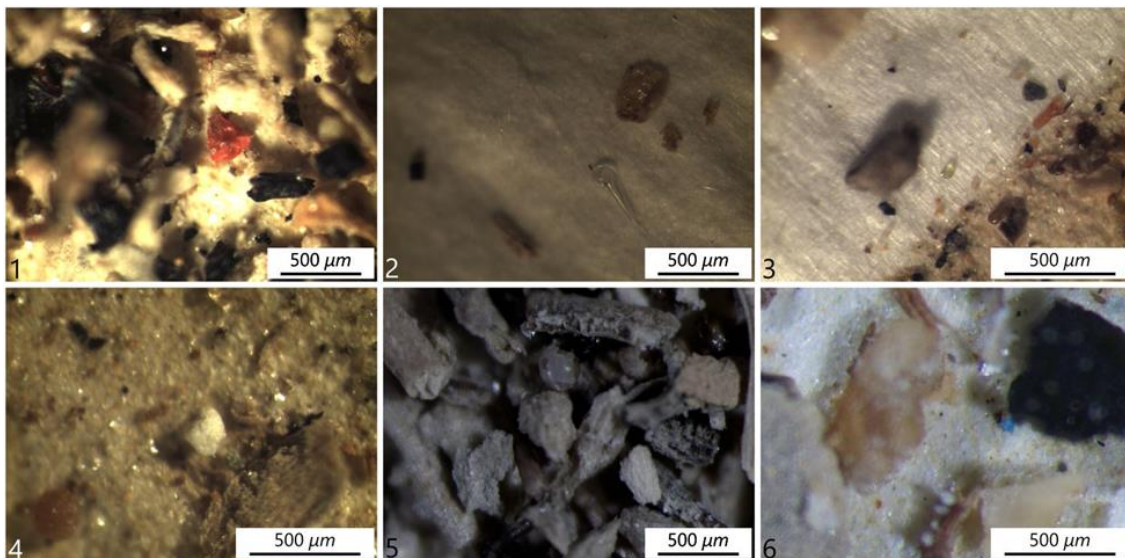
Figure 4.91. Pictures of microplastics found in MOC3. 1. Red fragment; 2. Transparent microbead; 3. Yellowish microbead; 4. White fragment; 5. Transparent film; 6. Blue fragment.

4.5.3   MOC4 – MOC5

This couple of samples comes from an inner portion respect to the previous three samples.

They represent, as MOC1 and MOC2, sediments deposited both under tractional condition and settling (*figure 4.92*).

Figure 4.92. Sandy ripples in cross lamination draped by finer sediments deposited during the waning phase.

4. Results

MOC5

The MOC5 sample represents the sandy ripples in cross lamination formed under tractional conditions. The microscopic analysis led to the identification of 22 microplastic items. Figures 4.93 and 4.94 show forms and abundance of microplastics within the sample.

Figure 4.93. Forms and abundance of microplastics in MOC5.

Figure 4.94. Pictures of microplastics found in MOC5. 1. Blue fibre; 2. Blue fragment; 3. Red fibre; 4. Transparent fragment; 5. Transparent fibre.

4. Results

MOC4

The MOC4 sample is made of finer sands draping ripples deposited for settling. The microscopic analysis led to the identification of 22 microplastic items. Figures 4.95 and 4.96 show forms and abundance of microplastics within the sample.
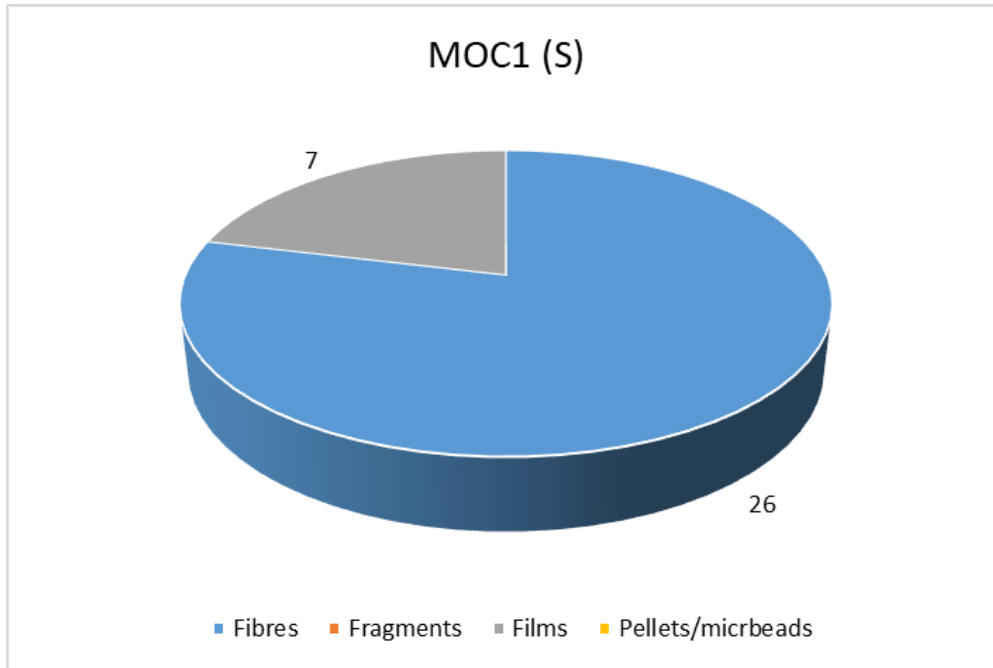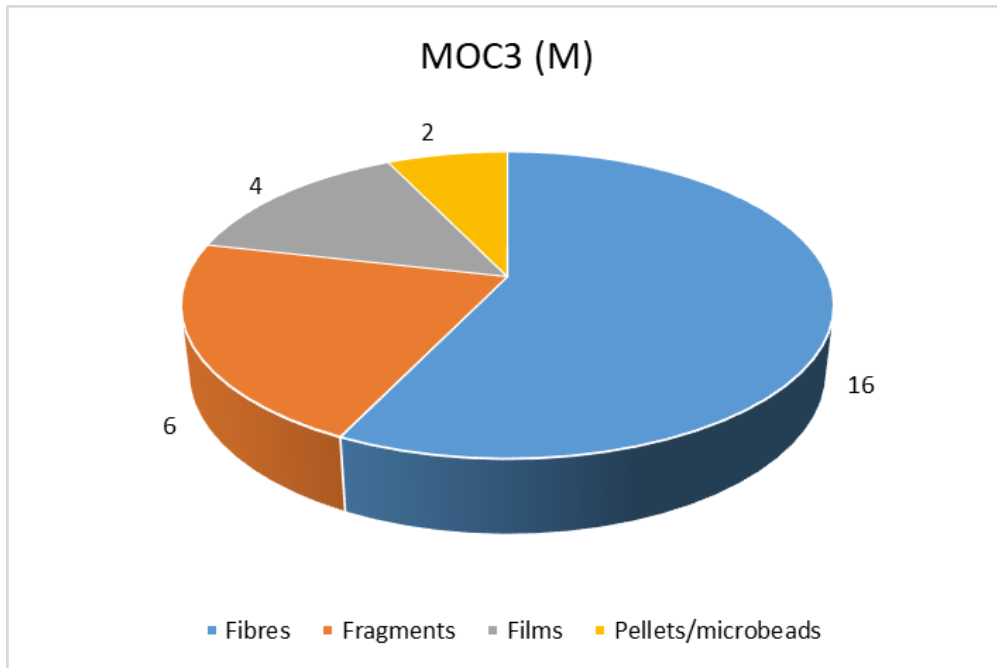

Figure 4.95. Forms and abundance of microplastics in MOC4.
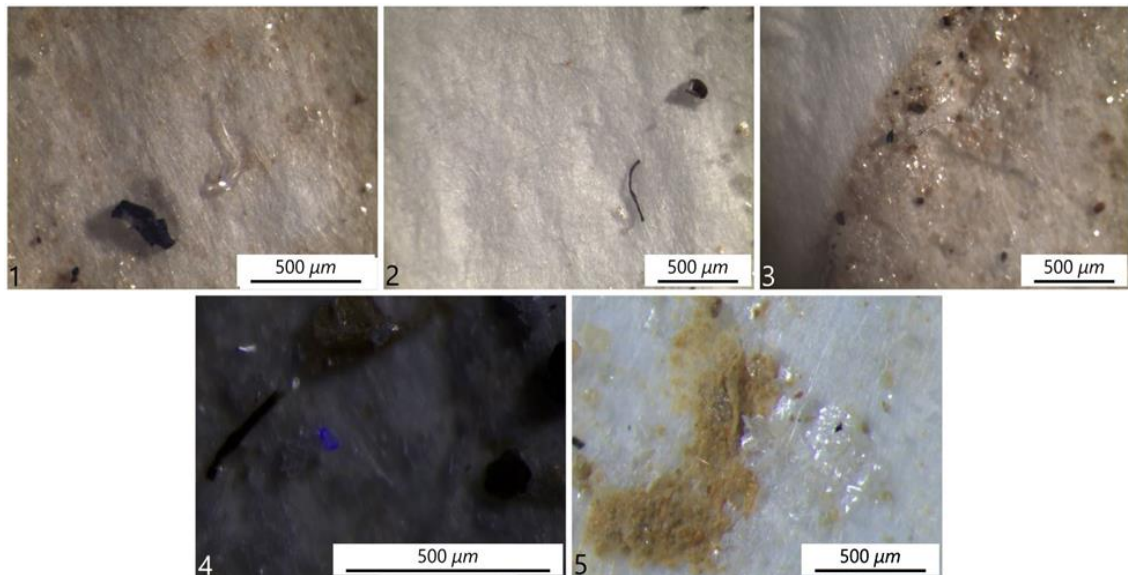
Figure 4.96. Pictures of microplastics found in MOC4. 1. Transparent fibre; 2. Black fibre; 3. Transparent fibre; 4. Transparent fragment under UV light; 5. Transparent film.

4.5.4   MOC6

The last sample comes from the floating vegetational debris collected at the tip of the tail, located $700\ m$ downstream from the other five samples (*figure 4.97*).

Figure 4.97. MOC6. Vegetational debris collected at the tip of the tail.

This vegetational debris appeared "heavier" than the previous ones (MOC11, MOC16 and MOC17), indeed testing his capacity to float in clean water, resulted that a higher quantity of material tended to sink (*figure 4.98*).
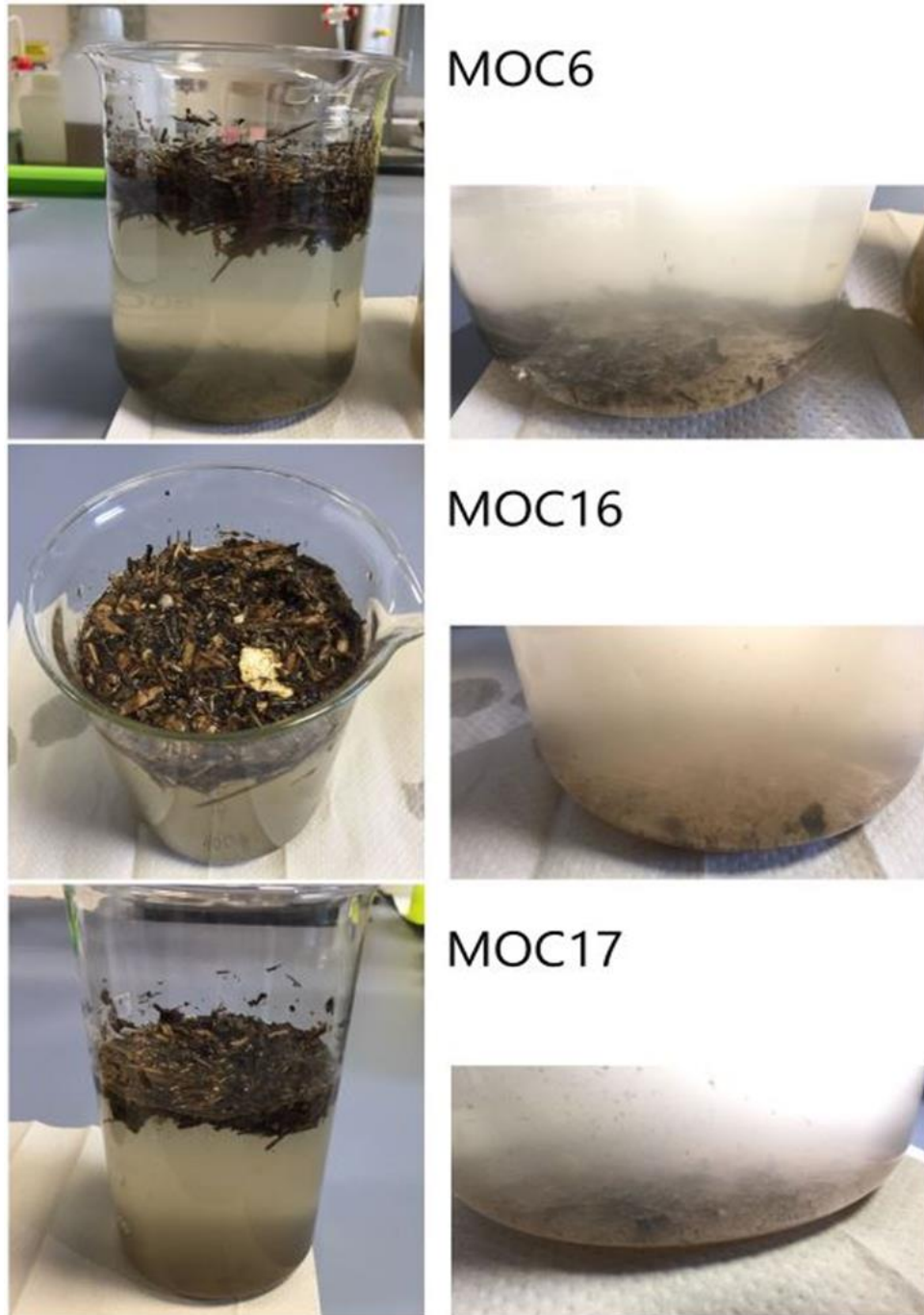
Figure 4.98. Floating test on three different vegetational samples. MOC6 presents a higher sinking component.

4. Results

The microscopic analysis led to the identification of 26 microplastic items. Figures 4.99 and 4.100 show forms and abundance of microplastics within the sample.
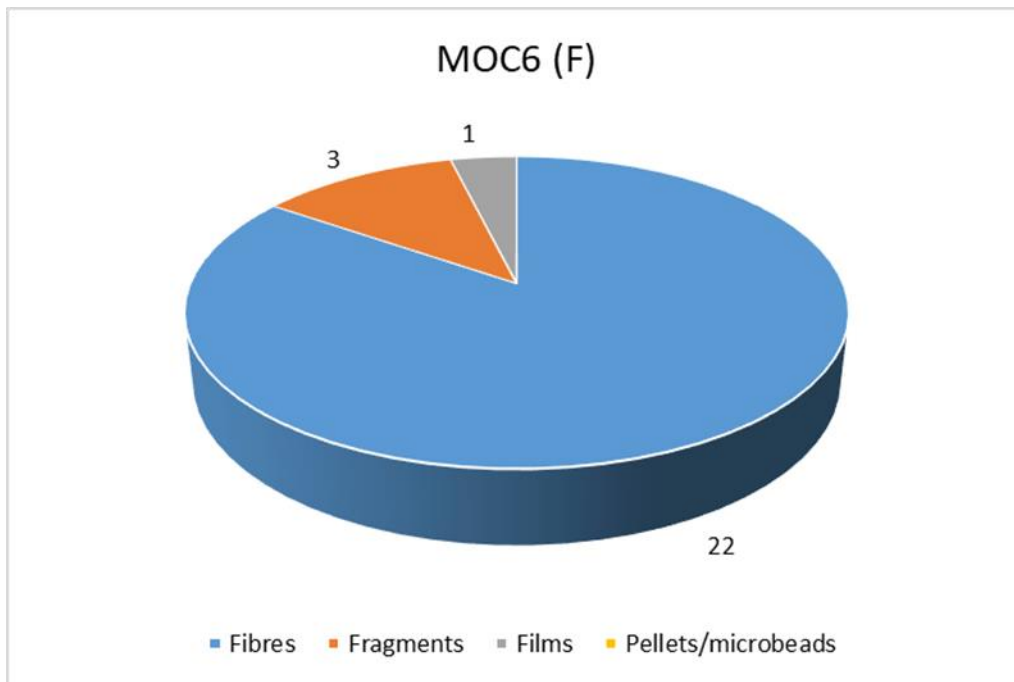
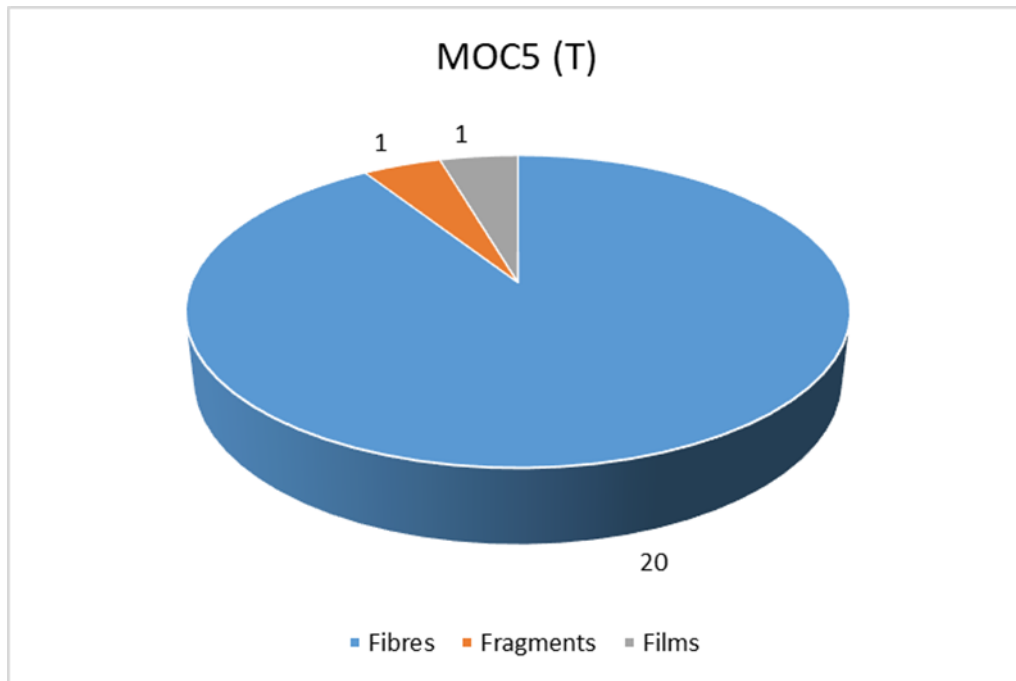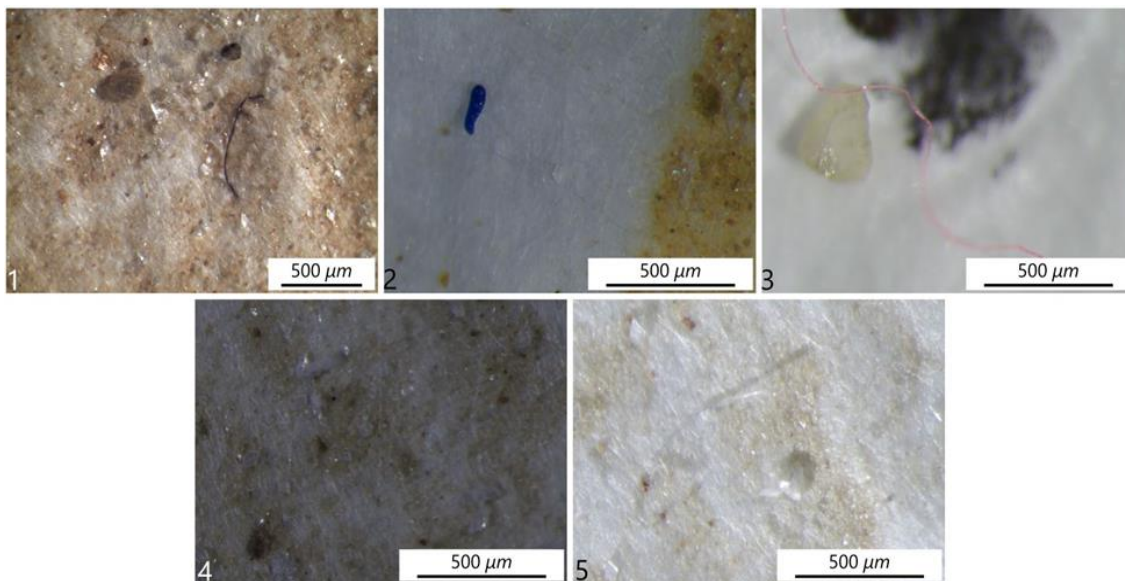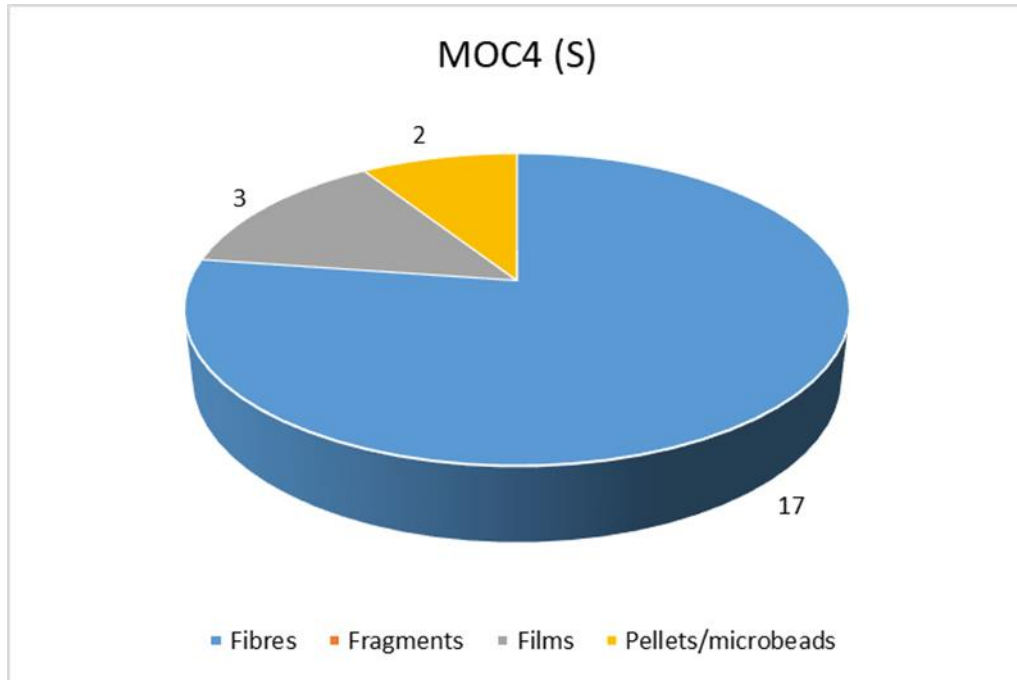*Figure 4.99. Forms and abundance of microplastics in MOC6.*
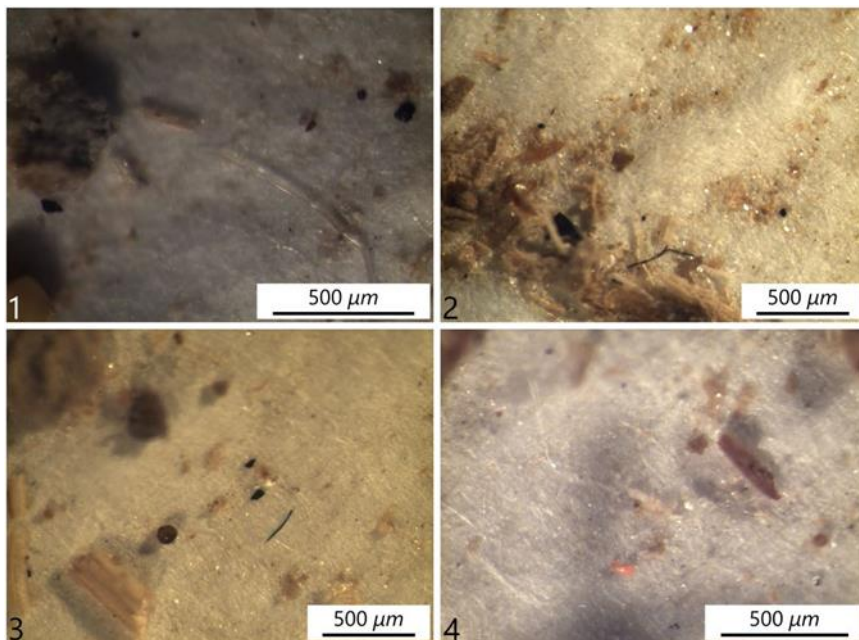
Figure 4.100. Pictures of microplastics found in MOC6. 1. Transparent fibre; 2. Black fibre; 3. Blue fibre; 4. Pink fragment.

4. Results

4.6   Summary

Table 7 summarise the main features of the 37 samples analysed.

	Sample	TYPE	Fibres	Fragments	Films	Pellets/microbeads	Total	Concentration MPs/g
BAR 1	MOC12	S	24	3	1	1	29	0,96
	MOC13	T	9	0	2	0	11	0,88
	MOC14	S	19	0	2	3	24	0,96
	MOC15	T	22	0	0	0	22	1,44
	MOC16	F	23	0	1	0	24	1,12
	MOC17	F	22	0	0	0	22	1,32
BAR 2	P1	T	64	7	7	2	80	1,12
	P2	S	111	24	6	1	142	1,12
	P3	S	48	4	7	1	60	0,88
	P4	M	35	4	3	3	45	0,88
	P5	T	41	7	11	2	61	1,04
	P6	S	44	7	8	2	61	0,76
	P7	S	20	5	1	0	26	1,32
	P8	S	60	6	0	3	69	1,68
	P9	T	31	1	6	2	40	0,88
	P10	S	88	18	16	8	130	2,8
	P11	T	18	2	3	1	24	1,16
	P12	S	66	5	14	3	88	0,44
	P13	M	41	2	12	1	56	0,96
	P14	M	49	0	1	1	51	0,88
	P15	M	16	1	3	1	21	6,67
BAR 3	MOC7	S	16	3	0	0	19	2,75
	MOC8	T	29	2	2	0	33	3,2
	MOC9	S	30	11	1	0	42	5,68
	MOC10	T	17	2	3	0	22	2,4
	MOC11	F	11	3	0	0	14	1,8
BAR 4	G2	T	20	2	2	0	24	2,44
	G3	S	12	4	6	0	22	2,44
	G4	T	22	2	0	0	24	1,04
	G5	S	29	3	4	0	36	2,76
	G12	S	21	4	2	1	28	1,6
BAR 5	MOC1	S	26	0	7	0	33	5,2
	MOC2	T	25	1	2	0	28	0,96
	MOC3	M	16	6	4	2	28	3,52
	MOC4	S	17	0	3	2	22	2,24
	MOC5	T	20	1	1	0	22	2,04
	MOC6	F	22	3	1	0	26	0,84

Table 7. Microplastic forms, quantities, and concentration of the analysed samples.

4. Results

Considering the five bars it is possible to see that microplastic concentrations in the sediments analysed are not uniforms.

The samples containing the highest concentration in microplastics generally represent the sediments settled during the waning phase (S samples), in accordance with the lower densities of the microplastics, while the sediments deposited under tractional conditions (T samples) show lower values. The T samples deposited in correspondence to an increase of the energy of the system and, for hence, the flow intensity. This led to the coarser sediments to be transported as bedload and deposit under tractive condition. The S samples, on the other hand, deposited during brief periods of standing water level which led to a decrease in flow intensity and thus to the settling of fine-grained sediments.

The floating vegetational debris (F samples) contain a large number of microplastics, considering the small portions of material analysed, with microplastic concentration peaks up to $6.67 \, MPs/g$.

5   Discussion

The Arno River sediments show a very variable microplastic concentrations, influenced by the depositional setting from which they accumulated. Microplastic concentration ranges from $0.44 \, MPs/g$ to $6.67 \, MPs/g$. These values are comparable with some of the concentrations found in rivers worldwide (*table 8*).

River	MPs/g	State	Reference
West River	2,56 - 10,24	China	Huang et al., 2021
Pearl River	0,08 - 9,59	China	Lin et al., 2018
Amazon Rivers	0,42 - 8,18	Brazil	Gerolin et al., 2020
Tisza River	0,53 - 8,07	Hungary	Kiss et al., 2021
St. Lawrence River	0,065 - 7,56	Canada	Crew et al, 2020
Arno River	0,44 - 6,67	Italy	This study
Mersey River	2,81 - 6,35	England	Hurley et al., 2018
Atoyac River	2,23 (mean)	Mexico	Shruti et al., 2019
Nakdong River	1,97 (mean)	South Korea	Eo et al., 2019
Rhine River	0,23 - 3,76	Germany	Klein et al., 2015
Citarum river	1,67 (mean)	Indonesia	Sembiring et al., 2020
Wei River	0,36 - 1,32	China	Ding et al., 2019
Pearl River	0,68 (mean)	China	Fan et al., 2019
Thame tributaries	0,13 - 0,74	England	Horton et al, 2016
Vistula River	0,19 - 0,58	Poland	Sekudewicz et al., 2021
Yangtze River	0,1 - 0,58	China	Fan et al., 2021
Maozhou River	0,03 - 0,56	China	Wu et al., 2020
River Kelvin	0,16 - 0,43	Scotland	Blair et al., 2018
Ciwalengke River	0,01 - 0,05	Indonesia	Cahya Alam et al., 2019

Table 8. Microplastic concentrations in river sediments worldwide.

The Arno River appears to be one of the most polluted rivers among those listed in table 8. However, excluding the values obtained from the F samples, which have concentrations sharply higher than the mean values, the average concentration results to be $1.72 \, MPS/g$. Additionally, this value is not comforting considering that the Arno has a small drainage basin ($8220 \, km^2$) compared to other rivers in the table, or that the population density of the study area reaches a maximum of $800 \, inhabitants/km^2$. Although Rhine River in Germany or Pearl River in China are larger than the Arno River and they cross areas with higher population density (respectively 2907 and $2004 \, inhabitants/km^2$), the microplastic concentrations are similar.

5. Discussion

Actually, the reason why there is such a large range of values may be due to a yet early stage for these types of studies, and related methodologies used to isolate microplastics. Therefore, there may be methodological issues related to sediment sampling, microplastic extraction and analysis that could influence the microplastic counting.

The presence of microplastics was observed in all the samples analysed, irrespective of their nature, with a predominance of fibres over fragments, films, and pellets (*figure 5.1*). These finding agree with previous studies confirming that fibres are more likely to be trapped within the sediments than any other form (Kane and Clare,2019; Horton et al., 2017).
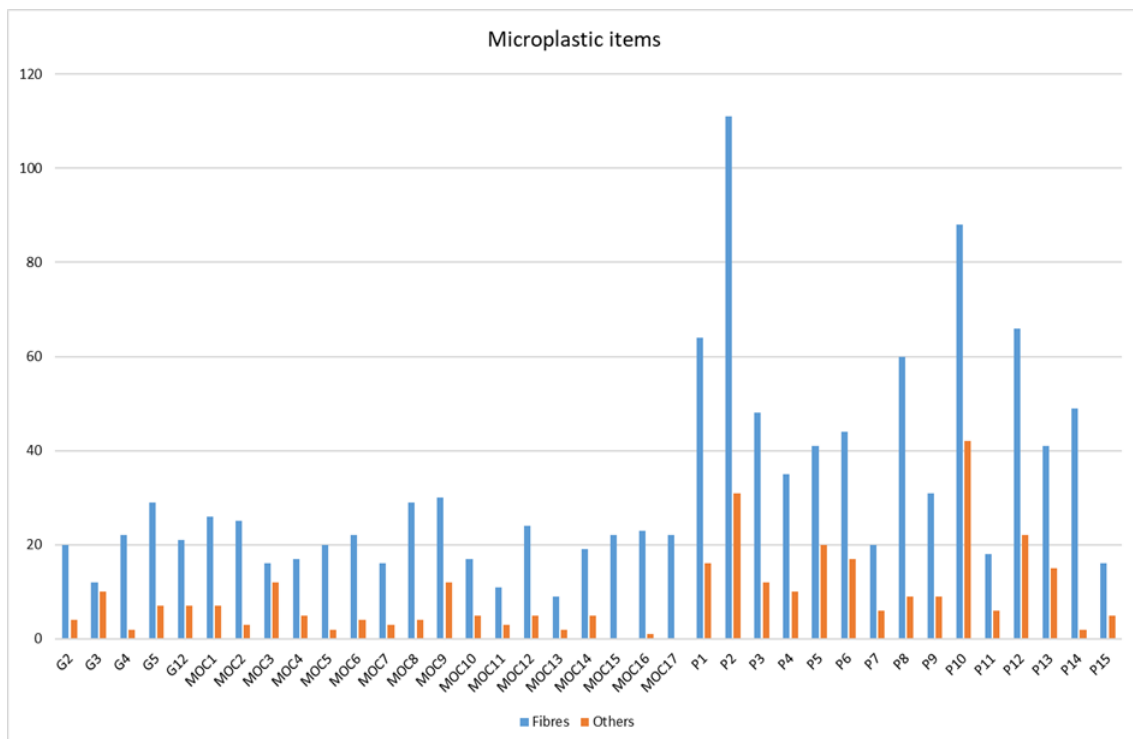
Figure 5.1. Forms and relative abundances per each sample.

Bar 2 shows a higher average microplastic concentration than other samples. In this bar, samples were collected with more frequency and both bar head and tail were investigated. The sediments containing the highest number if microplastics are located in the bar tail, with a maximum concentration value of $5.68 \, MPs/g$. Sediments collected in the bar head (from P9 to P15) have variable concentrations, even though values are not so different from the bar tail.

5. Discussion

The other bars were sampled mainly on the tail, although they do not show such high concentrations as Bar 2.

Different reasons can be suggested for the higher microplastic content of Bar 2 in comparison with the other bars. A first explanation could be related to the different analytical procedures. In fact, for the P-series, cellulose acetate filters were used for microscopic analysis. These filters, compared to glass microfiber filters, gave a clearer view of microplastics, so it is possible that the use of glass microfiber filters led to an underestimation of microplastics. Furthermore, Bar 2 is placed where the Arno River crosses an urban centre, where several minor creeks enter the main channel. A direct discharge of waste may, therefore, have locally influenced the concentrations.

The analytical approach adopted in order to evaluate transport and deposition of microplastics during different phases of flood depositional events, revealed to be appropriated as it led to the recognition of several intriguing points dealing with microplastic transport and accumulation processes. These points are discussed below and are about transport of microplastic: i) as floating elements, ii) in slough-water markers, iii) from settling processes and iv) during different flood stages.

5.1 Floating transport

During floods, the increase in hydrodynamic regime allows the rivers to transport large volume of sediments along with coarse grains. During these events, large volumes of vegetational debris are transported on water top surface, as floating debris.

Due to its low density, the plant debris floats on the water surface until it deposits as the flood falls, interacting with suspended microplastic particles. When the current is in contact with the rhizome of the plants, the flow velocity becomes unsteady. Under the influence of a convection current, the microplastics in water are difficult to transport and thus settle easily. In addition, for rigid plants, a trailing vortex will be produced when the water flows through it, consequently leading to the settling of the microplastic. (Yin et al., 2021).

The microscopic analysis highlighted that most of the microplastics associated with floating plant debris are fibres, suggesting that such forms are more likely to be trapped

as they tend to knot at the frustules. The results provided from the analysed floating vegetational debris (F samples) clearly show that in such samples there are peaks in microplastic concentrations significantly higher than the average (*figure 5.2*).
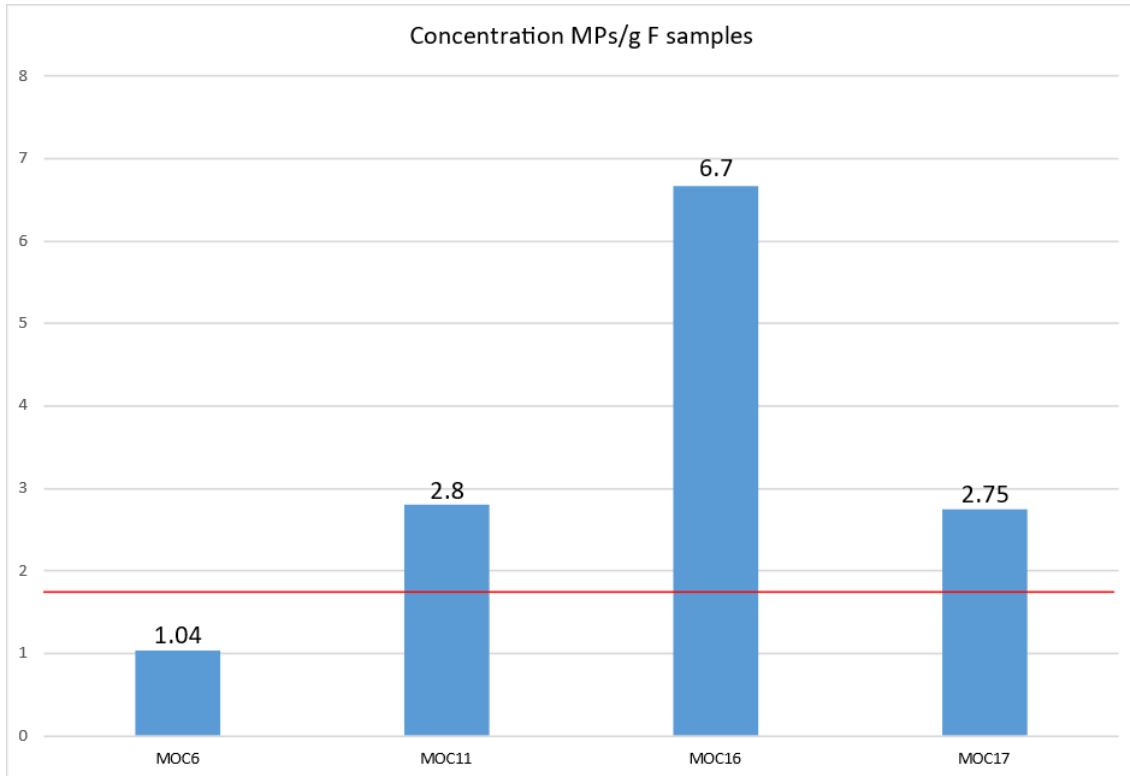

Figure 5.2. Microplastics concentration in F samples. In red, the average concentration excluding F samples.

Among the F samples, only MOC6 shows countertrend values whose meaning is not really clear. It is possible that its low microplastic concentration should be due to the nature of the deposit which, as seen in figure 4.98, appears "heavier" than any other F samples, with more material which tend to sink.

5.2 Slough-water markers

After a flood event reaches his peak, the water level tends to fall and reach a steady condition. The waning phase is characterized by phases in which water level stands, allowing the deposition of finer sediments, frustules and microplastics. When the water level restarts to fall, the material previously accumulated will mark the level at which water temporarily stationed. This condition is clearly favourable to the accumulation of microplastics, according to their physical properties. The evidence of slough water conditions has been observed both on the bar tail (within sandy sediments) and the head (within gravelly sediments). The five M samples show microplastic concentrations

5. Discussion

slightly higher than the average values (*figure 5.3*), in particular for those samples collected in bar head (**P**13 **P**14 **P**15).
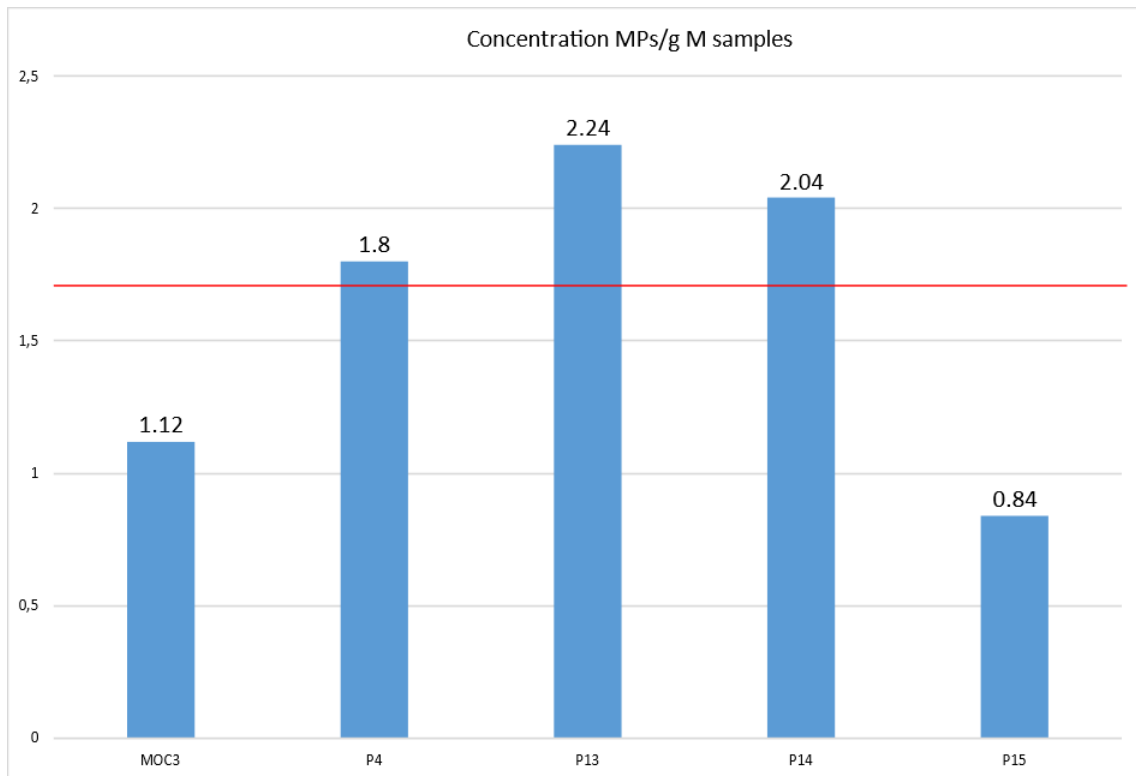
Figure 5.3. Microplastics concentration in M samples. In red, the average concentration excluding F samples.

Such high microplastic concentrations in gravelly beds can be explained if considering the infiltration behaviour of fine particulates within coarser sediments.

Recent studies show how microplastics infiltration capability strongly depend on their size rather than their density (Waldschläger & Schüttrumpf, 2020). Two fibres with same length but different density will infiltrate at similar depths, whereas two fibres with different lengths will reach different depths. In natural sediments, the matrix gives an indication of whether microplastic particles with specific diameters are able to infiltrate or not.

The only values which contrast with such an explanation are those from MOC3 and the P15 samples.

MOC3 has been collected from Bar 5, where the average concentration of microplastics per gram is clearly lower than Bar 2, where the P samples were collected (respectively 1.06 versus $2.55\ MPs/g$). However, if considered only the samples collected in Bar 5,

the MOC3 sample has a microplastic concentration higher than the mean values, thus confirming the favourable condition for microplastics to accumulate during phases of water standing.

The "anomalous" value of P15 can be easily explained considering the related depositional environment. P15 was actually collected in the zone of maximum erosion, where the finest portion of sediment was effectively scarce. It is therefore plausible that the bypass processes could have prevailed even during the waning phase, flushing out the finest portion and associated microplastics.

5.3   Settling processes

During the latest waning phase, the low energy of the flood does not allow the larger sediments such as gravels and pebbles to be transported. During this stage only the finer sediments can be transported, mainly as suspended load. The decrease in flow intensity makes a perfect condition for finer sediment and microplastics to settle in muddy to sandy layers, during the temporary standing of the water level.

Microplastic removal from the water column and retention within river sediments is strongly affected by the particle density. Settling deposition is favourited for microplastic particles with larger size or, for smaller particulate, thanks to the heteroaggregation, the aggregation of nano- and microplastic with suspended solids. With increasing size of the plastic particles, removal of singular particles from the water phase occurs earlier, whereas settling of smaller plastic particles is dependent on their aggregation with suspended solids. (Besseling et al., 2016).

In the bar tail, the suspended particulates – as the flow intensity decreases – tend to settle and drape the sediments deposited under tractional conditions. The finest portion in the bar head, instead, infiltrates within the gravels and pebbles.

The head is the most erosive area of a fluvial bar, and it is difficult for the finest portion to not be flushed away. But, against the odds, the infiltration process proved to be an efficient process for microplastics to be trapped. Fine sediments and microplastics seem to find repair in the shadow zones of larger clasts (gravels and pebbles) and the resulting increase in grip retains microplastics more efficiently in the sediment.

5. Discussion

The microplastic concentrations of the sediments settled during the waning phase (S samples) are indicated in figure 5.4.
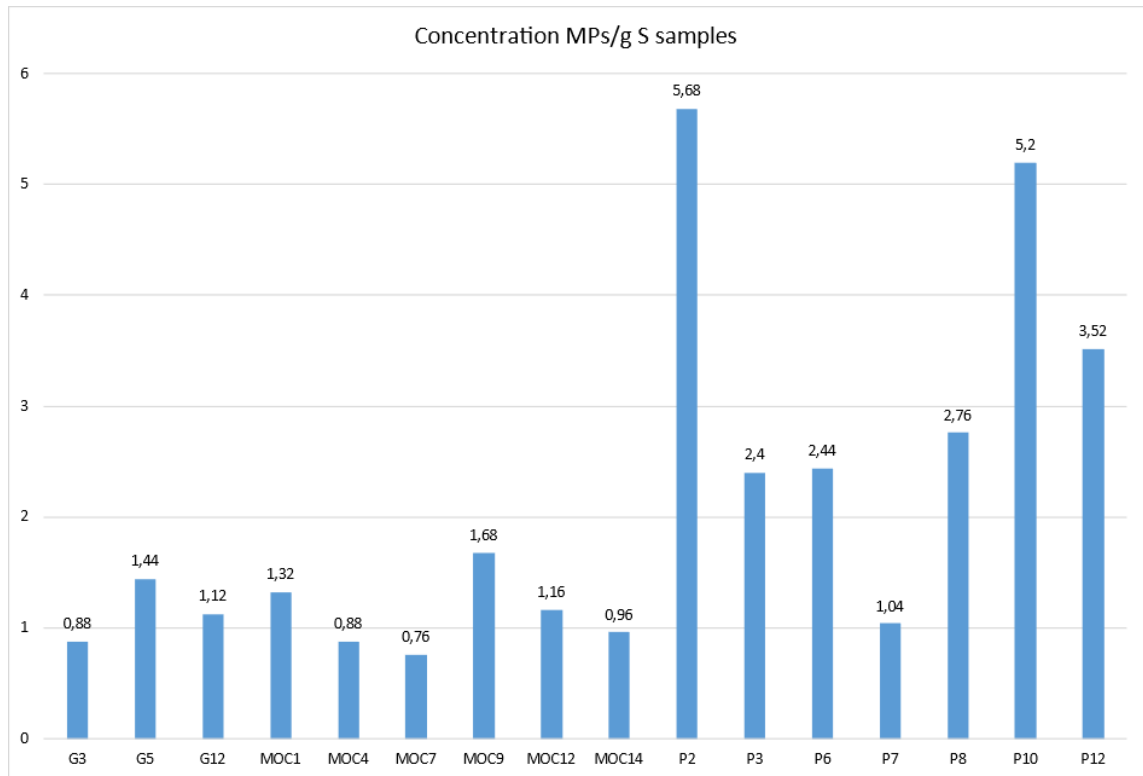

Figure 5.4. Microplastic concentrations in S samples.

The P10 and P12 samples come from the finest portion infiltrated within the gravels in the bar head. Their microplastic concentrations confirm the efficiency of gravel beds to retain microplastics, as their values (respectively 5.2 and 3.52 MPs/g) are clearly higher than the average.

5.4 Microplastic deposition during different flood stages

The sediments deposited during under tractional conditions differ from the sediment deposited for settling. Comparing the samples representing different flood stages, the microplastic concentration in sediments deposited for settling during the waning phase (S samples) is expected to be higher than in those sediments deposited under tractional conditions (T samples).

5. Discussion

Observing the data provided by the analyses on coupled samples it is possible to determine a trend valid for 8 couples out of 10 (*figure 5.5*). Most surface sediments contain microplastics in higher concentrations than associated sediments sampled at $10 - 15\ cm$ depth.
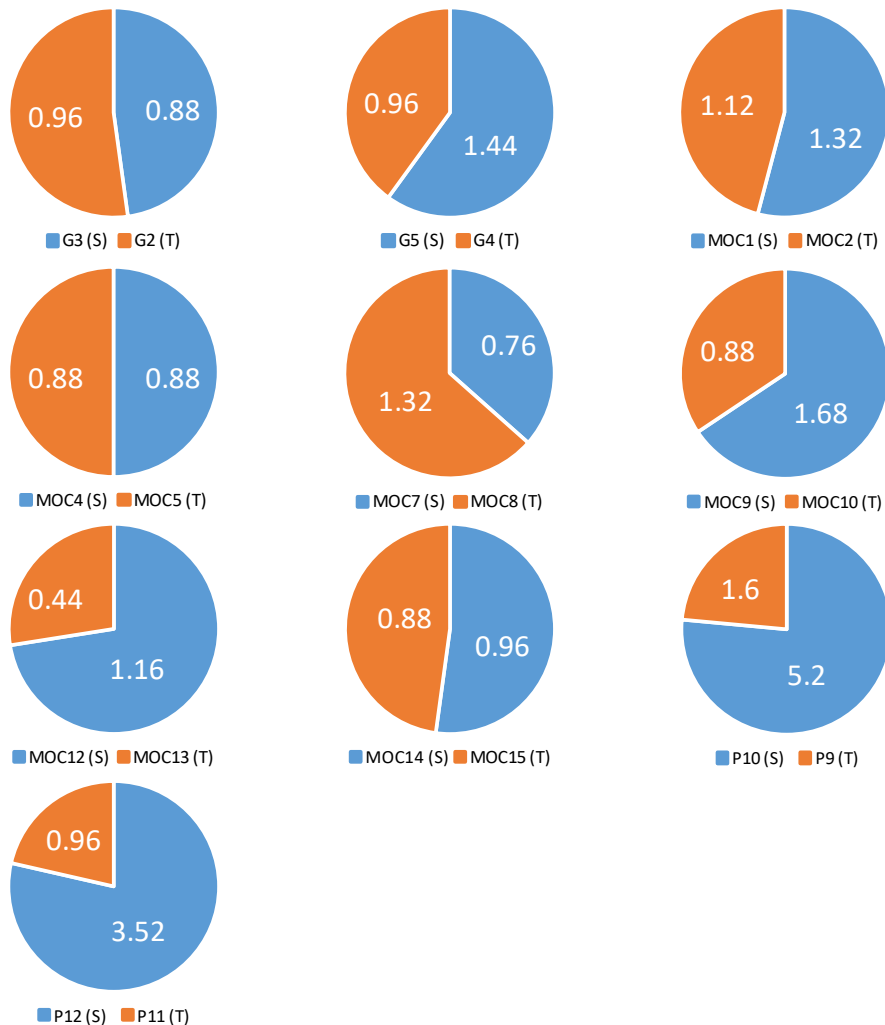
Concentration MPs/g

Figure 5.5. Microplastic concentration per gram relative to each couple of samples.

This trend confirms therefore the expectations, as during the waning phase the smaller and lighter particles, such as microplastics, find the perfect conditions to settle and to be trapped within the sediment.

Despite this expected result, due to the physical properties of the microplastics, it is surprising to observe that such a difference was not so overwhelming compared to the concentration of microplastics in sediments deposited under tractive conditions, when
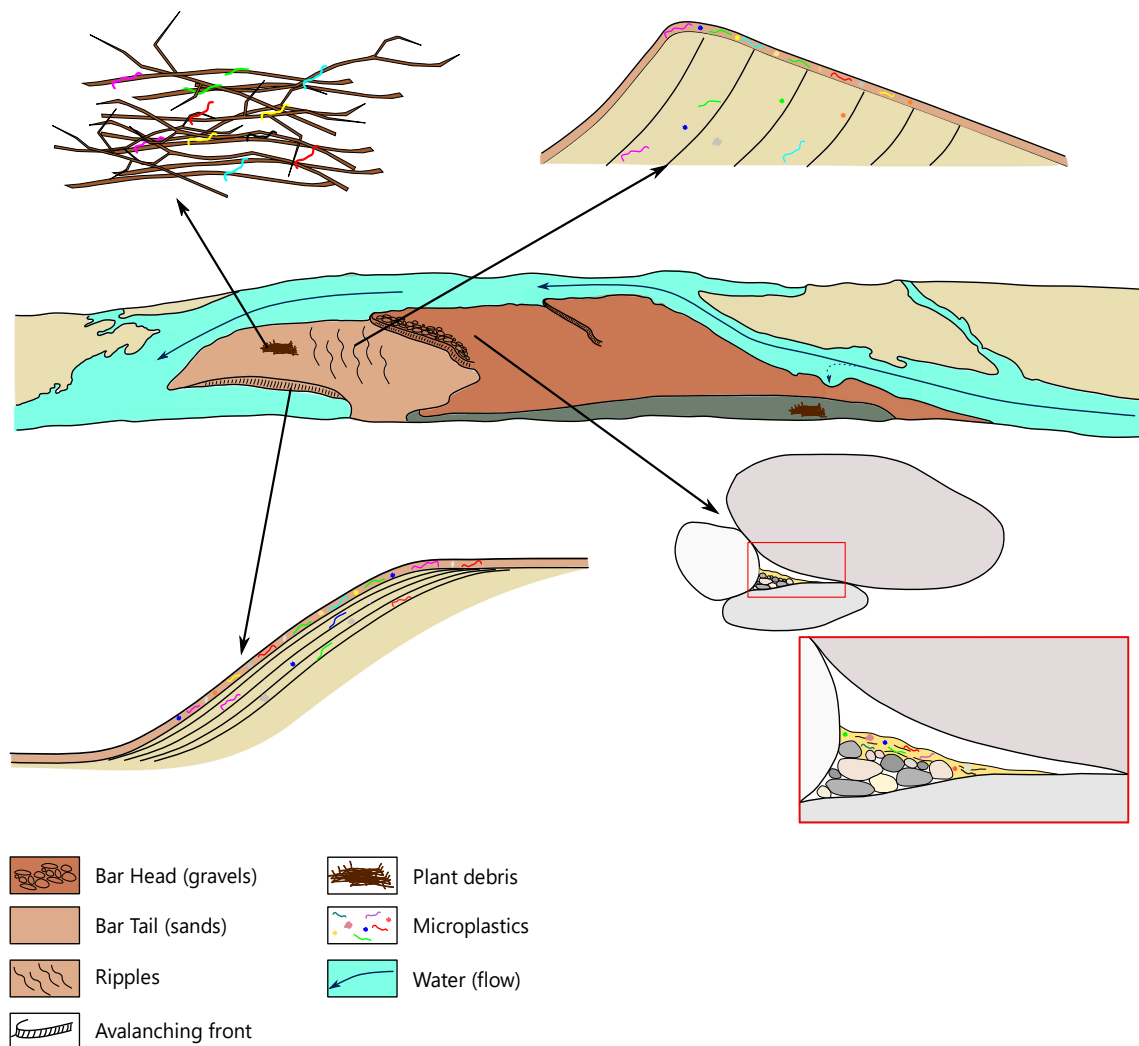
5. Discussion

the tractional forces prevent sediment settling. Under low-flow condition at the early rising limb of the flood, the bed develops an armour layer which serves to stabilise the bed surface and thus limits microplastic "winnowing" or release, such that the sediment bed acts as a sink (Ockelford et al., 2020).

5.5   Microplastic distribution during floods

This study highlights microplastic transport and deposition mechanisms in rivers during flood events.

During floods, microplastics have been seen to distribute in different concentrations within the bar deposits (*figure 5.6*).

Figure 5.6. Microplastics distribution in river sediments after flood events.

5. Discussion

The hydrodynamic regime strongly influences the deposition of microplastics, as their low density makes them better deposited during the waning phase, when flows are less sustained and allow them to settle. Despite this, a large number of microplastics were also found in sediments deposited under tractional conditions, indicating that, although in lower concentrations, they can be deposited even at higher water flows.

Increased grip seems to play a key role in retaining microplastics within the deposit.

As seen in floating plant debris, microplastic concentrations can reach high values, up to $6.67\ MPs/g$. This factor is particularly relevant even in areas mainly affected by erosion processes, such as bar heads. In fact, the finer sediment infiltrated within the gravels and pebbles unexpectedly showed quite high concentrations of microplastics, especially when sheltered in shadow areas of larger clasts.

6   Conclusions

The present study aims to provide our knowledge about processes governing distribution of microplastics in river sediments. To achieve this goal, 37 sediment samples from 5 alternate bars were picked up in different settings and analysed by means of a stereomicroscope.

This work shed some lights on several features concerning the transport and accumulation processes of microplastics, which can be summarised as follows:

Independently from location the study sample, a prevalence of microfibres over all other forms was always observed, thus confirming that fibres are extremely diffuse and have also a greater trapping potential.

Settling from standing of slowly-flowing water seems to be the best ways for microplastics to deposit.

Plant debris allows the entrapment of larger quantities of microplastics, thanks to the disturbing action on water flows, favouring settling processes.

The capability of fine sediment and microplastics to infiltrate within coarser clasts results in high concentrations of microplastics being found even in area which are mainly affected by by-pass processes, like bar head-zones.

The comparison between samples deposited during different flood stages confirms that sediments deposited by settling have higher concentrations of microplastics. However, sediments deposited under tractive conditions yield unexpectedly significant concentrations of microplastics.

The approach proposed here should be considered for future studies to improve our knowledge on microplastics transport and deposition in riverine systems, as they are the main carriers for microplastics in marine environments. Delving into this issue must therefore be the first step in raising public awareness to fight plastic pollution.

References

Alam, F. C., Sembiring, E., Muntalif, B. S., & Suendo, V. (2019). 'Microplastic distribution in surface water and sediment river around slum and industrial area (case study: Ciwalengke River, Majalaya district, Indonesia).' *Chemosphere*, *224*, 637–645. https://doi.org/10.1016/j.chemosphere.2019.02.188

Besseling, E., Quik, J. T. K., Sun, M., & Koelmans, A. A. (2017). 'Fate of nano- and microplastic in freshwater systems: A modeling study.' *Environmental Pollution*, *220*, 540–548. https://doi.org/10.1016/j.envpol.2016.10.001

Blair, R. M., Waldron, S., Phoenix, V. R., & Gauchotte-Lindsay, C. (2019). 'Microscopy and elemental analysis characterisation of microplastics in sediment of a freshwater urban river in Scotland, UK.' *Environmental Science and Pollution Research*. https://doi.org/10.1007/s11356-019-04678-1

Bonotto, G. (2020) 'Analisi di microplastiche in sedimenti fluviali.' Tesi di laurea magistrale inScienze e Tecnologie per l'Ambiente e il Territorio

Caporali, E., Rinaldi, M., & Casagli, N. (2005). 'The Arno River Floods.' *Giornale Di Geologia Applicata*, *1*, 177–192. https://doi.org/10.1474/GGA.2005-01.0-18.0018

Carpenter, E. J., Smith Jr., K. L., (1972) 'Plastics on the Sargasso Sea Surface.' *Science*, *175* (4027), 1240-1241. doi: 0.1126/science.175.4027.1240.

Claessens, M., Meester, S. de, Landuyt, L. van, Clerck, K. de, & Janssen, C. R. (2011). 'Occurrence and distribution of microplastics in marine sediments along the Belgian coast.' *Marine Pollution Bulletin*, *62*(10), 2199–2204. https://doi.org/10.1016/j.marpolbul.2011.06.030

Cole, M., Lindeque, P., Fileman, E., Halsband, C., Goodhead, R., Moger, J., & Galloway, T. S. (2013). 'Microplastic ingestion by zooplankton.' *Environmental Science and Technology*, *47*(12), 6646–6655. https://doi.org/10.1021/es400663f

References

Crew, A., Gregory-Eaves, I., & Ricciardi, A. (2020). 'Distribution, abundance, and diversity of microplastics in the upper St. Lawrence River.' *Environmental Pollution*, *260*. https://doi.org/10.1016/j.envpol.2020.113994

Ding, L., Mao, R. fan, Guo, X., Yang, X., Zhang, Q., & Yang, C. (2019). 'Microplastics in surface waters and sediments of the Wei River, in the northwest of China'. *Science of the Total Environment*, *667*, 427–434. https://doi.org/10.1016/j.scitotenv.2019.02.332

Eo, S., Hong, S. H., Song, Y. K., Han, G. M., & Shim, W. J. (2019). 'Spatiotemporal distribution and annual load of microplastics in the Nakdong River, South Korea.' *Water Research*, *160*, 228–237. https://doi.org/10.1016/j.watres.2019.05.053

Eriksen, M., Mason, S., Wilson, S., Box, C., Zellers, A., Edwards, W., Farley, H., & Amato, S. (2013). 'Microplastic pollution in the surface waters of the Laurentian Great Lakes.' *Marine Pollution Bulletin*, *77*(1–2), 177–182. https://doi.org/10.1016/j.marpolbul.2013.10.007

Fan, J., Zou, L., & Zhao, G. (2021). 'Microplastic abundance, distribution, and composition in the surface water and sediments of the Yangtze River along Chongqing City, China.' *Journal of Soils and Sediments*, *21,* 1840–1851. https://doi.org/10.1007/s11368-02102902-5/Published

Fan, Y., Zheng, K., Zhu, Z., Chen, G., & Peng, X. (2019). 'Distribution, sedimentary record, and persistence of microplastics in the Pearl River catchment, China'. *Environmental Pollution*, *251*, 862–870. https://doi.org/10.1016/j.envpol.2019.05.056

Frias, J., Pagter, E., Nash, R., & O'Connor, I. (2018). '*Standardised protocol for monitoring microplastics in sediments*.' https://doi.org/10.13140/RG.2.2.36256.89601/1

Gerolin, C. R., Pupim, F. N., Sawakuchi, A. O., Grohmann, C. H., Labuto, G., & Semensatto, D. (2020). 'Microplastics in sediments from Amazon rivers, Brazil'. *Science of the Total Environment*, *749*. https://doi.org/10.1016/j.scitotenv.2020.141604

References

González-Pleiter, M., Edo, C., Aguilera, Á., Viúdez-Moreiras, D., Pulido-Reyes, G., González Toril, E., Osuna, S., de Diego-Castilla, G., Leganés, F., Fernández-Piñas, F., & Rosal, R. (2021). 'Occurrence and transport of microplastics sampled within and above the planetary boundary layer.' *Science of the Total Environment*, *761*. https://doi.org/10.1016/j.scitotenv.2020.143213

He, B., Wijesiri, B., Ayoko, G. A., Egodawatta, P., Rintoul, L., & Goonetilleke, A. (2020). 'Influential factors on microplastics occurrence in river sediments.' *Science of the Total Environment*, *738*. https://doi.org/10.1016/j.scitotenv.2020.139901

Horton, A. A., Svendsen, C., Williams, R. J., Spurgeon, D. J., & Lahive, E. (2017). 'Large microplastic particles in sediments of tributaries of the River Thames, UK - Abundance, sources and methods for effective quantification.' *Marine Pollution Bulletin*, *114*(1), 218–226. https://doi.org/10.1016/j.marpolbul.2016.09.004

Huang, D., Li, X., Ouyang, Z., Zhao, X., Wu, R., Zhang, C., Lin, C., Li, Y., & Guo, X. (2021). 'The occurrence and abundance of microplastics in surface water and sediment of the West River downstream, in the south of China.' *Science of the Total Environment*, *756*. https://doi.org/10.1016/j.scitotenv.2020.143857

Kane, I. A., & Clare, M. A. (2019). 'Dispersion, accumulation, and the ultimate fate of microplastics in deep-marine environments: A review and future directions.' In *Frontiers in Earth Science* (Vol. 7). Frontiers Media S.A. https://doi.org/10.3389/feart.2019.00080

Kiss, T., Fórián, S., Szatmári, G., & Sipos, G. (2021). 'Spatial distribution of microplastics in the fluvial sediments of a transboundary river – A case study of the Tisza River in Central Europe'. *Science of the Total Environment*, *785*. https://doi.org/10.1016/j.scitotenv.2021.147306

Klein, S., Worch, E., & Knepper, T. P. (2015). 'Occurrence and spatial distribution of microplastics in river shore sediments of the rhine-main area in Germany.' *Environmental Science and Technology*, *49*(10), 6070–6076. https://doi.org/10.1021/acs.est.5b00492

References

Lebreton, L. C. M., van der Zwet, J., Damsteeg, J. W., Slat, B., Andrady, A., & Reisser, J. (2017). 'River plastic emissions to the world's oceans.' *Nature Communications*, *8*. https://doi.org/10.1038/ncomms15611

Lebreton, L., Slat, B., Ferrari, F., Sainte-Rose, B., Aitken, J., Marthouse, R., Hajbane, S., Cunsolo, S., Schwarz, A., Levivier, A., Noble, K., Debeljak, P., Maral, H., Schoeneich-Argent, R., Brambini, R., & Reisser, J. (2018). 'Evidence that the Great Pacific Garbage Patch is rapidly accumulating plastic.' *Scientific Reports*, *8*(1). https://doi.org/10.1038/s41598-018-22939-w

Li, W. C., Tse, H. F., & Fok, L. (2016). 'Plastic waste in the marine environment: A review of sources, occurrence and effects.' In *Science of the Total Environment* (Vols. 566–567, pp. 333–349). Elsevier B.V. https://doi.org/10.1016/j.scitotenv.2016.05.084

Lin, L., Zuo, L. Z., Peng, J. P., Cai, L. Q., Fok, L., Yan, Y., Li, H. X., & Xu, X. R. (2018). 'Occurrence and distribution of microplastics in an urban river: A case study in the Pearl River along Guangzhou City, China.' *Science of the Total Environment*, *644*, 375–381. https://doi.org/10.1016/j.scitotenv.2018.06.327

Masura, J., Baker, J., Foster, G., & Arthur, G. (2015). 'Laboratory Methods for the Analysis of Microplastics in the Marine Environment: Recommendations for quantifying synthetic particles in waters and sediments.'

Mishra, A. K., Singh, J., & Mishra, P. P. (2021). 'Microplastics in polar regions: An early warning to the world's pristine ecosystem.' In *Science of the Total Environment* (Vol. 784). Elsevier B.V. https://doi.org/10.1016/j.scitotenv.2021.147149

Napper, I. E., Bakir, A., Rowland, S. J., & Thompson, R. C. (2015). 'Characterisation, quantity and sorptive properties of microplastics extracted from cosmetics.' *Marine Pollution Bulletin*, *99*(1–2), 178–185. https://doi.org/10.1016/j.marpolbul.2015.07.029

References

Nocita, A. (2007). 'La fauna ittica del bacino dell'Arno Museum reserches View project Silurus glanis control action in Tuscany View project.' https://www.researchgate.net/publication/263018785

Ockelford, A., Cundy, A., & Ebdon, J. E. (2020). 'Storm Response of Fluvial Sedimentary Microplastics'. *Scientific Reports*, *10*(1). https://doi.org/10.1038/s41598-020 58765-2

PlascticsEurope. (2020). 'Plastics-the Facts 2020 An analysis of European plastics production, demand and waste data.'

Rinaldi, M. Surian N., Comiti F., Bussettini M. (2011). 'Manuale tecnico – operativo per la valutazione ed il monitoraggio dello stato morfologico dei corsi d'acqua.'

Rodrigues, S., Claude, N., Juge, P., & Breheret, J. G. (2012). 'An opportunity to connect the morphodynamics of alternate bars with their sedimentary products.' In *Earth Surface Processes and Landforms* (Vol. 37, Issue 2, pp. 240–248). https://doi.org/10.1002/esp.2255

Sekudewicz, I., Dąbrowska, A. M., & Syczewski, M. D. (2021). 'Microplastic pollution in surface water and sediments in the urban section of the Vistula River (Poland).' *Science of the Total Environment*, *762*. https://doi.org/10.1016/j.scitotenv.2020.143111

Sembiring, E., Fareza, A. A., Suendo, V., & Reza, M. (2020). 'The Presence of Microplastics in Water, Sediment, and Milkfish (Chanos chanos) at the Downstream Area of Citarum River, Indonesia.' *Water, Air, and Soil Pollution*, *231*(7). https://doi.org/10.1007/s11270-020-04710-y

Shruti, V. C., Jonathan, M. P., Rodriguez-Espinosa, P. F., & Rodríguez-González, F. (2019). 'Microplastics in freshwater sediments of Atoyac River basin, Puebla City, Mexico.' *Science of the Total Environment*, *654*, 154–163. https://doi.org/10.1016/j.scitotenv.2018.11.054

References

Tacconi Stefanelli, C., Casagli, N., & Catani, F. (2020). Landslide damming hazard susceptibility maps: a new GIS-based procedure for risk management. *Landslides*, *17*(7), 1635–1648. https://doi.org/10.1007/s10346-020-01395-6

Tartaro, G. (1989). La canalizzazione dell'Arno nel Valdarno Superiore, un intervento sul territorio nel XVII secolo. Accademia valdarnese del Poggio-Montevarchi, quaderni 2, S. Giovanni Valdarno

Waldschläger, K., & Schüttrumpf, H. (2020). 'Infiltration Behavior of Microplastic Particles with Different Densities, Sizes, and Shapes-From Glass Spheres to Natural Sediments.' *Environmental Science and Technology*, *54*(15), 9366–9373. https://doi.org/10.1021/acs.est.0c01722

Wu, P., Tang, Y., Dang, M., Wang, S., Jin, H., Liu, Y., Jing, H., Zheng, C., Yi, S., & Cai, Z. (2020).'Spatial-temporal distribution of microplastics in surface water and sediments of Maozhou River within Guangdong-Hong Kong-Macao Greater Bay Area.' *Science of the Total Environment*, *717*. https://doi.org/10.1016/j.scitotenv.2019.135187

Yin, L., Wen, X., Huang, D., Zeng, G., Deng, R., Liu, R., Zhou, Z., Tao, J., Xiao, R., & Pan, H. (2021).'Microplastics retention by reeds in freshwater environment.' *Science of the Total Environment*, *790*. https://doi.org/10.1016/j.scitotenv.2021.148200

Yurtsever, M. (2019). 'Glitters as a Source of Primary Microplastics: An Approach to Environmental Responsibility and Ethics.' *Journal of Agricultural and Environmental Ethics*, *32*(3), 459–478. https://doi.org/10.1007/s10806-019-09785-0

Supplementary material

Grain size distributions
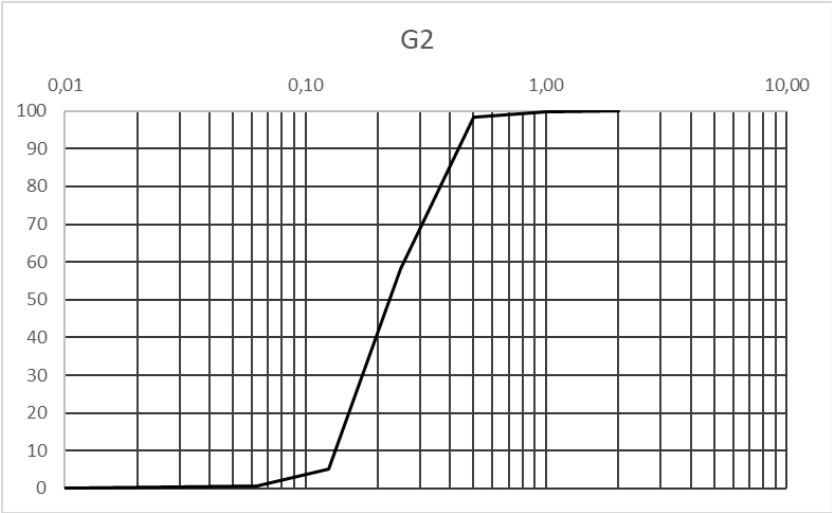
Figure a. Grain size distribution of the G2 sample.
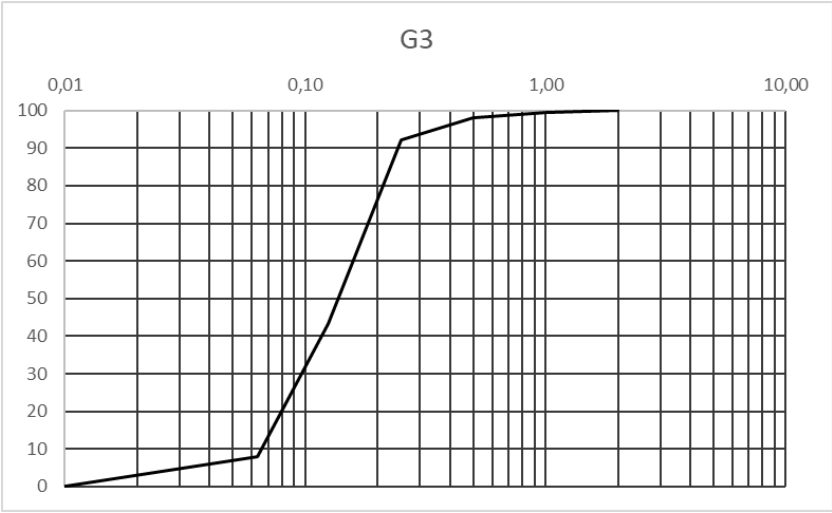
Figure b. Grain size distribution of the G3 sample.
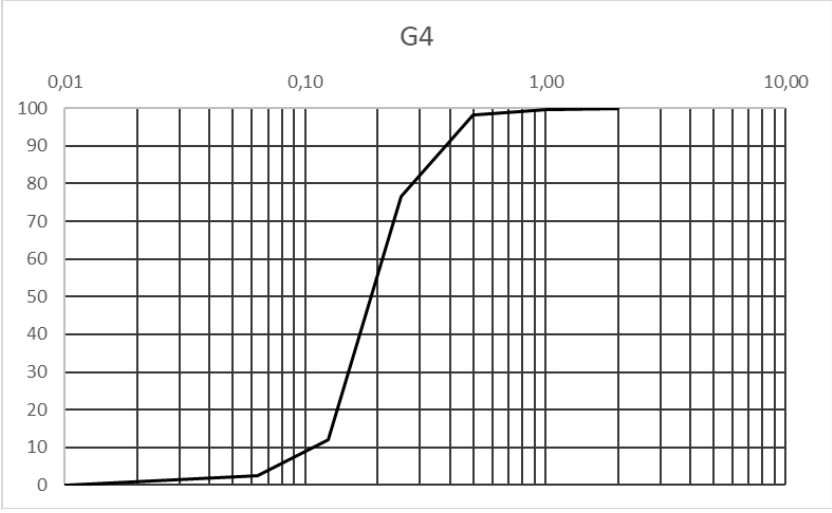
Figure c. Grain size distribution of the G4 sample.
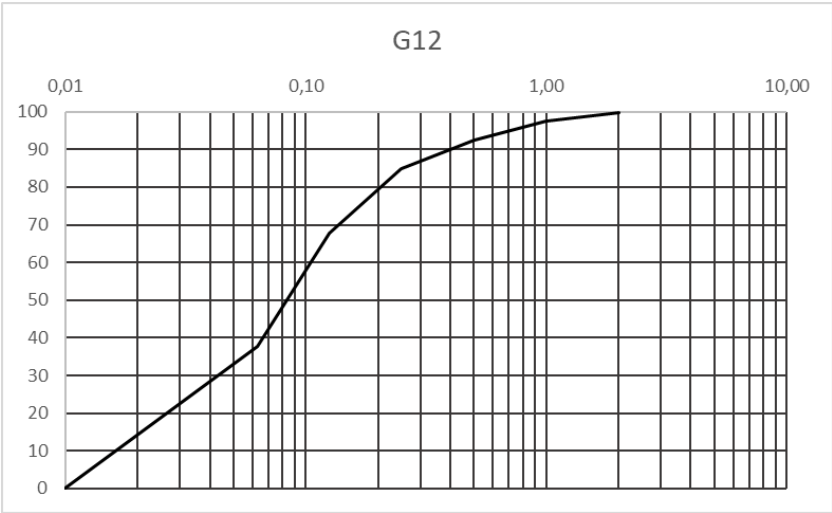
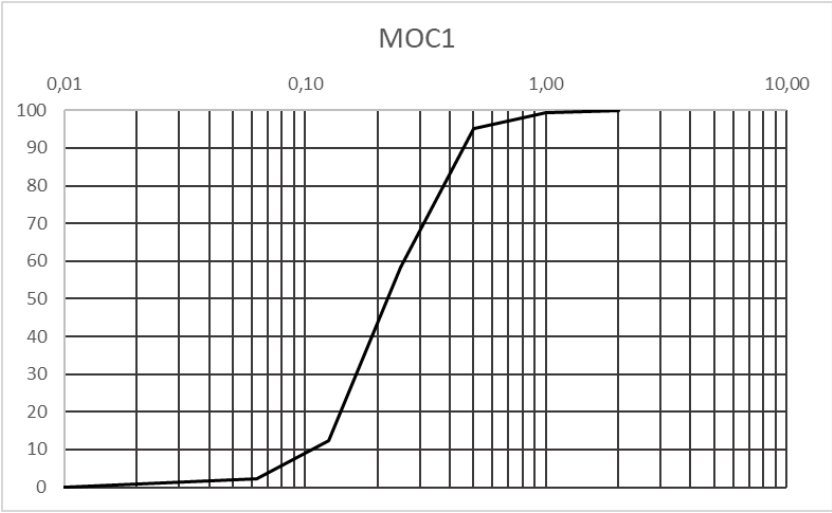*Figure d. Grain size distribution of the G12 sample.*

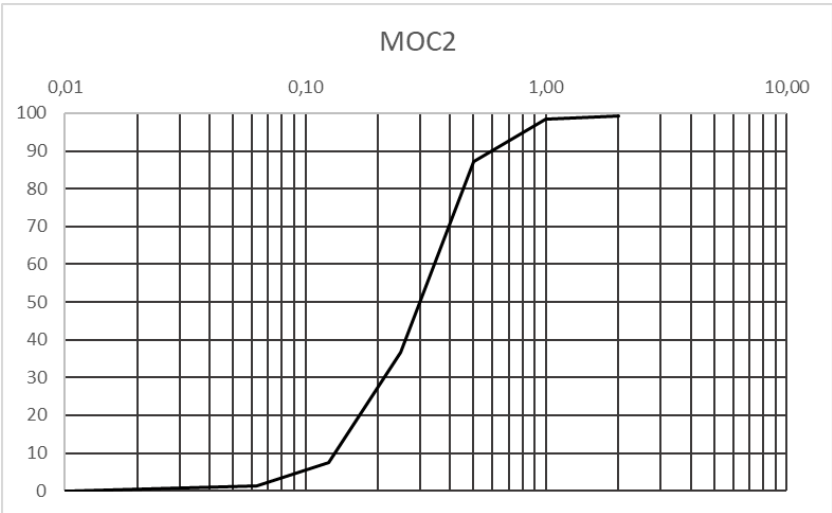*Figure e. Grain size distribution of the MOC1 sample.*

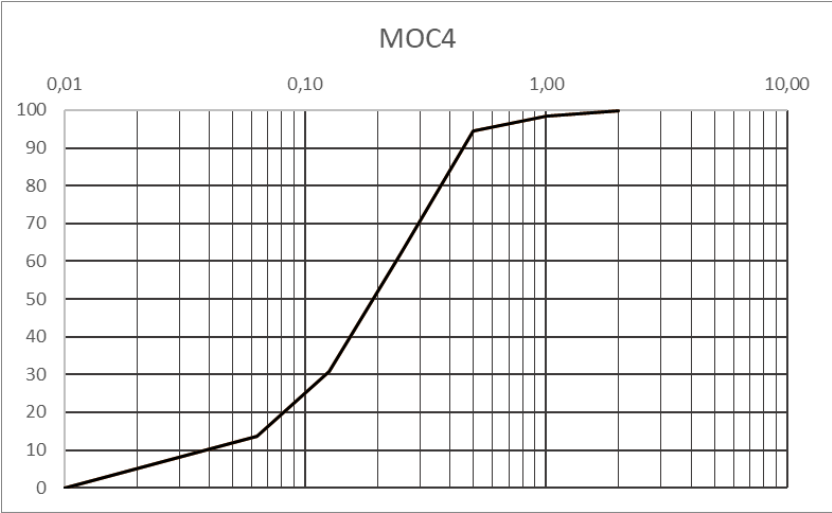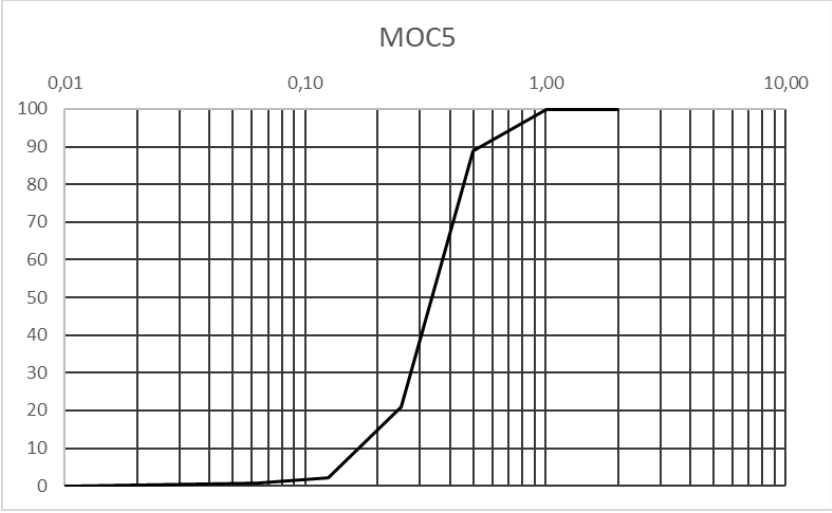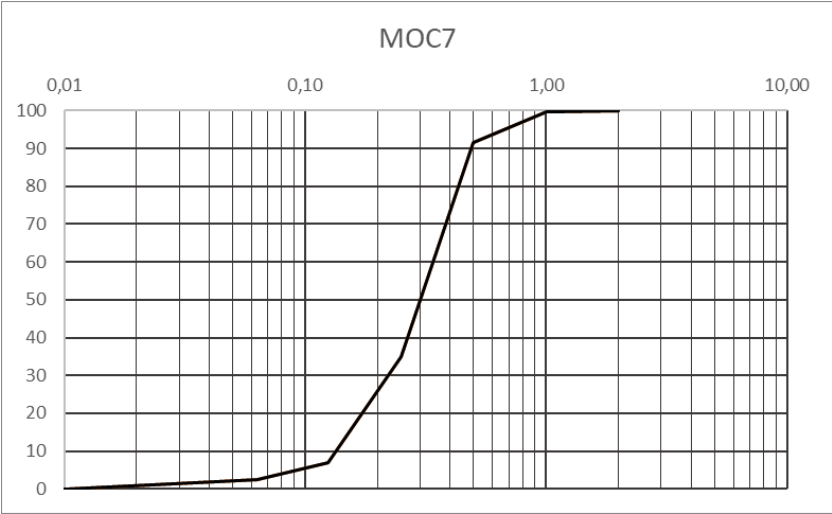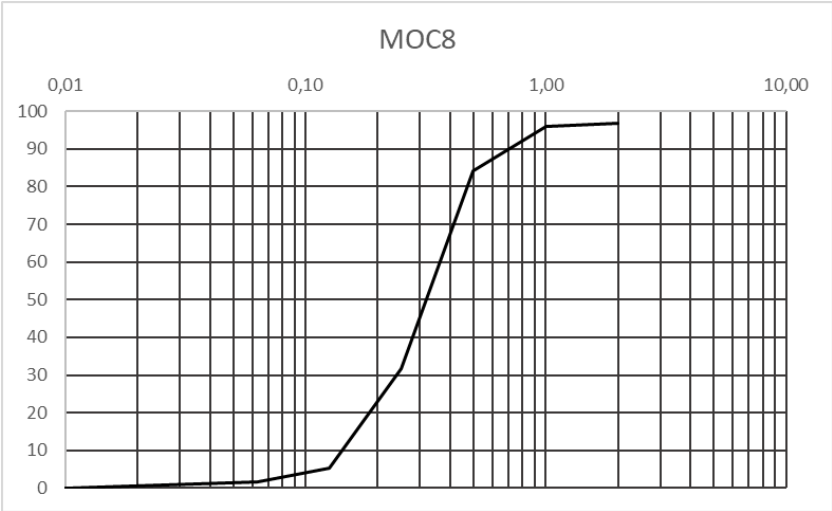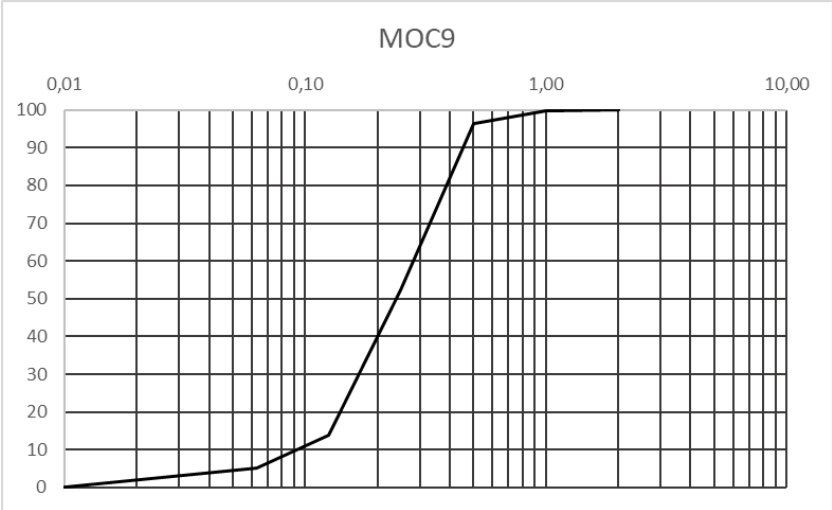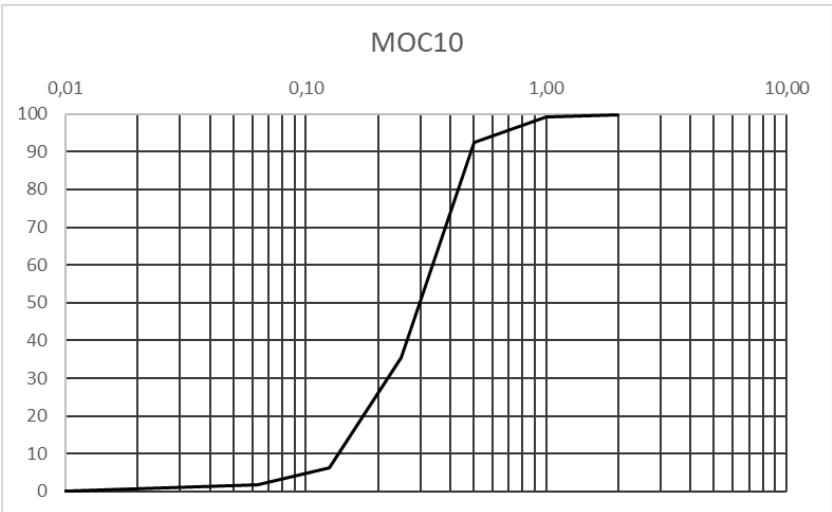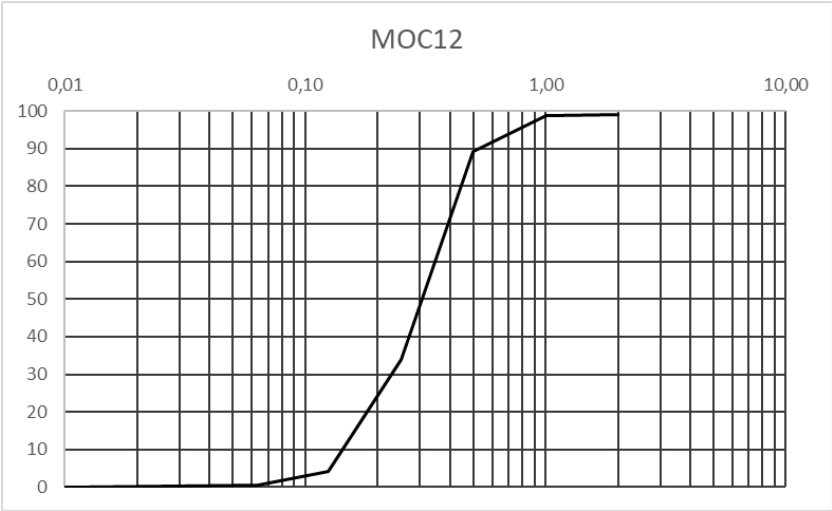*Figure f. Grain size distribution of the MOC2 sample.*

Figure g. Grain size distribution of the MOC4 sample.

Figure h. Grain size distribution of the MOC5 sample.

Figure i. Grain size distribution of the MOC7 sample.

Figure j. Grain size distribution of the MOC8 sample.

Figure k. Grain size distribution of the MOC9 sample.

Figure l. Grain size distribution of the MOC10 sample.

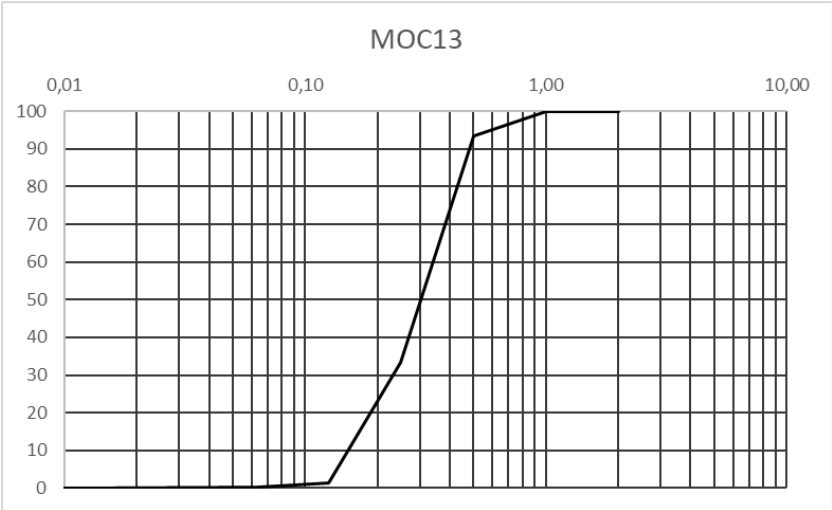*Figure m. Grain size distribution of the MOC12 sample.*
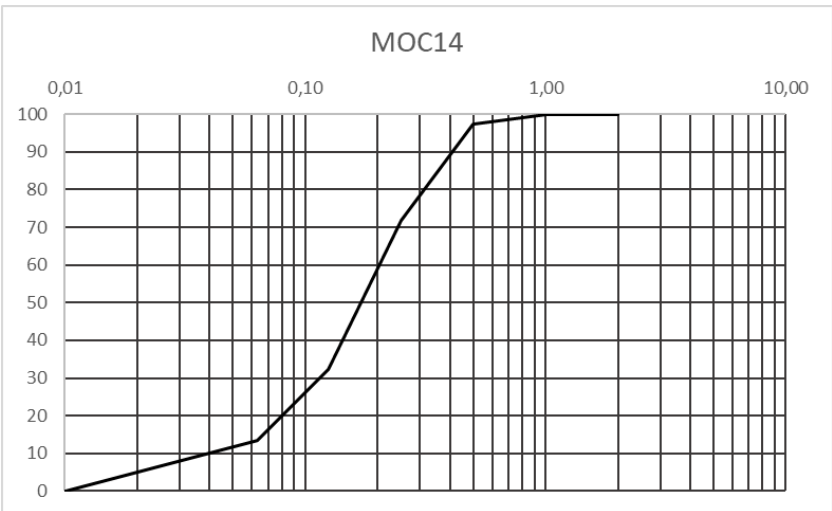

Figure n. Grain size distribution of the MOC13 sample.
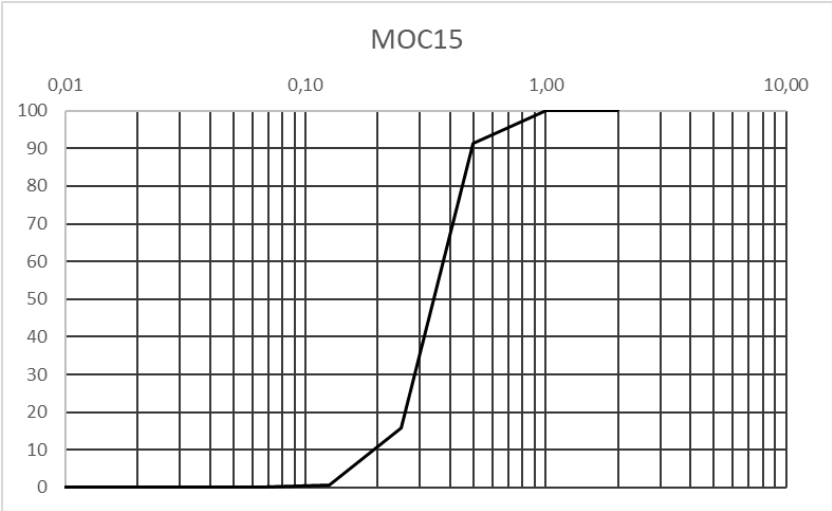

Figure o. Grain size distribution of the MOC14 sample.

Figure p. Grain size distribution of the MOC15 sample.